International Atomic Energy Agency

INDC(IND)-046
Distr. G

INDC INTERNATIONAL NUCLEAR DATA COMMITTEE

PROGRESS REPORT ON NUCLEAR DATA ACTIVITIES IN INDIA FOR THE PERIOD JULY 1992 TO MARCH 1995

Compiled by

S. Ganesan

Neutron Physics Division
Bhabha Atomic Research Centre
Bombay, India

1995

IAEA NUCLEAR DATA SECTION, WAGRAMERSTRASSE 5, A-1400 VIENNA

Reproduced by the IAEA in Austria
November 1995

INDC(IND)-046
Distr. G

PROGRESS REPORT ON NUCLEAR DATA ACTIVITIES IN INDIA FOR THE PERIOD JULY 1992 TO MARCH 1995

Compiled by

S. Ganesan

Neutron Physics Division
Bhabha Atomic Research Centre
Bombay, India

Abstract

The present progress report on Nuclear Data Activities in India covers the work carried out during the period from July 1992 to March 1995. It contains brief description on various activities such as measurements, evaluations, compilations, processing of nuclear data, validation of nuclear data through experimental analysis and other related works being carried out in India, at Bhabha Atomic Research Centre, Bombay and at Indira Gandhi Centre for Atomic Research, Kalpakkam. The report gives extended abstracts of the work carried out mainly in the above-mentioned two centres.

1995

PREFACE

The present progress report on Nuclear Data Activities in India is the nineth report, the first of which was brought out in the year 1981. This report covers the work carried out during the period from July 1992 to March 1995. It contains brief description on various activities such as measurements, evaluations, compilations, processing of nuclear data validation of nuclear data through experimental analysis and other related works being carried out in India, mainly at Bhabha Atomic Research Centre at Bombay and Indira Gandhi Centre of Atomic Research at Kalpakkam.

The work related to basic and applied nuclear physics including studies on nuclear structure, excitation modes, decay of nuclei, low and medium energy charged particle nuclear reactions, nuclear instrumentation, experimental techniques, accelerator based basic and applied research, and heavy ion physics being carried out at Pelletron accelerator at Bombay and Variable Energy Cyclotron at Calcutta has not been included in this report which can be found in the proceedings of the DAE Symposium on Nuclear Physics, Vol.36B, held at the University of Calicut, Calicut from December 27-30, 1993 and in the proceedings of the DAE Symposium on Nuclear Physics, Vol.37B, held at Utkal University Utkal from December 26-30, 1994.

This report basically gives the extended abstracts of the work carried out and these are not to be regarded as publications or quoted without permission from authors.

Dr. S.S. Kapoor
Director, Physics Group, BARC &
Member, International Nuclear Data Committee

INDEX

SUPERFLUID MODEL BASED LEVEL DENSITY PARAMETERS FOR NUCLEAR DATA EVALUATION

S.B.Garg and Ashok Kumar
Bhabha Atomic Research Centre
Trombay, Bombay-400 085

It is well known that nuclear level density parameter is one of the basic inputs to determine interaction cross-section in a nuclear model calculation. Several recipes /1-4/ are available for its evaluation. In this paper, recipe based on superfluid model /3/ has been employed to estimate the level density parameters of a large no. of nuclides in the mass range 40 to 250. The procedure of Ref./5/ has been adopted . Accordingly, the level density parameter 'a' is represented by

$$a(U) = a(*)\ [1 + E_{sh}/U\ \{\ 1-\exp(-\tau\ U)\}] \quad .....(1)$$

Where a(*) is the asymptotic level density parameter to which a(U) converges at high excitation energies and τ is a damping parameter given by $\tau = 0.40\ (A)^{-1/3}$. E_{sh} is the shell energy correction given by the difference of the experimental mass and the liquid drop model based mass of the nucleus i.e. $E_{sh} = M_{exp} - M_{ld}$. M_{ld} is calculated with the formulation of Ref./6/ with the pairing energy corrections of Cook et al /7/ by accounting for the deformation energy. Level density expression of Gilbert and Cameron /1/ is employed to calculate 'a' at the neutron binding energy by fitting the s-wave resonance level spacing according to the following expression:

$$1/\langle D\rangle_0 = f\ (U, J=1/2) \qquad \text{for } I=0$$
$$= f\ (U, J=I+1/2) + f\ (U, J=I-1/2) \qquad \text{for } I\neq 0$$

In this procedure, first a(*) is inferred and then using expression (1) 'a' is estimated. We have taken the recently evaluated s-wave resonance spacings from Ref./8/ and computed 'a(*)' and 'a' for a large no. of nuclides. These parameters are plotted against the mass no. A in Figs.1 and 2. It is shown in Fig.1 (solid curve) that a(*) can be approximated by a quadratic in A of the type:

$a(*) = b_0 + b_1 A + b_2 A^2$ with $b_0 = {}_{-5}0.75925$, $b_1 = 0.13788$ and $b_2 = -11.5631\ (10)$. This expression can be easily built into the existing nuclear model codes for the evaluation of nuclear level density and thereby nuclear data. It may be stressed that the level density parameter based on this methodology accounts for the shell closure effect and is energy dependent.

References. 1. A. Gilbert and A.G.W Cameron; Can. J Phys. 43, 1446(1967) 2. W. Dilg et al; Nucl. Phys. A 217, 269(1971) 3. A.V. Ignatyuk et al; Sov. J. Nucl. Phys. 21, 255 (1975) 4. S.K. Kataria et al; Phys. Rev. C18, 988(1978) 5. A. Mengoni and Y. Nakajima; J. Nucl. Sci. Technol 31, 151(1994). 6. W.D. Myers and W.J. Swiatecki ; Nucl. Phys. 81, 1(1966). 7. J.L. Cook et al; Aust. J. Phys. 20, 477(1967). 8. H. Zhongfu et al; Comm. of Nucl. Data Prog. No. 9, 60 (1993).

Acknowledgement:

This work has been carried out under the IAEA Research Contract No. 8067/RB.

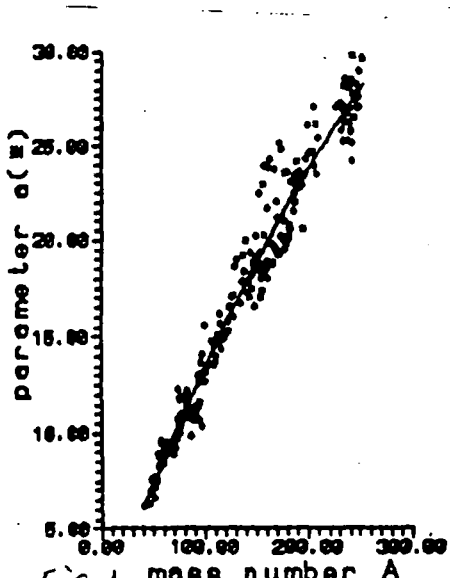

Fig. 1

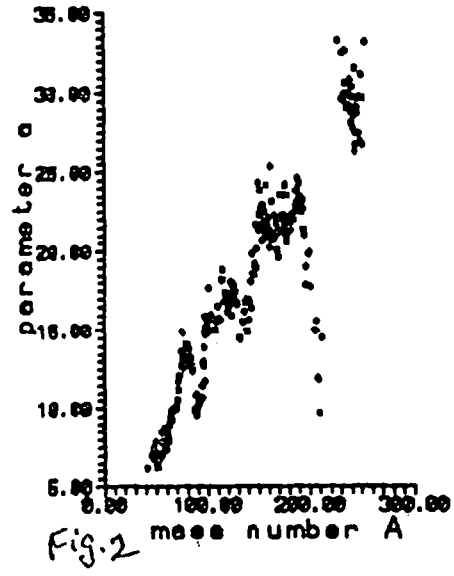

Fig. 2

(N,2N) CROSS-SECTIONS OF TUNGSTEN AND ITS ISOTOPES

S.B.Garg
Neutron Physics Division
Bhabha Atomic Research Centre
Trombay , Bombay- 400 085

Tungsten and its isotopes W-182,W-183,W-184 and W-186 are important nuclides from the considerations of their application in neutron dosimetry and fusion technology. The measured cross-section data are usually not available over the energy range extending up to 30 MeV and tungsten is no exception. Nuclear models are,therefore,employed to extrapolate or interpolate the measured data.In this context,we have been utilizing various nuclear model schemes and based on several analyses,we are of the opinion that the multistep Hauser-Feshbach scheme /1/ with a provision for the pre-equilibrium decay process /2/ reproduces the measured data rather well and it qualifies for adoption as a data prediction tool.To provide a further test of this hypothesis and to generate the desired data for technological applications in the energy range extending up to 30 MeV we have computed multiparticle reaction cross-sections of the above listed isotopes by accounting for neutron,proton,alpha-particle and gamma-rays in the outgoing channels.(N,2N) cross-sections of natural tungsten have been inferred and are given in Fig.1 by considering the isotopic abundances.

Analysis has been carried out by adopting the level density recipes of Gilbert and Cameron /3/ and of Ignatyuk et al /4/ with the pairing energy corrections of Cook et al /5/.Neutron optical model potential parameters of Delaroche et al /6/ are utilized to compute reaction cross-section and transmission coefficients.Potential parameters of Beccheti and Greenlees /7/ and of Mc Fadden and Satchler /8/ have been used for proton and alpha-particle respectively. Discrete energy levels of all the nuclides taking part in the reactions have been compiled from Nuclear Data Sheets.Giant resonance parameters for transmission coefficients of gamma-rays are taken from the literature.

Geometry dependent hybrid model /9/ is also employed to compute cross-section data for W-182 to bring out the comparison. The results are shown in Fig.2. To save space computed data for W-183,W-184 and W-186 are not given but the trend is similar to that of W-182. It may be noted that the measured data /10/ are well reproduced. In the case of W-182 the Gilbert-Cameron and the Ignatyuk level density recipes yield similar results. Predictions of the geometry dependent hybrid model are,however, higher. The computed (n,3n) cross-sections are also shown in Fig.2 for W-182.

References:1.W.Hauser and H.Feshbach; Phys. Rev.87, 366(1952).2.C. Kalbach; Z.Phys. A283, 401(1977). 3.A.Gilbert and A.G.W.Cameron;Can. J.Phys.43,1446 (1965). 4.A.V. Ignatyuk et al; Sov.J.Nucl.Phys.21,255 (1975). 5. J.L.Cook et al;Aust.J.Phys. 20,477 (1967).6.J.F.Delaroche et al;Intern.Nucl.Data Conf. Knoxville , USA, 336(1979).7.F.D.Becchti and G.W.Greenlees; Phy.Rev.182,1190(1969) 8. L.Mc Fadden and G. R.Satchler; Nucl.Phys. 84,177 (1966). 9. M. Blann and H.K.Vonach; Phys. Rev. C28 , 1475 (1983). 10. J.Frehaut et al;Report BNL-NCS-51245 Vol.I,399(1980)

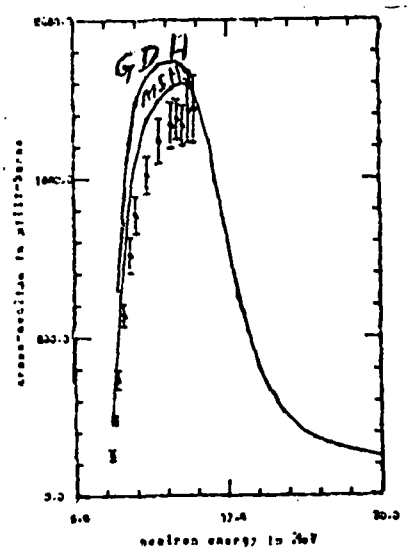

Fig.1 (n,2n) cross-sections of natural tungsten with MSMF and GDH models

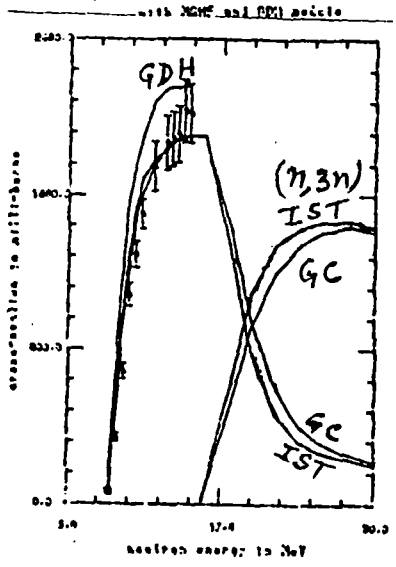

Fig.2 (n,2n) and (n,3n) X-sections of W-182 with MSMF and GDH models and IST and GC level densities

MULTINEUTRON EMISSION CROSS-SECTIONS OF Pb-208 AND Bi-209 FOR USE IN FUSION TECHNOLOGY

S.B. Garg
Neutron Physics Division
Bhabha Atomic Research Centre
Trombay, Bombay - 400 085, India

ABSTRACT

Pb-208 and Bi-209 are considered as promising materials for fusion blankets because of their superior neutron multiplying characteristics. In this paper, emission cross-sections for neutrons, protons, alpha-particles and gamma-rays are investigated for these nuclides in the energy range 8-30 MeV using the framework of the multistep Hauser-Feshbach statistical theory combined with the Kalbach exciton model for the pre-equilibrium decay and the Brink - Axel model of the giant dipole resonance to account for the radiative capture competition.

Appropriate optical model potential parameters are selected to evaluate the compound nucleus reaction cross-sections at different neutron incident energies. (n,n'), (n,2n), (n,3n), (n,4n) and the total production cross-sections for neutrons, protons, alpha-particles and gamma-rays are inferred by performing consistent calculations.

I. INTRODUCTION

Pb-208 and Bi-209 are considered as promising materials for application in fusion blankets because of their superior neutron multiplying characteristics. Emission of charged particles from these nuclides is limited to the minimal because of their large Coulomb potential barriers. However, the generation of gamma rays may be the other important deciding characteristic to determine their suitability for fusion applications because of the radiation transport and shielding considerations. In this paper, all these factors have been examined by carrying out detailed cross-section calculations in the framework of the multistep Hauser-Feshbach statisticai theory /1/, which includes Kalbach-exciton model /2/ to allow for the pre-equilibriuim decay and the Brink-Axel model /3/ of the giant depole resonance to account for the radiative capture competition. Geometry dependent hybrid model /4/ is also employed in the case of Bi-209 to bring out the limitations of these models in the data prediction. Discussion is limited to (n,2n), (n,3n), (n,4n), total neutron emission, total proton emission, total alpha-particle emission and total gamma-ray emission cross-sections in the energy range 8-30 MeV. Level density recipes used in the continuum energy region to compute the equilibrium-part of the reaction products include the improved Gilbert-Cameron option /5,6/ and the Ignatyuk-Smirenkin-Tishin option /7/ with the pairing and shell energy corrections taken from Cook et al /8/. In the pre-equilibrium reaction mechanism, Williams' formalism /9/ is employed for the computation of particle-hole state densities. Discrete energy levels with the parities, spins and gamma-ray branching ratios taken from the Nuclear Data Sheets are adopted for the target, composite and residual nuclides involved in the reaction decay chains. In the case of geometry dependent hybrid model which makes use of the Weisskopf-Ewing evaporation model /10/ to describe the equilibrium process, the level density parameter for the doubly or singly closed shell nuclides Pb-208 and Bi-209 is taken as A/20-A being the mass no. of the composite nuclide; pairing energy corrections as defined by Blann and Bisplinghoff /11/ are applied in the back shifted fashion and the energy dependent single particle level density is used for neutrons and protons.

II. MODEL COMPUTATIONS

The compound nucleus reaction cross - sections and transmission coefficients for neutrons, protons and alpha

- particles are calculated with the spherical optical model based code SCAT-2/12/. Multiparticle reaction cross-sections are computed with the GNASH code /13/ in the case of Hauser-Feshbach statistical theory and with ALICE91 code /14/ in the case of geometry dependent hybrid model. Neutron optical model potential parameters for Pb-208 and Bi-209 are taken from Cheema and Finlay /15/ and Bersillon /16/ respectively. Proton and alpha-particle optical model potential parameters of Perey /17/ and Huizenga and Igo /18/ are adopted. Gamma-ray strength functions are derived using the average s-wave resonance level spacings from Cook et al and the average gamma-ray level widths from Mughabghab and Garber /19/. Dipole resonance parameters are taken from Dietrich and Berman /20/ to account for the gamma-ray cascades in the calculations. The average reaction matrix constant to determine the exciton transition rates in the pre-equilibrium decay mode is fixed at 150 (MeV) cubed in the case of Kalbach exciton model.

III. RESULTS AND CONCLUSIONS

The computed (n,2n), (n,3n) and (n,4n) cross-sections for Bi-209 and Pb-208 are compared with the corresponding measured data /21,22/ in Figs.1 and 2. It is noted that in the case of Bi-209, the energy dependent IST level density option leads to a better reproduction of the measured (n,2n) and (n,3n) cross-sections compared to the often used GC level density option. However, GC option has an edge over the IST option in the case of doubly magic Pb-208. Since no (n,3n) data for Pb-208 and no (n,4n) data for both Pb-208 and Bi-209 are measured, this study serves to predict these data and also extrapolates the measured data beyond the energy range of their measurements. The predictions of the geometry dependent hybrid model shown in Fig.1 for Bi-209 are acceptable if quick estimates are desired with the accuracies in the range of 50% or so. It may be noted that the IST level density option reproduced the measured (n,2n) and (n,3n) crosssection data within 10% over a wide energy range of investigation. Based on this analysis, it may be concluded that the IST level density option represents the measured data better in these heavy nuclides.

Fig.3 depicts the total production cross-sections for neutrons, protons, alpha-particles and gamma-rays computed with the IST level density option for Pb-208 and Bi-209. It is noted that the total neutron emission cross-sections in both these nuclides are identical over the entire energy range. Proton and alpha emission cross-sections of Bi-209 are, however, higher than those of Pb-208 but their absolute magnitudes (<100 mb) are too low to play any significant role in nuclear safety or shielding considerations of fusion systems. Gamma emission cross-sections of Pb-208 are higher than those of Bi-209 over most of the investigated energy range and their magnitudes are high, of the order of

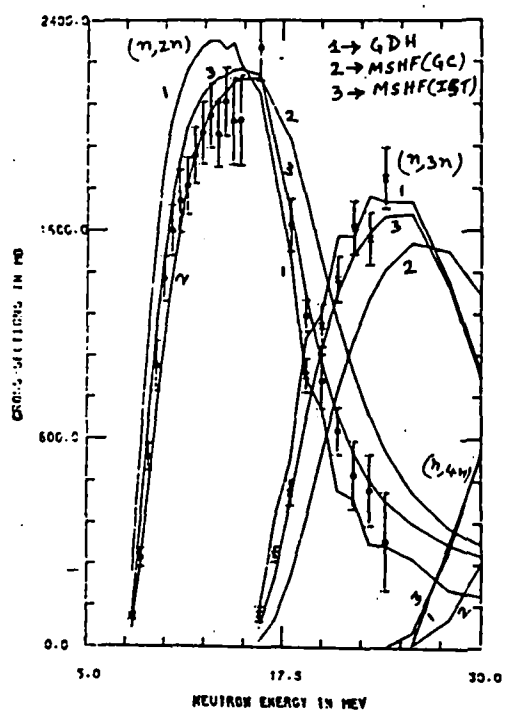

Fig.1 Neutron Emission X-Sections of Bi- 209 with IST and GC level densities.

several thousand millibarns. This aspect may be important in gamma transport and shielding evaluations. On this count, Bi-209 appears to be superior to Pb-208 for application in fusion blankets.

No explicit discussion of (n,n') reaction has been made in the text of this paper.It may, however, be mentioned that above the neutron incident energy of 14 MeV, both the GC and IST options yield similar data for (n,n') reaction ; but below 14 MeV, IST and GC predictions

differ - range varying upto 25%.

REFERENCES

1.W. Hauser and H. Feshbach : Phys. Rev. 87, 366 (1952) 2.C. Kalbach : Z. Phys. A283, 319 (1977) 3.D.M. Brink : Thesis, Oxford University (1955), P. Axel : Phys. Rev. 126, 671 (1972) 4.M. Blann and H.K. Vonach : Phys. Rev. C28, 1475 (1983) 5.A. Gilbert and A.G.W. Cameron:Can. J. Phys. 43, 1446 (1965) 6.U.E. Facchini and E. Saetta-Menichla Energy.Nucl.15,54 (1968) 7.A.V. Ignatyuk, G.N. Smirenkin and A.S. Tishin :Sov. J. Nucl. Phys. 21, 255 (1975) 8.J.L. Cook, H. Ferguson and A.R. Musgrove : Aust. J. Phys.20, 477 (1967) 9.F.C. Williams : Nucl. Phys. A116, 231 (1971) 10.V.F. Weisskopf and D.H. Ewing : Phys. Rev. 57, 472 (1940) 11.M.Blann and J. Bisplinghoff : Report UCID - 19614 (1982) 12.O. Bersillon : Report CEA-N-2227 (1981) 13.P.G. Young and E.D. Arthur : Reports LA-6947 (1977), LA-UR-88-382 (1988) 14.M.Blann : Private Communication (1991) 15.T.S. Cheema and R.W. Finlay : Nucl. Phys. A443, 249 (1985) 16.O. Bersillon : Report NEANDC-222U (1986) 17.F.G. Perey : Phys. Rev. 131,745 (1963) 18.J.R. Huizenga and G. Igo; Nucl. Phys. 29, 462 (1962) 19.S.F. Mughabghab and D.I. Garber: Report BNL-325 Vol.I (1973) 20.S.S. Dietrich and B.L. Berman : At. and Nucl. Data Tables,38,199(1988)21.J. Frehaut, A. Bertin, R. Bois and J. Jary : Report BNL-NCS-51245 Vol.I, 399 (1980) 22.L.R. Veeser, E.D. Arthur and P.G. Young : Phys. Rev. C16, 1792 (1977)

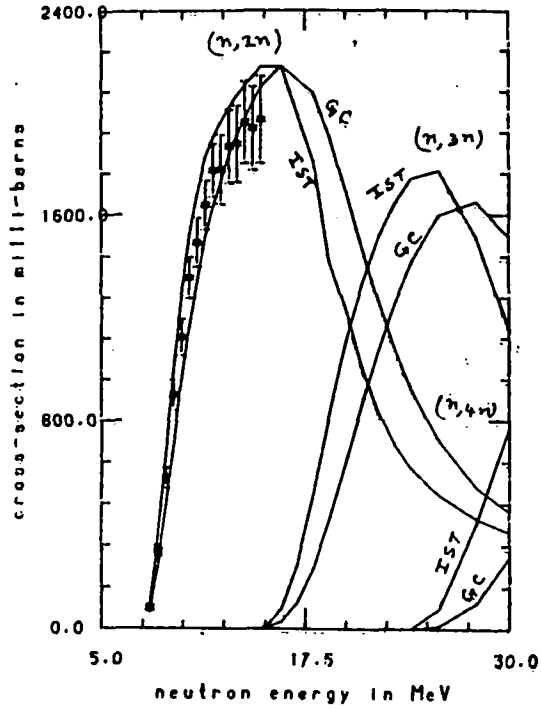

Fig.2 (n,2n),(n,3n),(n,4n) X-Sections of Pb-208 with IST and GC level densities.

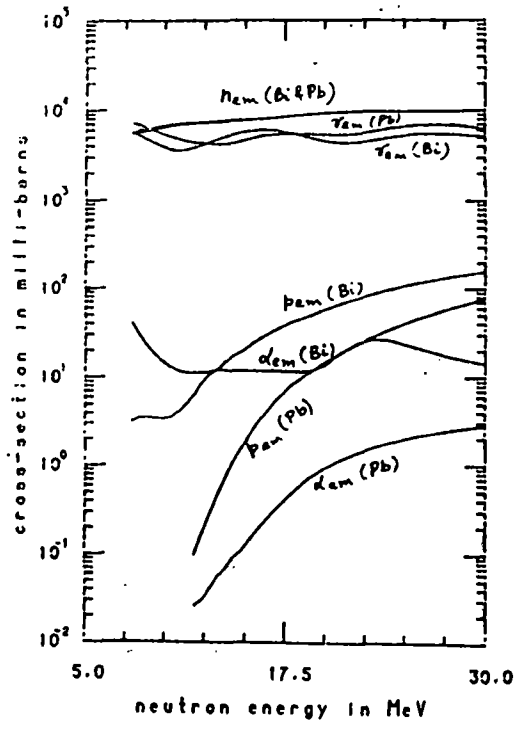

Fig.3 Particle Emission X-Sections with IST and GC level density options.

NUCLEAR LEVEL DENSITY EFFECTS ON THE EVALUATED CROSS-SECTIONS OF NICKEL ISOTOPES

S.B. Garg
Neutron Physics Division
Bhabha Atomic Research Centre
Trombay, Bombay - 400085, India

ABSTRACT

A detailed investigation has been made to estimate the effect of various level density options on the computed neutron induced reaction cross-sections of Ni-58 and Ni-60 covering the energy range 5-25 MeV in the framework of the multistep Hauser-Feshbach statistical model scheme which accounts for the pre-equilibrium decay according to the Kalbach exciton model and gamma-ray competition according to the giant dipole radiation model of Brink and Axel. Various level density options considered in this paper are based on the Original Gilbert-Cameron, Improved Gilbert-Cameron, Back-Shifted Fermi gas and the Ignatyuk-Smirenkin-Tishin approaches. The effect of these different level density prescriptions is brought out with special reference to (n,p), (n,2n), (n,α) and total production cross-sections for neutron, hydrogen, helium and gamma-rays which are of technological importance for fission and fusion based reactor systems.

I. INTRODUCTION

It is well known that nuclear level density plays a vital role in determining the neutron nuclear reaction cross-sections of a given nuclide. In this paper, a detailed study has been carried out to investigate the effect of the various level density options on the neutron induced interaction cross-sections of Ni-58 and Ni-60 in the energy range of 5-25 MeV. The following four level density prescriptions have been examined :

i)Original Gilbert-Cameron Recipe (OGC) /1/, ii) Improved Gilbert-Cameron Recipe (IGC) /2/, iii) Back-shifted Fermi Gas Recipe (BSFG) /3/ and iv) Ignatyuk-Smirenkin-Tishin Recipe (IST) /4/.

The study has been conducted in the framework of the multistep Hauser-Feshbach statistical model scheme /5/ which includes Kalbach-exciton model /6/ to allow for the pre-equilibrium emission and the Brink-Axel giant dipole radiation model /7/ to facilitate gamma - decay competition of the reaction. The effect of these various level density options is demonstrated by considering (n,p), (n,α), (n,2n) and total neutron, hydrogen, helium and gamma-ray production cross sections of Ni 58 and Ni 60 which are the constituents of stainless steel, frequently used as a structural material in fission and fusion based reactor systems.Pairing and shell energy corrections are taken from Cook et al/8/ and in the case of the back-shifted Fermi gas recipe level density and energy correction parameters are taken from Ivascu et al /9/.

II. DATA COMPUTATION

Cross-sections have been computed in the framework of the multistep Hauser - Feshbach statistical theory as already stated with the emission competition of neutron, proton alpha - particle and gamma-rays included at every stage of the compound reaction mechanism where as in the pre- equilibrium stage only particle emission is included and gamma-ray competition is excluded. Transmission coefficients for neutrons are calculated with the optical model potential parameters of Prince /10/; for protons with the potential parameters of Mani /11/ and for alpha-particles with the parameters of Strohmaier et al /12/. Gamma-ray transmission coefficients are determined from the S-wave gamma-ray strength function with the dipole resonance parameters of Reffo /13/. Energy, spin, parity and gamma-ray branching ratios of the discrete levels of all the nuclides taking part in the reaction decay chains are taken into account. In the pre-equilibrium process, internal transition rates to the various exciton states are determined in terms of the average two body interaction matrix element as defined by Kalbach /14/. The exciton state densities are calculated

according to the Williams' formulation /15/. The K-parameter of the average reaction matrix element has been extracted as 135 (MeV) cubed in this analysis by matching the calculated and measured neutron emission spectrum at 14.1 MeV for Ni-58 by Garg /16,17/. The same value has been adopted for Ni-60. The computations are performed with GNASH Code /18/.

III. RESULTS

(i) (n,p) Cross-sections : Fig.1 represents these cross-sections. In the case of Ni-58, OGC and IGC recipes yield similar results up to 12 MeV. IST and BSFG predictions are, however, lower; variations being ~20%. Above 12 MeV all the four recipes predict data within 15% of one-another. In the case of Ni-60, IGC and IST results are similar upto 10 MeV; BSFG and OGC predicts vary from 15% to factors of 2 or 3. Above 10 MeV all the four results are within 15%. In both the cases the experimental data are represented well by IGC, IST and OGC recipes.
(ii) (n,α) Cross-sections : These data are depicted in Fig.2. In the case of Ni-58, BSFG data are lower than other predictions by factors of 2 or more upto 12 MeV. Above this energy the data prediction is quite close at several energy points although deviations upto 30% are also noted among the different sets of data. It is also noted that IST, IGC and OGC reproduce experimental data within the given uncertainties. In the case of Ni-60, BSFG data are again low by a factor of 2 upto 10 MeV. Between 10 and 16 MeV, deviations vary upto 25% and above 16 MeV, deviations upto 50% are noted among the different sets of data.

No explicit discussion has been made in the text for (n,2n) and the total production cross-sections of neutron,hydrogen,helium or gamma-rays because of space limitation. However,some comments have been made about these entities in the following conclusions.

IV. CONCLUSIONS

The following conclusions are drawn:

(a) Total neutron production cross-sections given by the four level density prescriptions are within 10% and (n,2n) cross-sections are within 30% for both the nuclides, Ni-58 and Ni-60.

(b) (n,p) and hydrogen production cross-sections are not well represented by BSFG recipe upto about 10 MeV. Above this energy the various predictions are within 20% of one another.

(c) (n,α) and total helium production cross-sections are adversely affected in the BSFG option as they show deviations by factors of 2 to 4 in the case of Ni-60 and by about 50% in the case of Ni-58. IGC, IST and OGC data also show deviations.

(d) Gamma-ray production cross-sections in all the cases are acceptable since the variations are within 30%.

(e) IST, IGC and OGC generated data for several of the reactions investigated in this paper are close or within about 30% of one-another. Any one of these options can thus be used for data prediction. Since the IST option accounts for the energy dependence of the 'a' parameter and the effect of shell closures, it may be taken as a preferred option in the nuclear data evaluations.

(f) Better systematics for level density and energy shift parameters are desired for the BSFG option.

REFERENCES

1. A. Gilbert and A.G.W. Cameron : Can. J. Phys. 43,1446 (1965) 2.U.E.Facchini and E.Saetta-Menichla : Energ. Nucl.15,54(1968) 3.W. Dilg, W. Schantl, H. Vonach and M. Uhl : Nucl. Phys. A 217, 269 (1971) 4.A.V. Ignatyuk, G.N. Smirenkin and A.S. Tishin : Sov. J. Nucl. Phys. 21, 255 (1975)5. W. Hauser and H. Feshbach : Phys. Rev. 87, 366 (1952) 6. C. Kalbach : Z. Phys. A283, 319 (1977) 7.D.M. Brink : Thesis, Oxford University (1955); P. Axel : Phys. Rev. 126, 671(1972) 8.J.L. Cook, H. Ferguson and A.R. Musgrove : Aust. J. Phys. 20, 477 (1967) 9.M. Ivaseu, V.

Avrigeanu and M. Averigeanu : Rev. Roum. Phys. 32, 697 (1987) 10.A. Prince : Int. Conf. Nucl. Data for Sci. & Technol., Antwerp, 574 (1983) 11.G.S. Mani : Nucl. Phys. A165, 225 (1977) 12.B. Strohmaier, M. Uhl and W. Reiter : Paper presented at the IAEA Advisory Group Meeting on Nuclear Data for Radiation Damage Assessment and Related Safety Aspects, Vienna, 12-16 October, 1981 13.G. Reffo : Particle and Gamma-ray Spectra Calculations in Structural Material, Paper presented at the IAEA Advisory Group Meeting on Structural Material, Vienna, November 2-4, 1983 14.C. Kalbach : Z. Phys. A287, 319 (1978) 15.F.C. Williams : Nucl. Phys. A116, 231 (1971) 16.S.B. Garg : Investigation of Neutron Induced Reaction Cross-sections of Ni-58 and Ni-60 with various Nuclear Model Evaluation Schemes, Paper Presented at the IAEA Research Co-ordination Meeting, Vienna, June 20-22 (1990) 17.S.B. Garg : Effect of Different Level Density Prescriptions on the Calculated Neutron-Nuclear Reaction Cross-sections, Paper presented at the IAEA Research Co-ordination Meeting, Vienna, June 20-22 (1990) 18. E.D. Arthur : The GNASH Pre-equilibrium Statistical Model Code, Los Alamos National Laboratory Manuscript LA-UR-88-382 (1988); P.G. Young and E.D. Arthur : Los Alamos National Laboratory Report LA-6947 (1977)

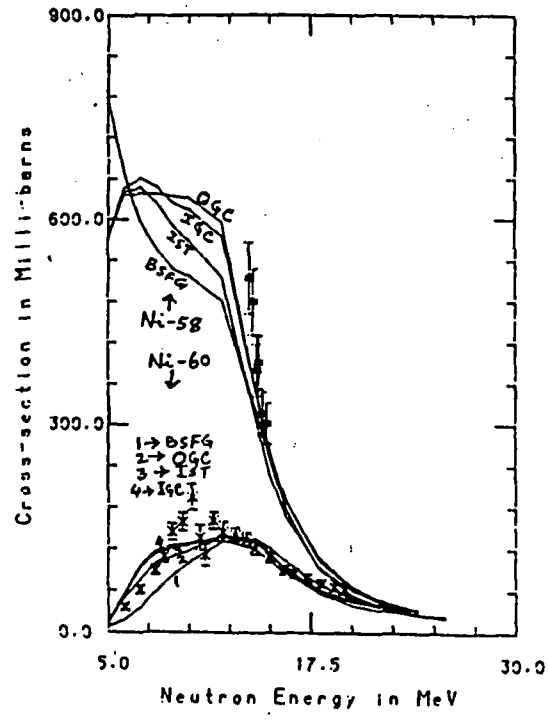

Fig.1 (n,p) X-sections with different level density options.

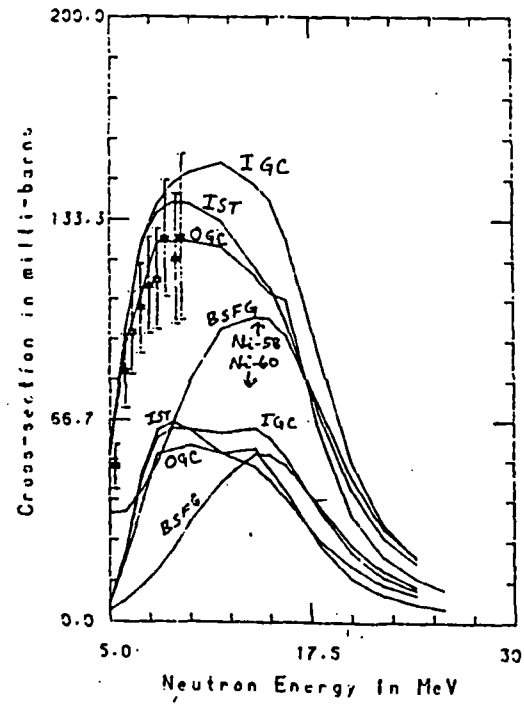

Fig.2 (n,alpha) X-Sections with different level density options.

REPORT ON FIRST CRP MEETING ON "DEVELOPMENT OF REFERENCE INPUT PARAMETER LIBRARY FOR NUCLEAR MODEL CALCULATIONS OF NUCLEAR DATA" SPONSORED BY IAEA AND HELD AT CERVIA, ITALY DURING SEPT. 19-23 , 1994.

Summary by S.B.Garg
Neutron Physics Division

The first Co-ordinated Research Programme Meeting on "Development of Reference Input Parameter Library for Nuclear Model Calculations of Nuclear Data" was held at Grand Hotel, Cervia (Italy) during Sept. 19-23, 1994. The Meeting was inaugurated by Dr. G.Reffo of ENEA, Bologna (Italy) and was attended by nine participants from eight countries including Italy , Russia , USA , Austria, Japan, China, Hungary and India. Besides these participants there were three observers, two from Italy and one from China. The International Atomic Energy Agency was represented by the Research Programme Co-Ordinator.

The main motivation to hold this Meeting was to recognize that nuclear reaction models have reached considerable degree of reliability and that these models can be utilized to produce a variety of nuclear cross-section data for application in reactor and other allied scientific technologies. It is also recognized that all required cross-section data cannot be generated through measurements because of vanishing resources and complexity of measuring techniques. In such circumstances nuclear models can be advantageously employed to estimate the required cross-section data. However, complete reliability of the computed data is dependent on the basic input parameters and this Meeting was primarily concerned with the basic input data which are broadly categorized into the following six segments:

1. Atomic masses, shell corrections and deformations
2. Discrete level schemes
3. Average resonance parameters
4. Optical model potential parameters
5. Level density parameters and
6. Gamma-ray strength functions

Papers on all these topics were presented at this Meeting and it was decided that the participants would transmit their data to the International Atomic Energy Agency according to a time bound programme . These basic parameter data would then be analysed and compiled in a starter file for use. Responsibility was also fixed for the various segments. It was agreed that BARC and Los Alamos National Laboratory, USA would critically examine the optical model potential parameters and make their recommendation over the period of next three years. During this period close collaboration between BARC and LANL is foreseen.

BARC Contribution to the First CRP Meeting: The following paper was presented at the First CRP Meeting;

OPTICAL MODEL AND LEVEL DENSITY PARAMETERS FOR NUCLEAR DATA EVALUATION

Optical model potential parameters based on spherical and deformed models were compiled and analysis of measured data was carried out in several cases using these parameters. Level density parameters based on Fermi gas and Back-shifted Fermi gas models were compiled for a large number of nuclides of interest in basic and applied research together with the pairing and energy shell corrections. Level density parameters were also derived using the super-fluid model of the nucleus for a large number of elements in the mass range 40 t0 250. In these derivations shell energy corrections were estimated with the liquid drop model of Myers and Swiatecki by including the pairing energy corrections of Cook et al and using the recent s-wave resonance spacings taken from literature.

Level density parameters evaluated with the Gilbert-Cameron formulation in the cross-section analysis of several nuclides carried out at BARC were also compiled. All these data have been transmitted to IAEA as the initial BARC contribution.

In the second phase of the IAEA Research Contract optical model potential parameters given by various participants of the Research Contract would be re-cast in the SCAT-2 format in collaboration with Dr.P.G.Young of Los Alamos National Laboratory ,U.S.A and a starter file would be created for global use. These parameters would be tested in certain representative cases.Optical model potential parameters proposed to be compiled and analysed would deal with neutron, proton , deuteron , triton , helium-3 , and alpha particles.

Participants

1. **Dr. S.B.Garg**
2. **Dr. Ashok Kumar**

A 75 GROUP NEUTRON-PHOTON COUPLED CROSS-SECTION LIBRARY WITH P5-ANISOTROPIC SCATTERING MATRICES

S.B.Garg
Neutron Physics Division
Bhabha Atomic Research Centre
Trombay , Bombay - 400 085.

1. **INTRODUCTION:** In the past we had developed 27 group and 35 group neutron cross-section libraries /1 , 2/ and 25 group and 100 group photon interaction cross-section sets for application in reactor and shielding technologies. However , recently an accute need was felt by the users' community for a multigroup neutron - photon coupled cross-section library so that the transport of neutrons and photons might be simultaneously investigated in reactor assemblies , shields and other media of scientific applications. Such a library is also needed for oil logging and mineral exploration studies. In order to meet these requirements a 75 group neutron-photon has been developed using the basic cross-section files ENDF/B-IV /3/ for neutrons and DLC-7F /4/ for photons. This library comprises 50 neutron groups and 25 gamma energy groups and contains 42 nuclides of direct interest in reactor technology. P5 - anisotropic scattering matrices are generated in order to treat well the anisotropic behaviour of the scattered neutrons and photons.

Requisite computer codes have been developed and updated for the inhouse computer to generate multigroup neutron cross-sections ; photon interaction cross-sections ; and gamma-ray production cross-sections via neutron interactions. Selection of group energy structure has been carefully done so that all vital aspects of the various physical processes are well represented and the number of energy groups remains manageable even for small computing machines.

2. **COMPUTER CODES:** The following computer codes have been extensively modified and utilized in the production runs of the data on inhouse computer:

i. **XLACS-IIA CODE /5/:** This code processes neutron resonances and generates multigroup cross-sections for all the neutron induced reactions together with the anisotropic scattering matrices of any order.

ii. **LAPHNGAS CODE /6/:** This code generates multigroup gamma-ray production cross-sections due to neutron interactions.

iii. **SMUG CODE /7/:** This code produces multigroup photon interaction cross-sections and the anisotropic scattering matrices of any order utilizing basic DLC-7F cross-section file.

iv. **CHOX CODE /8/:** This code combines multigroup neutron, gamma-ray production and photon interaction cross-section libraries to produce a coupled master file by suitably arranging and merging the various types of reaction cross-sections.

v. **NITAWL CODE /9/:** This code makes use of the master file to yield the desired neutron-photon coupled cross-section library for the simultaneous transport of neutrons and photons.

3. **NUCLIDES INCLUDED:** The following 42 nuclides are included in this library:

H-2, He-3, He-4, Li-6, Li-7, Be-9, B-10, B-11, C, N, O, Na, Mg, Al, Si, K, Ca, V, Cr, Mn, Fe, Co, Ni, Cu, Nb, Mo, Pb, Th, Pa-233, u-233, U-234, U-235, U-236, U-238, Pu-238, Pu-239, Pu-240, Pu-241, Pu-242, Am-241, Am-243, and Cm-244.

4. **REFERENCES:**

1) S.B.Garg ; Multigroup Resonance Self - Shielding Factors and Cross-sections of Main Reactor Elements, Report BARC-1002 (1979)

2) S.B.Garg and Amar Sinha ; BARC 35 - A 35 Group Cross-section Library with P3 - Anisotropic Scattering Matrices and Resonance Self - Shielding Factors, Report BARC-1222 (1984).

3) D.Garber, C.Dunford, and S.Pearlstein ; Data Formats and Procedures for the Evaluated Nuclear Data File , ENDF ,Report BNL-NCS-50496 (ENDF-102) (1975).

4) DLC-7F ; Evaluated Photon Interaction Library in ENDF Format , Radiation Shielding Information Centre, Oak Ridge National Laboratory , USA.

5) G.S.Robson ; XLACS-IIA : A Modified Version of XLACS-II for Processing ENDF Data into Multigroup Neutron Cross-sections in AMPX Master Library Format , RSIC Informal Memo (1981) , PSR-182 (1982).

6) W.E.Ford III and J.L.Lucius ; LAPHNGAS : Ampx Module for Generating Multigroup Secondary Gamma-Ray Production Cross-sections , Report ORNL PSR-63 (1978).

7) J.L.Lucius and W.E.Ford III ; SMUG : An AMPX Module for Generating Multigroup Photon Cross-sections , Report ORNL PSR-63 (1978).

8) N.M.Greene and J.E.White ; CHOX : The AMPX Module for Cross-section Interface Manipulation , Report ORNL PSR-117 (1978).

9) L.M.Petrie et al ; NITAWL : AMPX Module for Resonance Self-Shielding and Working Library Production , Report ORNL PSR-117 (1978).

Validation of Nuclear Data for Heavy Water Reactor Lattices Using WIMS and WIMKAL-80 Nuclear Data Libraries

P.D. Krishnani
Th.P.D., 5 th Floor, Central Complex
Bhabha Atomic Research Centre
Trombay, Bombay - 400 085
India

Introduction

Integral measurements of various types provide valuable data to assess the adequacy of the cross sections used in predicting the nuclear characeristics of reactors. In this context measurements of reactivity, relative reaction rates and neutron balance assume fundamental importance. We have analysed [1] these parameters for heavy water moderated systems by using WIMS and WIMKAL-80 cross section libraries both of which have 69 energy groups. The analysis has been carried out by the lattice analysis code CLUB [2-4]. It employs a method based on combination of interface current formalism and collision probability (CP) method.

Cross Section Libraries Used

The WIMS library is a 69-group library with 14 fast groups (10 Mev $\leq$ E $\leq$ 9.118 kev), 13 resonance groups (9.118 kev $\leq$ E $\leq$ 4.0 ev) and 42 thermal groups (4.0 $\leq$ E $\leq$ 0.0 ev). This library has been derived from UK Nuclear Data Library. There are tables for few resonance materials like U-235, U-238, Pu-239 etc. which give resonance integrals as a function of effective potential cross section and temperatures for the resonance groups. In the following analyses, resonance tables 235.4 and 2238.5 or 2238.4 (WIMS notation for identifying resonance tables) were used for U-235 and U-238, respectively.

The fission spectrum available in the WIMS library is based on measurements of Doner which may be approximated by a Maxwellian spectrum with kT value of 1.3 Mev. Subsequently, it was replaced with a harder spectrum of kT value of 1.43 Mev. In the following analysis, we have used both the fission spectra.

The WIMKAL-80 library [5] is the 1980 version of WIMS KAERI library. The energy group structure of this library is same as in the WIMS library. It consists of multigroup cross sections for 130 materials generated for thermal reactor applications using the NJOY nuclear data processing system [6]. Most of the evaluated nuclear data were taken from the ENDF/B-V or IV, but some data, not available from the reduced ENDF/B files, were taken from the JENDL-2 (Rev-1) and ENDL-84.

Fission spectra of U-235 were generated from Watt spectrum data of ENDF/B-V. Most actinides have the self-shielded resonance integral data/tables given as a function of temperature and background cross sections. The capture and fission cross sections of U-238 and Th-232 were processed from ENDF/B-V data.

Results

We have analysed three sets of experiments done in Canada with 7-, 19- and 28-rod fuel clusters with heavy water, and air coolants. The following parameters are compared :

Keff - effective multiplication factor
δ - ratio of U-238 fissions to U-235 fissions
γ - ratio of captures in U-238 to absorptions in U-235

In addition to the above parameters, we have also compared the various neutron density ratios.

Table 1 gives average Keff and its standard deviation for various experiments. It can be seen from this table that the Keff increases by approximately 2-3 mk when harder fission spectrum is used. Further, the Keff is underpredicted with the resonance table 2238.5 and that the Keff is closer to unity for resonance table 2238.4. However, there is a reduction of trend in Keff with lattice pitch with the resonance data of 2238.5. The Keff is on the average overpredicted with WIMKAL-88 library and the overprediction is of the order of 0.5 %.

It was seen [1] that there was an improvement in the fast fission ratio when the fission spectrum with kT=1.43 Mev is used. They are usually unerpredicted by both the libraries and the error can be of the order of 10 % in some of the cases. It was also seen that the error in the initial conversion ratio (γ) was of the same order of (1-2 %) in both the libraries which can be considered satisfactory. However, they are usually underpredicted.

After this, we analysed neutron density measurements for 7-, 19- and 28-rod fuel clusters. It was observed that the results of calculations were within experimental error by both the libraries.

Conclusions

In conclusion, it can be stated that it is appropriate to consider an harder fission spectrum in the WIMS library. The Keff is better predicted with 2238.4 resonance data. However, there is a definite trend in Keff with lattice pitch which indicates a systematic error. On the other hand, the Korean library WIMKAL-88 overpredicts the Keff and the overprediction is of the order of 0.5 %. There is no perceptible difference in the prediction of other reaction rates and neutron density ratios for the two libraries.

REFERENCES

[1] P.D. Krishnani, "Validation of Nuclear Data for Heavy Water Reactor Lattices Using WIMS and WIMKAL-88 Nuclear Data Libraries", Note No. ThPD/426, 1994.

[2] P.D. Krishnani and K.R. Srinivasan, Nucl. Sci. Engg. 78, 97 (1981).

[3] P.D. Krishnani, Ann. nucl. Energy, 9, 255 (1982).

[4] P.D. Krishnani, Ann. nucl. Energy, 9, 207 (1982).

[5] Jung-Do Kim, "WIMKAL-88 The 1988 Version of WIMS-KAERI Library", Korea Atomic Energy Research Institute, 1990.

[6] R.E. McFarlane et al., "The NJOY Nuclear Data Processing System", LA-9303-M, 1982.

Table 10
Average Keff and its Standard Deviation from the Mean
For All the Experiments

Fuel Cluster/ Coolant		WIMS 2230.4 kT=1.30 Mev	WIMS 2230.4 kT=1.43 Mev	WIMS 2230.5 kT=1.30 Mev	WIMS 2230.5 kT=1.43 Mev	WIMKAL
7-Rod D_2O	Keff	0.9981	1.0005	0.9934	0.9958	1.0037
	Std	±0.0037	±0.0037	±0.0020	±0.0020	±0.0006
7-Rod Air	Keff	0.9971	0.9995	0.9923	0.9948	1.0022
	Std	±0.0024	±0.0024	±0.0014	±0.0013	±0.0029
19-Rod D_2O	Keff	0.9973	0.9997	0.9929	0.9953	1.0019
	Std	±0.0019	±0.0009	±0.0011	±0.0001	±0.0025
19-Rod Air$	Keff	0.9990	1.0012	0.9952	0.9975	1.0042
	Std	±0.0030	±0.0031	±0.0015	±0.0015	±0.0009
28-Rod D_2O	Keff	0.9998	1.0024	0.9956	0.9982	1.0054
	Std	±0.0019	±0.0019	±0.0010	±0.0010	±0.0009
28-Rod Air	Keff	1.0006	1.0032	0.9966	0.9992	1.0056
	Std	±0.0025	±0.0024	±0.0015	±0.0015	±0.0020

$ Case of Pitch=18 cm has not been considered for calculating Mean Keff (Keff) and its standard deviation (Std) for this case

USE OF HAUSER-V CODE FOR NUCLEAR DATA EVALUATION

H.M. JAIN
Reactor Physics & Nuclear Engineering Section
Reactor Services & Maintenance Division
Bhabha Atomic Research Centre
Bombay - 400 085
India

This Statistical (HAUSER-FESHBACH Theory) optical model based code was used for calculating the fission cross sections for ^{239}Pu and ^{241}Am as a part of International Code Intercomparison exercise. The results submitted are compared with other eight different contributions and has been published in the following report compiled by H. Derrien of OECD, Nuclear Energy Agency, France.

"Results of an International Code Intercomparison for Fission Cross Section Calculations" by H. Derrien, NEA/P&T Report No.8, NEA/NSC/DOC(94)6, February, 1994.

This code has been modified for further work on nuclear data evaluations to calculate the total cross section also. This code use the Gilbert-Cameron constant temperature at low energy and the Fermi-gas model at higher energy (or the back-shifted Fermi-gas model) for calculation of level density of the nuclei at high excitation energies where there are many energy levels. For fission channel density, it uses the enhancement factor for level density calculation. In our fission cross section calculations for the exercise, the enhancement factors are adjusted in order to reproduce the experimental values of the fission cross section. Presently, the work is continued for these enhancement factors f_k and level density parameters a.

U-233 PRODUCTION IN A THORIA-AND-WATER MULTILAYERED ASSEMBLY USING A 14-MeV NEUTRON SOURCE#

D.V.S. Ramakrishna, V.R.Nargundkar and O.P. Joneja*
Neutron Physics Division, Bhabha Atomic Research Centre, Bombay
* Institut de Genie Atomique, EPFL, Lausanne, Switzerland

A programme to study the neutronics of various fusion blanket assemblies was initiated at B.A.R.C. using 14 MeV (d,t) neutrons obtained from an indigenously built 150 KeV accelerator. The objective is to carry out systematic studies of the fusion blanket systems containing lithium and thorium and evolve a conceptual hybrid blanket design.

In the first set of experiments to measure U-233 breeding, thorium oxide rods were arranged in a multilayered configuration consisting of alternate layers of ThO2 and water. ThO2 rods were made out of 1.054 cm dia ThO2 pellets stacked in a 1.26 cm dia Al clad tube with an active length of 55.0 cm and 2.5 cm top and bottom Al plugs.The average weight of ThO2 in each rod was 455.5 g. The blanket assembly consisted of ThO2 rods arranged in a rectangular geometry in two Al tanks filled with water as shown in Fig.1. The tank was 70 cm high, 60 cm wide and 50 cm long. The water tanks were placed symmetrically on either side of the 14 MeV (d,t) neutron source with a separation of 15 cm to accommodate the target tube. Each tank had 7 rows of rods, each row consisting of 45 rods touching each other. The gap between the two rows was 1.3 cm. Thus there were alternate layers of ThO2 and water forming a multilayer configuration. The height of the water column in the tank was adjusted so that there was an effective 5 cm top water reflector. The tanks were placed on a 30 cm polypropylene block to form the bottom reflector.

Thorium Nitrate powder packed in perspex containers of size 24 mm dia and 5 mm depth were used as probes. 7 such probes were placed at the centre of each layer touching ThO2 rods for radial distribution measurement of U-233 production rate. In the second experiment 9 probes were symmetrically placed in central region of the second layer of ThO2 covering 15cmX15cm area for the integral measurement. The irradiation was carried out for 6 hrs and the induced activities of the probes were measured by counting 312 keV gammas of Pa-233 using a 45 cc HPGe detector. The profile of the radial distribution of U-233 production rate is shown in Fig.2. The measured U-233 production rate of all the Thoria rods in 15cmX15cm area was found to be (9.40±2.0)E-03 as compared to the predicted value of (9.01±1.3)E-03 obtained from MCNP calculation using BMCCS2 cross section library.

Paper published in Fusion Technology, V01 23 (419) 1993.

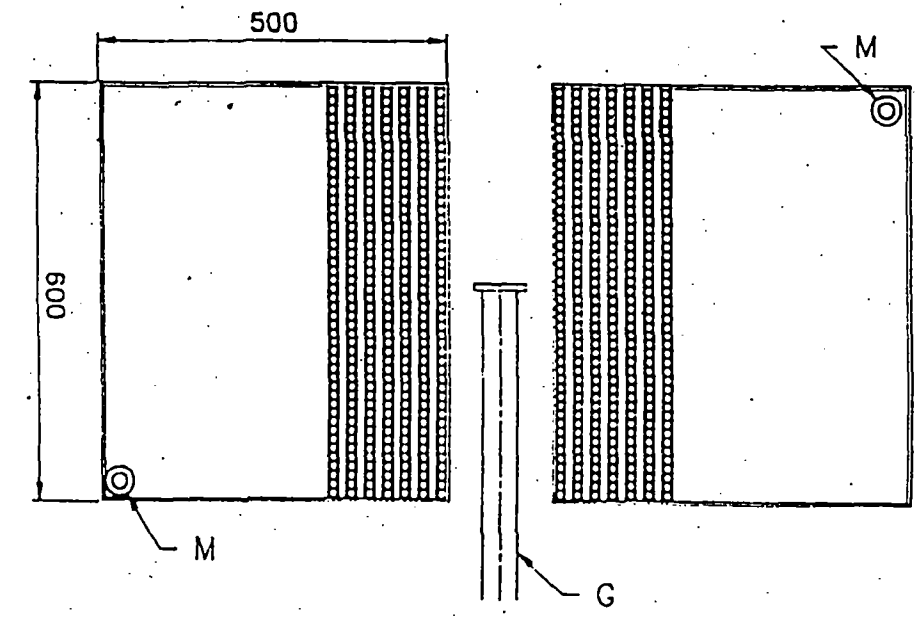

FIG. 1:—EXPERIMENTAL ASSEMBLY
(Horizontal section)

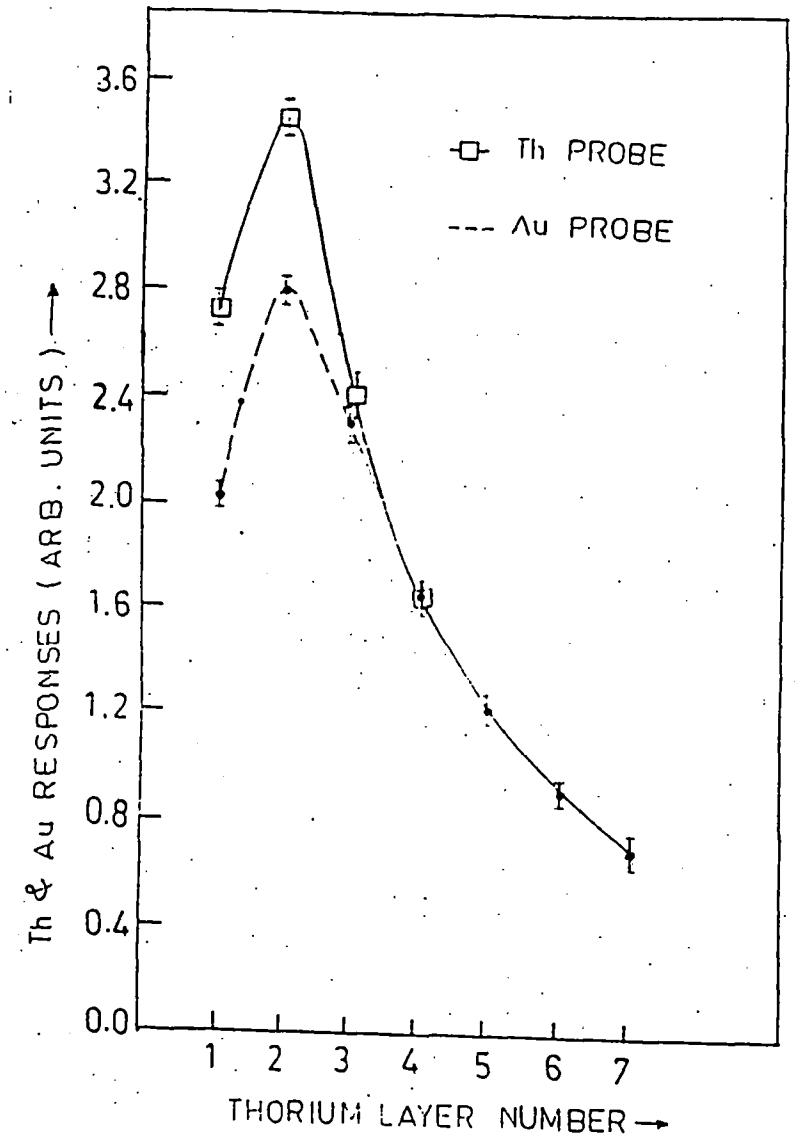

FIG. 2 REACTION RATE PROFILES FOR Th & Au IN THE BLANKET ASSEMBLY (EXPERIMENT)

INTEGRAL MEASUREMENTS FOR THE VALIDATION OF NEUTRON CROSS SECTION DATA IN FUSION BLANKET ASSEMBLIES CONTAINING THORIUM[#]

T.K.Basu, D.V.S.Ramakrishna, R.P.Anand, S.A.Hayashi[*]& C.Ichihara[**]
Neutron Physics Division, Bhabha Atomic Research Centre, Bombay
* Visiting Scientist from Rikkyo University, Yokosuka, Japan
** Visiting Scientist from KURRI, Kyoto University, Osaka, Japan

Activation studies were carried out in a ThO2 blanket assembly in a fusion neutron environment to check the validity of neutron cross section data. Reaction rate Measurements of various threshold detectors such as F(n,2n), Zr(n,2n), Nb(n,2n), Al(n,α), Fe(n,p), In(n,n'), Th(n,γ) and Au(n,γ) were carried out in a cylindrical ThO2 blanket assembly surrounding a 14 MeV (d,t) neutron source. The blanket consisted of 858 ThO2 rods made of 10.54 mm ThO2 pellets stacked in 12.6 mm Al clad tubes of active length of 55 cm and with 2.5 cm top and bottom Al-plugs. The rods were arranged in a hexagonal geometry consisting of 11 rings. A central hexagonal channel of height 8.36 cm was provided for inserting neutron generator tube. ThO2 rods were supported by hexagonal Al-rings only at two ends. Two channels of 3 mm thick Al were provided along the horizontal diagonal of the assembly; each channel can accommodate 11 demountable rods. Thorium oxide assembly was surrounded by 40 cm thick polypropylene reflector. Fig.1 shows the schematic view of the assembly.

Thin foils of the threshold detectors of 10 mm dia. were inserted at various axial and radial locations in between the ThO2 pellets of the demountable rods. The blanket assembly was irradiated with 14 MeV (d,t) neutrons for a period of 4 to 10 hrs. The induced gamma activities of the irradiated foils were measured using a high efficiency HPGe detector. The reaction rates were estimated using the photo peak areas of the characteristic gammas. The reaction rates for these materials were also calculated at different locations in the assembly using the Monte Carlo code MCNP with BMCCS2 cross section library. Figs. 2-6 show the calculated reaction rate distribution profiles in radial direction. The reaction rates are normalized with respect to the value at the first rod position. The normalized experimental points are also shown in the figures. As seen from the figures the normalized experimental points fall on the calculated profiles within the experimental uncertainties showing general agreement between experimental and calculated trends. Further evaluations are being done to establish the consistency by comparing the absolute reaction rates ratios of the threshold detectors having different neutron energy response.

Paper published in the Proc. International Conference on Nuclear Data for Science and Technol., Vol.2, 947, Gatlinburg, USA, 1994

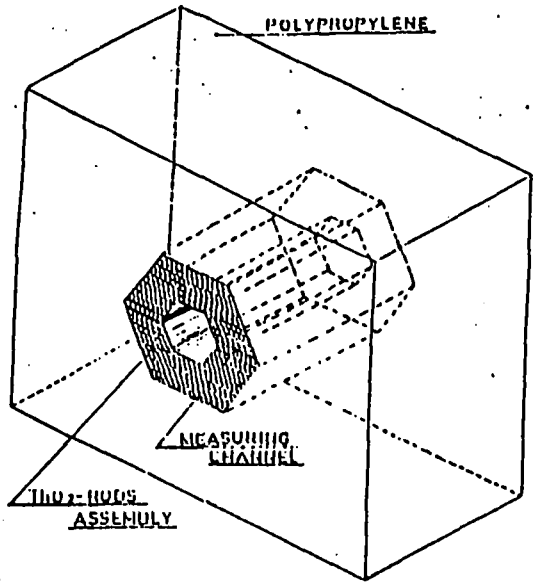

Fig.1 Schematic of the assembly

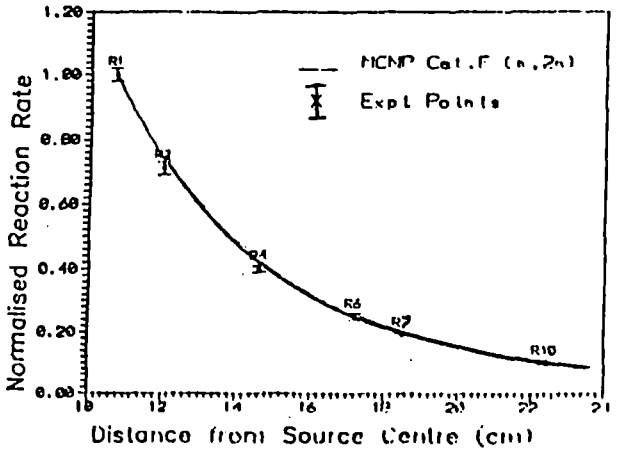

Fig.2 Radial distribution of F-19

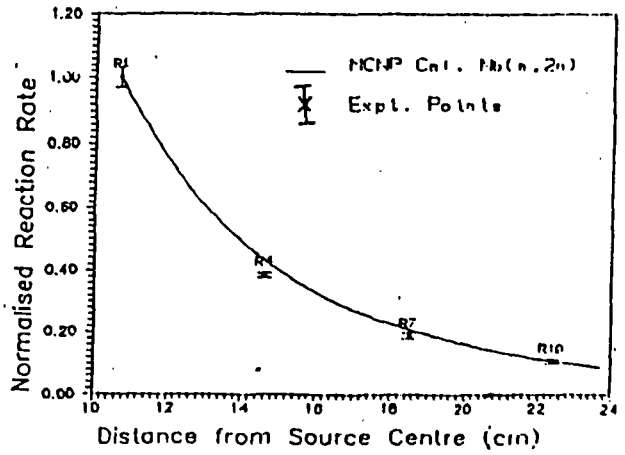

Fig.3 Radial distribution of Nb-93

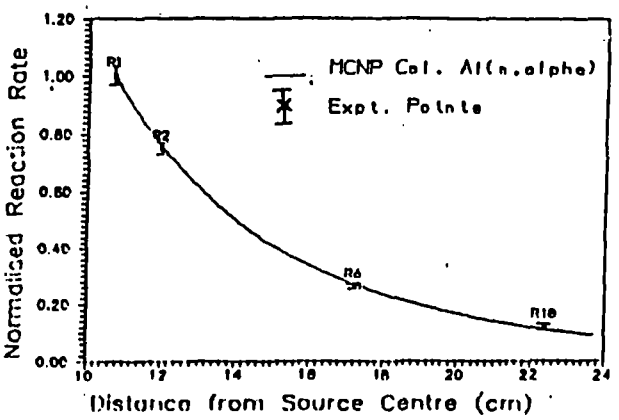

Fig.4 Radial distribution of Al-27

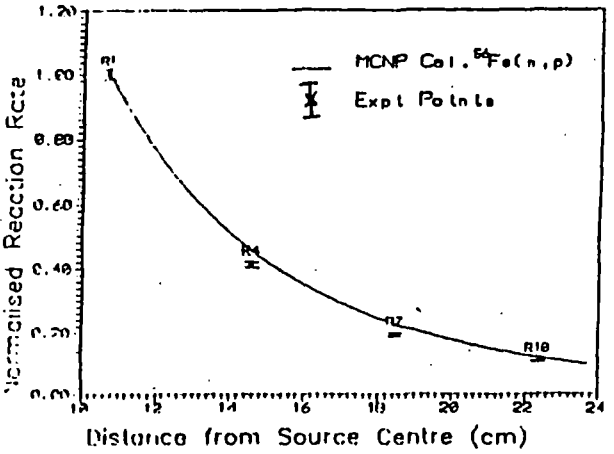

Fig.5 Radial distribution of Fe-56

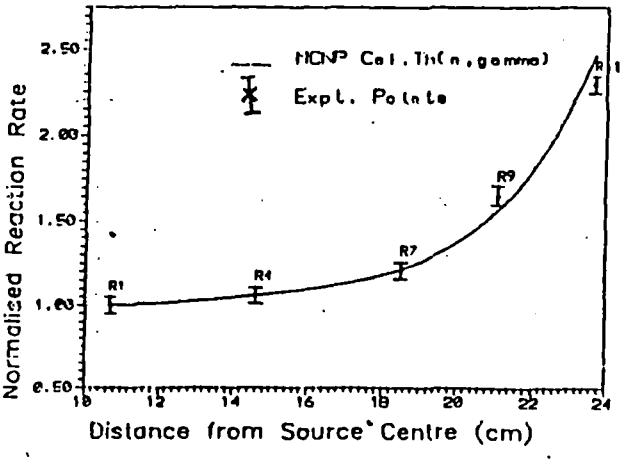

Fig.6 Radial distribution of Th-232

U-233 BREEDING MEASUREMENTS IN THORIUM OXIDE BLANKET ASSEMBLY USING A (D,T) ACCELERATOR NEUTRON SOURCE

D.V.S. Ramakrishna, R.P. Anand and T.K. Basu
Neutron Physics Division, Bhabha Atomic Research Centre, Bombay

Under the experimental programme to study the neutronics of fusion blanket systems, U-233 breeding measurements were carried out in a compact cylindrical thorium oxide assembly followed by polypropylene reflector.

The assembly was made by arranging 858 Aluminum clad ThO2 rods of 60 cm length and 1.26 cm dia. in hexagonal geometry consisting of 11 rings. It had a central through hexagonal channel of height 8.36 cm to insert the beam tube containing Tritium target. The assembly was surrounded by polypropylene reflector as shown in Fig.1. In order to obtain the integral U-233 breeding in the assembly, 120 Thorium oxide probes (10 mm dia. and 1.5 mm thick) were inserted inside the rods made specifically for this purpose at different axial and radial locations in the assembly. The 14 MeV neutron yield was determined by the activation technique using Nb, Zr and Teflon(F) foils.

The irradiation was carried out for 25 hours spread over three days. 312 keV gammas emitted by Pa-233 produced in the probes due to neutron captures in thorium was measured using a high efficiency HPGe detector. The measured values in each rod were fitted with a third order polynomial to obtain axial distribution and thereby the total production rate in the rod. Similarly the values of the total production rates in the rods thus obtained were fitted to get the radial distribution and by integrating it, the total U-233 production rate was obtained in the entire assembly. The whole measurement was repeated to check the consistency. The two measured values were found to be 0.361 ± 0.02 and 0.367 ± 0.02 which are consistent with each other.

The total U-233 production rate in the assembly was also calculated using a 3-D MCNP code taking into account the exact geometry of the ThO2-blanket assembly, using the BMCCS2 cross section data set based on ENDF/B-IV library. Table 1 shows the measured and calculated values of U-233 production rates at various axial positions in different rings of the assembly normalized to the value at the central position (P6) of seventh ring (R7). It can be seen that the C/E ratios at most of the positions is very close to unity (within 5%) except for few positions. The total integral calculated value of U-233 production rate for the whole assembly was 0.347 ± 0.007 which is in very good agreement with the average measured value of 0.364 ± 0.02.

Table 1

Experimental and Calculated Normalized U-233 Production Rates
Normalised with respect to central probe (P6) of Ring 7(R7)

Rod No		P1	P2	P3	P4	P5	P6
Posn.		5 cm	10 cm	15 cm	20 cm	25 cm	30 cm
R1	E	0.277	0.400	0.496	0.693	0.718	0.836
	C	(0.266)	(0.421)	(0.521)	(0.685)	(0.768)	(0.806)
C/E		*0.96*	*1.05*	*1.05*	*0.99*	*1.07*	*0.96*
R4	E	0.263	0.437	0.596	0.705	0.817	0.861
	C	(0.271)	(0.441)	(0.568)	(0.762)	(0.865)	(0.834)
C/E		*1.03*	*1.01*	*0.95*	*1.08*	*1.06*	*0.97*
R7	E	0.291	0.524	0.674	0.842	0.974	1.000
	C	(0.279)	(0.478)	(0.673)	(0.883)	(0.986)	(1.000)
C/E		*0.96*	*0.91*	*1.00*	*1.05*	*1.01*	*1.00*
R9	E	0.425	0.703	0.959	1.184	1.324	1.327
	C	(0.353)	(0.603)	(0.840)	(1.040)	(1.221)	(1.279)
C/E		*0.83*	*0.86*	*0.88*	*0.88*	*0.90*	*0.96*
R10	E	0.497	0.759	1.030	1.341	1.526	1.594
	C	(0.430)	(0.740)	(1.024)	(1.259)	(1.471)	(1.511)
C/E		*0.87*	*0.97*	*0.99*	*0.94*	*0.96*	*0.95*
R11	E	0.693	1.044	1.388	1.662	1.844	1.922
	C	(0.540)	(0.986)	(1.387)	(1.660)	(1.926)	(1.995)
C/E		*0.78*	*0.94*	*1.00*	*1.00*	*1.04*	*1.04*

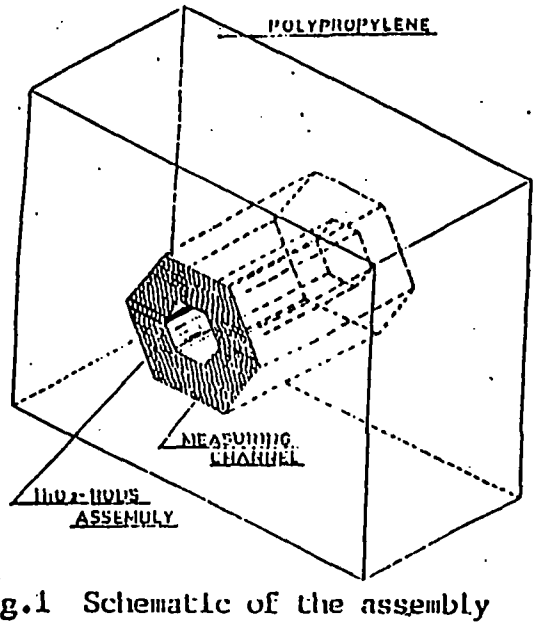

Fig.1 Schematic of the assembly

OPTIMIZATION OF ZONAL THICKNESS FOR TRITIUM BREEDING IN BLANKET ASSEMBLY CONTAINING THORIUM OXIDE AND LITHIUM ALUMINATE

R.P. Anand, T.K. Basu and D.V.S. Ramakrishna
Neutron Physics Division, Bhabha Atomic Research Centre, Bombay

In the next set of experiments, tritium and U-233 breeding measurements will be carried out in lithium aluminate and thorium oxide composite blanket assembly surrounded by polypropylene. The lithium aluminate rods were fabricated by stacking Γ-phase lithium aluminate pellets of 1.054 cm dia (density=1.83 g/cc) stacked in a 1.26 cm dia Al clad tube with an active length of 55.0 cm and 2.5 cm top and bottom Al plugs. The average weight of lithium aluminate in each rod was 87.2 g. The rods were similar to that of thorium oxide so that they can be arranged in a hexagonal compact geometry. The blanket assembly for this purpose was chosen so as to accommodate 13 rings instead of 11 rings used for U-233 breeding measurements. For this the height of the central through hexagonal channel was decreased to 6.12 cm from 8.36 cm which also brought the neutron source closer to the assembly.

MCNP calculations with the BMCCS2 cross section library were carried out to optimize the zonal thicknesses of lithium aluminate and thorium oxide blanket assembly for the maximum production rate of tritium with the available lithium aluminate rods (480). Table 1 summarizes the results of breeding calculations carried out for various combinations of Th and Li zonal thicknesses. It is observed that maximum tritium production (0.26) can be obtained when the assembly consists of 5 rings of lithium aluminate (480 rods) kept after 8 rings of thorium oxide (No.6). Without thorium, the tritium breeding in the full lithium blanket of 13 rings (936 rods) is only 0.17 (No.9). Thorium zone multiplies neutrons due to (n,xn) and (n,f) reactions thereby increasing the tritium breeding in lithium zone. By keeping a small zone of lithium before thorium zone and rest of lithium after thorium, fissions in thorium zone can be suppressed without sacrificing much on tritium breeding (No.13).

Based on these calculations, a blanket assembly has been built with 8 rings of thorium oxide followed by 5 rings of lithium aluminate in hexagonal geometry with a provision to introduce demountable rods. The blanket assembly is surrounded by 40 cm thick polypropylene as in the case of thorium assembly. Lithium carbonate and thorium oxide discs of size 9 mm dia and 3 mm thickness will be used as probes for the measurements of tritium and U-233 production rates respectively. Liquid scintillation technique will be employed to measure the β-activity of tritium and 312 KeV γ-activity of Pa-233 will be measured for U-233 production rate at different locations in the assembly.

Table 1

Calculated Tritium and U-233 Breeding Rate in Composite Blanket Assemblies Surrounded by 40 cm Thick Polypropylene

Sr No	Assembly (Rings)	No of rods		Th (n,f)	Breeding Ratio		
		Th	Li		U-233	Tritium	Total
1	13 Th	936	-	0.156	0.427	-	0.427
2	13 Th + 3 Li	936	360	0.159	0.257	0.235	0.492
3	12 Th + 4 1i	828	468	0.155	0.225	0.256	0.481
4	12 Th + 1 Li	828	108	0.154	0.271	0.188	0.459
5	10 Th + 3 Li	630	306	0.141	0.177	0.250	0.427
6	8 Th + 5 Li	456	480	0.127	0.122	0.261	0.383
7	5 Th + 8 Li	240	696		0.055	0.256	0.311
8	8 Li + 5 Th	480	456	0.047	0.144	0.090	0.234
9	13 Li	-	936	-	-	0.171	0.171
10	8 Li		456	-	-	0.146	0.146
11	4 Li	-	180	-	-	0.106	0.106
12	2Li + 8Th + 3Li	552	384	0.101	0.121	0.232	0.353
13	4Li + 6Th + 3Li	450	486	0.072	0.076	0.221	0.297
14	4Th + 5Li + 4Th	540	396	0.107	0.218	0.103	0.321

CREATION AND VALIDATION OF A NEUTRON-GAMMA COUPLED MULTIGROUP CROSS SECTION LIBRARY

K. Devan, V. Gopalakrishnan and S. M. Lee
Reactor Physics Division, Indira Gandhi Centre for Atomic Research, Kalpakkam-603 102

At IGCAR, a neutron-gamma coupled multigroup library (100n,21γ) called DLC-37 is being used extensively for fast reactor shield design calculations. It is meant for fusion reactor applications and has been found inadequate. Hence, the task of creating our own neutron-gamma coupled library was taken up. By using 1985 version of NJOY code system [1], a coupled set called IGC-DE4-S1 in ANISN format for 25 nuclides has been arrived at based on ENDF/B-IV neutron library and DLC-99 gamma library, with Legendre order of upto 5. The flow chart for the creation of coupled set is given in Fig 1. The code NGCOUP[2] was written to combine the neutron and gamma multigroup constants.

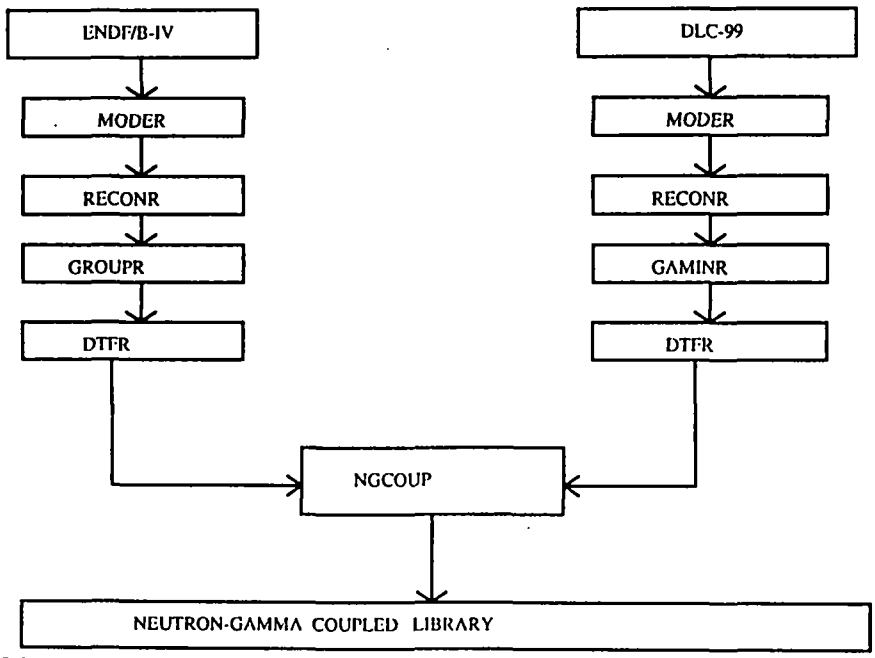

Fig. 1 Flowchart for the preparation of neutron - gamma coupled library at IGCAR

The weight functions used for multigrouping are:

For neutrons:

E exp (- E / 0.025), (Maxwellian) spectrum up to 0.414 eV

1/E spectrum between 0.414 eV and 820.85 keV

$\sqrt{E}$ exp (-E / 1.4 x 10^6), (Fission) spectrum above 820.85 keV

For gammas:

The gamma spectrum used are a 1/E at intermediate energies, a drop-off at low energies caused by photoelectric absorption and a shoulder at higher energies corresponding to the maximum Q value for capture.

The integral validation of IGC-DE4-S1 set was carried out as follows:

(1) Performing criticality calculations for four fast critical assemblies to check the neutron interaction data.

(2) Analysing a shielding benchmark[3] of a point Cs^{137} source in an infinite water by calculating scalar and angular fluxes at 2 and 3 mean free paths to check the gamma interaction data (results given in Table 1 and 2).

(3) To check the gamma production cross sections, gamma production cross sections averaged over a reported fast neutron (>1 MeV) spectrum for several nuclides were calculated and compared against the measured cross sections[4] (results given in Table 3).

There is no provision in the ANISN format to include self-shielding. The integral parameters obtained with this set, therefore, are subject to this limitation. Details of the creation and validation of the set are given in ref.5.

1. R. E. MacFarlane, D. W. Muir and R. E. Bolcourt, " The NJOY Nuclear Data Processing System: Volume -I", LA-9303-M, Vol.I (ENDF-324), 1982.

2. K. Devan, " NGCOUP : A Program to create a neutron-gamma coupled libray in ANISN format from DTFR outputs", Internal note , RPD/NDS/55 (1994).

3. ORNL-RSIC-25(ANS-SD-9), " Shielding Benchmark Problems", (1969).

4. R. E. Maerker, " SB3. Experiment on secondary gamma-ray production cross sections averaged over a fast-neutron spectrum for each of 13 different elements plus a stainless steel", ORNL-TM-5204 (ENDF-228), (1976).

5. K. Devan, V. Gopalakrishnan and S. M. Lee, " A neutron-gamma coupled multigroup cross section set for fast reactor shielding calculations from ENDF/B-IV and DLC-99 libraries by using NJOY system", Internal note, RPD/NDS/58 (1994).

TABLE 1. COMPARISON OF SCALAR GROUP GAMMA FLUXES

GAMMA GROUP	3 M.F.P (35.1 CM)		2 M.F.P (23.4 CM)	
	BENCHMARK	CALCULATED	BENCHMARK	CALCULATED
21	0.45503E-04	0.45677E-04	0.13280E-03	0.12536E-03
20	0.21774E-04	0.22872E-04	0.78153E-04	0.74927E-04
19	0.11511E-04	0.12283E-04	0.42845E-04	0.45060E-04
18	0.08008E-04	0.10799E-04	0.24524E-04	0.46108E-04

TABLE 2. COMPARISON OF GROUP GAMMA ANGULAR FLUXES AT 2 M. F. P

ANGLE (DEG.)	GROUP 21		GROUP 20		GROUP 19		GROUP 18	
	BENCHMARK	CALCULATED	BENCHMARK	CALCULATED	BENCHMARK	CALCULATED	BENCHMARK	CALCULATED
22.5	0.1759E-4	0.1476E-4	0.1389-04	0.1138E-4	0.1195E-4	0.1054E-4	0 .1868E-4	0.1017E-4
37.5	0.1501E-4	0.1341E-4	0.1029E-4	0.0900E-4	0.8249E-5	0.7344E-5	0.6166E-5	0.4319E-5
52.5	0.1382E-4	0.1225E-4	0.7686E-5	0.7776E-5	0.5665E-5	0.5489E-5	0.1221E-5	0.1999E-5
67.5	0.1025E-4	0.1127E-4	0.5732E-5	0.6730E-5	0.3537E-5	0.4278E-5		
82.5	0.9403-4	1.0025E-4	0.4832E-5	0.5538E-5	0.2227E-5	0.2936E-5		
97.5	0.9268E-5	0.8849E-5	0.5732E-5	0.6730E-5	0.1029E-5	0.1234E-5		
112.5	0.8160E-5	0.8099E-5	0.5185E-5	0.4596E-5	0.9451E-6	0.8974E-6		
127.5	0.7917E-5	0.7696E-5	0.3776E-5	0.4106E-5	0.5658E-6	0.7134E-6		
142.5	0.8487E-5	0.7464E-5	0.4272E-5	0.3894E-5	0.6095E-6	0.5641E-6		
157.5	0.8523E-5	0.7274E-5	0.4708E-5	0.3789E-5				
			0.5263E-5	0.3709E-5				

Table 3. Comparison of gamma production cross sections averaged over the fast neutron spectrum

Gamma Energy Interval (MeV)	Fe		Ni	
	Measured cross-* sections (mb)	Calculated cross-sections (mb)	Measured cross-* sections (mb)	Calculated cross-sections (mb)
1.0 - 1.5	278.0	211.94	790.0	792.60
1.5 - 2.0	132.0	106.70	179.0	184.96
2.0 - 2.5	101.0	103.41	68.0	55.91
2.5 - 3.0	74.0	66.81	43.0	39.66
3.0 - 3.5	44.0	47.35	37.0	42.19
3.5 - 4.0	33.0	40.05	17.0	15.83
4.0 - 4.5	8.7	7.94	11.5	10.06
4.5 - 5.0	5.6	4.99	4.8	4.43
5.0 - 5.5	3.8	4.15	< 4.7	2.94
5.5 - 6.0	2.4	2.48	< 3.4	2.12

* from ref. 4

Multigroup Cross sections for Iron, Chromium and Nickel from ENDF/B-VI

R. Saradhamani and V. Gopalakrishnan
Reactor Physics Division, Indira Gandhi Centre for Atomic Energy, Kalpakkam 603 102.

It is well known that Iron, Chromium and Nickel, being major constituents of stainless steel, are important as structural components in a reactor. Their atom densities in core, blanket and other regions are high enough to significantly influence the keff. They show resonances in regions extending to several hundred keV and their absorption as well as scattering cross sections are important. There are also dips in the elastic cross sections due to the interference of potential and resonance components, which cannot be ignored. Hence, for accurate reactor physics calculations, the cross sections of these materials must be obtained with little compromise.

In IGCAR, Cadarache Version2 set (1969 Adjusted French set) has been in use for over two decades for all core physics calculations. Cross sections of Cr and Ni have been suspected inadequate in this set. It is noticed that Cadarache Version 2 set performs better if the cross sections of Ni and Cr in it are replaced from JENDL-2 based set. Cadarache-2 set does not give self shielding factors for Cr and Ni. The resonance regions of these materials do not justify total neglect of self shielding effects. All the above observations, specifically that the recent set (JENDL-2) predicts better than the Cadarache-2, motivates one to look for the most recent data file. As a beginning to a systematic investigation, ENDF/B-VI (1990) has been chosen and the multigroup infinite dilution cross sections of Iron, Chromium and Nickel were compared/1/ with those from JENDL-2 and Cadarache-2. One group cross sections using FBTR and PFBR core spectra were also compared and given in Table 1, for elastic and capture reactions.

1. R. Saradhamani and V. Gopalakrishnan, Multigroup Cross sections of Iron, Chromium and Nickel from ENDF/B-VI, Internal Note RPD/NDS/61 (1994).

Table 1: Comparison of One group Cross sections

Spectrum	Cadarache-2	JENDL-2	ENDF/B-VI	% deviations wrt Cadarache-2 JENDL-2	ENDF/B-VI
Chromium Capture					
FBTR	3.9702E-03	5.8603E-03	5.5667E-03	48	40
PFBR	7.5368E-03	1.3894E-02	1.1584E-02	84	53
Iron Capture					
FBTR	5.6848E-03	8.3807E-03	7.6550E-03	47	34
PFBR	1.1236E-02	1.3301E-02	1.1965E-02	18	6
Nickel Capture					
FBTR	3.1969E-02	3.8658E-02	3.8701E-02	20	21
PFBR	1.8441E-02	3.4763E-02	3.0317E-02	88	64
Chromium Elastic					
FBTR	3.3682E+00	3.6934E+00	3.8764E+00	9	15
PFBR	4.4091E+00	5.1196E+00	5.4051E+00	16	22
Iron Elastic					
FBTR	3.1055E+00	3.4775E+00	3.6707E+00	11	18
PFBR	4.6927E+00	4.9737E+00	5.1975E+00	5	11
Nickel Elastic					
FBTR	5.1883E+00	5.3878E+00	5.4419E+00	4	5
PFBR	9.8556E+00	1.0192E+01	1.0216E+01	3	4

100 Group Displacement Cross sections from RECOIL Data Base

V. Gopalakrishnan
Reactor Physics Division, Indira Gandhi Centre for Atomic Energy, Kalpakkam 603 102.

Displacement cross sections in 100 nutron energy groups were calculated from the RECOIL data base[1] using the RECOIL program [1], for use in DPA (Displacements Per Atom) calculations for FBTR and PFBR materials.

DPA, which denotes the number of Displacements Per Atom of the target material due to neutron irradiation, is given in multigroup from, by

$$D = t \sum_{g_n} \sum_{g_R} \sigma(g_n, g_R)\, \upsilon(g_R)\, \phi(g_n)$$

where

$\sigma(g_n, g_R)$ is the cross section for a neutron energy group g_n to produce a primary knock on atom (pkA) in a (recoil) energy group g_R,

$\phi(g_n)$ is the neutron flux density,

$\upsilon(g_R)$ is the number of displacements the pkA could produce in the material in the subsequent cascade of interactions within the material,

and t is the irradiation time.

It can be rewritten as

$$D = t \sum_{g_n} \sigma_{dis}(g_n)\, \phi(g_n)$$

where

$$\sigma_{dis}(g_n) = \sum_{g_R} \sigma(g_n, g_R)\, \upsilon(g_R)$$

is known as the displacement cross section, in multigroup form.

RECOIL Data base gives multigroup kernels $\sigma(g_n, g_R)$, known also as the pkA spectrum in 105 neutron groups and 104 recoil groups. Program RECOIL calculates the displacement cross sections in the desired group structure.

100 group displacement cross sections were calculated/2/ using RECOIL-Data Base and RECOIL Program. Modifications were made in the data base to reduce space requirement, and in the the program for easy handling on a PC.

1. T. A. Gabriel et al., Radiation Damage Calculation: PrimaryRecoil Spectra, Displacement Rates, and Gas-Production Rates, Report ORNL/TM-5160(1979).

2. V. Gopalakrishnan, 100 Group Displacement Cross sections from RECOIL Data Base, Internal Note RPD/NDS/54 (1994).

Multigroup Activation Cross Sections

K. Devan
Reactor Physics Division, Indira Gandhi Centre for Atomic Research, Kalapakkam-603 102

For the estimation of the activation of various experimental foils as well as of materials present in a reactor the activation cross sections in specified group structure are required. We had created earlier [1,2] the activation cross sections for different materials in 25, 50 and 100 group structures to meet the above purposes.

Activation cross sections of Al^{27}, Mn^{55}, Fe, Co^{59}, Cu, Au^{197}, Th^{232} and U^{235} in 100 group structure were calculated from ENDL/84-V for use in estimation of activities of various foils in the proposed PFBR mock up shield experiment at APSARA reactor [3].

Activation cross sections of Zr and its isotpes were also calculated from ENDF/B-VI for activation studies in FBTR [4].

Though cross sections were required for specific reactions for the above purposes, cross sections for all reactions have been calculated and are available with us.

1. K. Devan, V. Gopalakrishanan and M. M. Ramanadhan, Activation Cross Sections of Sodium and Structural Nuclides in 25 and 100 Groups from JENDL-2, Internal Note RPD/NDS/32 (1990).

2. V. Gopalakrishnan, Activation Cross Sections in 50 Groups for Isotopes of Na, Fe, Cr, Ni, Cu, Co, Mo, and Mn With Two Different Weighting Spectra, Internal Note RPD/NDS/53 (1993)

3. K. Devan, Activation cross sections of Al^{27}, Mn^{55}, Fe, Co^{59}, Cu, Au^{197}, Th^{232} and U^{235} in 25 and 100 Group Structures from ENDL/84-V Library, Internal Note, RPD/NDS/56(1994).

4. K. Devan, 25 and 100 Group Activation Cross Sections of Zr and its Isotopes from ENDF/B-VI, Internal Note, RPD/NDS/60(1994)

Cross sections in 50 Groups for Isotopes of Na, Fe, Cr, Ni, Cu, Co, Mo and Mn With two Different Weighting Spectra.

V. Gopalakrishnan
Reactor Physics Division, Indira Gandhi Centre for Atomic Energy, Kalpakkam 603 102.

Multigroup cross sections for Sodium and for a few selected isotopes of some structural materials viz. Iron, Cobalt, Nickel, Chromium, Manganese, Copper and Molybdenum were calculated in 50 groups from the Japenese Evaluated Nuclear Data Library - Version 2 (JENDL-2 using two different weighting spectra, one suitable for a fast reactor core, and the other, for its shield. A comparison between these two sets was made, in order to have a feel of the relative differences introduced by the change in the weighting spectra. From the comparison, it was found that the difference due to the change in the weighting spectra is within 5% in most of the cases considered, though it exceeds 20% in some cases. It also has shown that there is generally an increase in the group cross sections when the standard E^n type weighting spectra (normally applied for obtaining unshielded group cross sections to be used for fast reactor core calculations) are replaced with a 1/E type spectra. Internal note/1/ gives greater details regarding group structure, ranges of weighting spectra, isotopes included etc. along with a table of comparison.

1. V. Gopalakrishnan, Activation Cross sections in 50 Groups for Isotopes of Na, Fe, Cr, Ni, Cu, Co, Mo and Mn With two Different Weighting Spectra, Internal Note RPD/NDS/53 (1993).

A Method for Generating Subgroup Parameters from Resonance Tables and the SPART Code

K. Devan and P. Mohanakrishnan
Reactor Physics Division, Indira Gandhi Centre for Atomic Research, Kalapkkam- 603 102

It is known that in certain neutron energy groups where the cross section varies significantly and in cases of interacting resonances due to the presence of many heavy isotopes, there is a loss of accuracy in the usual multigroup method. A finer group structure improves the accuracy but usually demands a large computer time. In such a situation, it is claimed, that the subgroup or multiband method [1-3] greatly improves the accuracy and is relatively economic. In this method, each group is divided into a number of total cross section ranges or bands and an average band cross section is defined in each band. Hence, the neutrons are allowed to interact not with only one cross section, as in the multigroup method, but rather with any one of the different band cross sections which are defined along with their associated statistical probabilities. Many people had used the subgroup method for fast reactors in the treatment of cell heterogeneity. Similar calculations were also done by R. J. Roth [2] for thermal reactors. At present, the subgroup method is found to be more flexible and easier to use when the spatial heterogeneity is considered.

As a first step in our attempts to implement the subgroup method for our fast reactor applications, D. E. Cullen's GROUPIE [3] code was tried to generate subgroup parameters. It was soon found that the code, as distributed by IAEA, does not include subroutines (due to restrictions) required for more than two bands. Hence we developed a method [4], which resembles Roth's method [2], to generate the subgroup parameters for any number of bands from the usual resonance tables containing multigroup unshielded cross sections and self shielding factors for a set of dilution cross sections and temperatures. A code SPART [4,5] was written which calculates the desired band parameters using the resonance tables available in Cadarache Version 2 format in binary mode.

The subgroup parameters are obtained from the resonance table by solving the following system of non-linear equations:

$$\sum_{k=1}^{N} \frac{\alpha_k}{\sigma_{tk} + \sigma_{0l}} = \frac{1}{\langle \sigma_t \rangle f_t(\sigma_{0l}) + \sigma_{0l}} \qquad \ldots\ldots (1)$$

$$\sum_{k=1}^{N} \frac{\alpha_k \sigma_{xk}}{\sigma_{tk} + \sigma_{0l}} = \frac{\langle \sigma_x \rangle f_x(\sigma_{0l})}{\langle \sigma_t \rangle f_t(\sigma_{0l}) + \sigma_{0l}} \qquad \ldots\ldots (2)$$

where α_k , σ_{tk} and σ_{xk} are subgroup parameters and k is the subgroup index. α_k is the band weight for k-th band and $f_t(\sigma_{ol})$ is the self-shielding factor for the total cross section for the dilution σ_{ol} .The index l gives the particular value of the dilution considered. Similarly, $f_x(\sigma_{ol})$ is the self-shielding factor for the reaction x (x = capture, elastic or fission) for the dilution σ_{ol} . $<\sigma_t>$ and $<\sigma_x>$ represent the unshielded cross sections for total and the reaction x and N is the total number of bands. The above set of equations satisfy the following constraints:

$$\sum_{k=1}^{N} \alpha_k = 1 \qquad \text{..... (3)}$$

$$\sum_{k=1}^{N} \alpha_k \sigma_{tk} = <\sigma_t> \qquad \text{..... (4)}$$

$$\sum_{k=1}^{N} \alpha_k \sigma_{xk} = <\sigma_x> \qquad \text{..... (5)}$$

$$\sum_{x} \sum_{k=1}^{N} \alpha_k \sigma_{xk} = <\sigma_t> \qquad \text{..... (6)}$$

The following steps were taken to solve the above set of non-linear equations with non-linear constraints:

(1) Convert eq. 1 into a polynomial equation and find its roots. The negative of these roots are the subgroup parameters for total cross section (σ_{tk}).

(2) Use σ_{tk}'s in eq. 1 and perform a least-squares fit with the constraints given by eq. 3 and 4 to find the band weights α_k 's.

(3) Use α_k and σ_{tk} in eq. 2 and perform a least-squares fit with the contraints given by eq. 5 and 6 to obtain σ_{xk}.

It should be noted that if N is the number of subgroups, the number of dilutions required to solve the above set of equations is 2N - 1. More details of the code SPART are given in ref.5.

Table 1 gives the subgroup parameters for Th-232 from JENDL-2 based multigroup binary cross section library [6] in two bands obtained using SPART. The subgroup parameters generated using GROUPIE from the JENDL-2 basic library is also given in Table 1. It should be kept in mind that SPART and GROUPIE differ in the method of generating subgroup parameters. Table. 2 gives the subgroup parameters for Pu-239 which was generated from the Cadarache Ver.2 cross section library in four bands.

1. L. B. Levitt, Nucl. Sci. Engg., 49, 450 (1972).

2. M. J. Roth, Report AEEW-R 921 (1974).

3. D. E. Cullen, Report UCRL-50400, Vol. 17, Part D (1980).

4. K. Devan and P. Mohanakrishnan, A Method of Generating Subgroup Parameters from Resonance Tables, in Proc. Tenth National Symposium on Radiation Physics (NSRP-10), Kalpakkam & Madras, Aug 17-20, 1993, p20.

5. K. Devan and P. Mohanakrishnan, SPART: A Code for Generating Subgroup Parameters from Resonance Tables, Internal Note RPD/NDS/51 (1993).

6. V. Gopalakrishnan et al., Internal Note, RPD/NDS/42 (1991)

Table 1. Subgroup parameters of Th-232 from JENDL-2 library for the broad group(276eV-101eV)

Code	Temp.	Band	Weights	Total	Capture	Elastic
SPART	300K	1	0.98281	17.810	3.703	14.10
		2	0.01719	1319.215	526.470	793.060
GROUPIE	0K	1	0.94661	10.067	0.500	9.568
		2	0.05339	593.000	245.070	347.93

Table 2. Subgroup parameters of Pu-239 from Cad. Ver.2 set at 300K for the group (22.6eV-3.06eV) using SPART code

Band	Weights	Total	Capture	Elastic	Fission
1	0.42213	15.884	1.819	9.693	4.123
2	0.32346	39.877	9.607	10.178	21.459
3	0.15690	190.880	53.301	14.307	117.010
4	0.09750	1051.300	436.210	65.548	556.190

ENDFIC - A Program for Indexing and Intercomparison of ENDFs

V. Gopalakrishnan and K. Devan
Reactor Physics Division, Indira Gandhi Centre for Atomic Energy, Kalpakkam 603 102.

Program **ENDFIC/1/** is a nuclear data utility program in FORTRAN. It was written under contract on '**Indexing and Intercomparison Programme of Evaluated Nuclear Data Files**' (No. **7866/RB/TC**), between Indira Gandhi Centre for Atomic Research, Kalpakkam, and the International Atomic Energy Agency, Vienna. The program can be used for the following two activities:

i. INFO activity: to find from a given ENDF/B formatted evaluated nuclear data library, information regarding the contents of the library,

ii. COMP activity: to do comparison of cross sections from several given ENDF libraries.

Features of ENDFIC

ENDFIC works with upto 5 ENDF libraries concurrently.
Under the INFO feature, ENDFIC can find for any desired nuclide,

- the ENDF format (4,5 or 6),
- the fissionability,
- the resolved resonance formalism, if any,
- availability of gamma production and covariance data,
- sections(MT) given under each file(MF),
- number of points given for each cross section type (MF=3),
- Q value of the reaction,
- whether the cross sections are linearised,
- number of records for chosen nuclide,
- starting record number for this nuclide, etc.

Under the COMP feature, cross sections from the given ENDF tapes can be compared, at specified (or built-in) energies. Cross sections of the same type or of different types may be compared.

The program being conversational, with builtin default options, having Rewind, Help and browsing facilities, is user friendly. The selection of nuclides may be either based on MAT number or on ZA value (Z *1000 + A). If, out of the selected libraries, the nuclide is specified only for the first, (by MAT or ZA) the program would choose the same nuclide (based on ZA) from the other libraries.

Limitations: ENDFIC itself cannot reconstruct resonance parameters into cross sections, a comparison at an energy in the resoance region may not be meaningful unless preprocessed ENDFs are input to the code.

1. V. Gopalakrishnan and K. Devan, ENDFIC - A Program for Indexing and Intercomparison of ENDFs, Internal Note RPD/NDS/57 (1994).

FORTDMPL - A Program to Prepare plot-codes in DMP Language to Drive Houston Insturments PC Plotter.

V. Gopalakrishnan
Reactor Physics Division, Indira Gandhi Centre for Atomic Energy, Kalpakkam 603 102.

A Houston Instruments PC plotter (model 695) has been installed in Nuclear Data Section, a few years ago. It could not be satisfactorily used for nuclear data plotting purposes for want of a suitable driver-software. The machine recognises DMPL command language. Though some standard commercial softwares like GRAPHER support this language, they are found to have restrictions on the number of points that can be plotted. Hence to suit the present needs, a program FORTDMPL was written in FORTRAN. This is a conversational program that generates DMPL codes to plot xy data on either A4 or A3 size paper. Usual requirements of linear/log axes, continuous/dashed lines, symbols, pen selection, curve smoothing, titles, legends etc. are incorporated. A tested version available at present can plot upto 10 curves on a frame each with upto 2000 points.

DETERMINATION OF FISSION YIELDS IN THE FAST NEUTRON INDUCED FISSION OF ^{238}U, ^{237}Np AND ^{243}Am USING FISSION TRACK ETCH-CUM GAMMA SPECTROMETRY

The absolute fission yields of 39 fission products in pure ^{238}U(99.9997 atom percent), 36 fission products in ^{237}Np and 30 fission products in ^{243}Am(99.998 atom percent) were determined in the fast neutron induced fission, employing fission track etch-cum gamma spectrometry[1]. The fissions were induced by a well defined reactor neutron spectrum (in a fixed position in the reactor) which was measured by using threshold detectors. The total number of fissions occurring in the target was obtained by recording the fission events in a lexan or mica solid state track detector strip immeresed in dilute solutions of uranium, neptunium and americium of known concentrations. The number of fission product atoms were determined mainly by direct high resolution gamma spectrometry except in the case of low yield symmetric and asymmetric products where a one or two step radiochemical separation followed by gamma spetrometry was employed. The yields of various fission products measured in the fast neutron induced fission of ^{238}U, ^{237}Np and ^{243}Am are given in the tables 1 to 3 and are being reported elsewhere[2-5]. For comparison the evaluated data from ENDF/B-VI or UKFY2 compilation are also given in the respective table of the fissioning systems. This work is part of an on-going IAEA research contract for the measurement of absolute fission yields in the fast neutron induced fission of several actinides[2]. Some important features/highlights of these measurements are as followes.

(i) All the fission yields data in pure ^{238}U[3] and ^{243}Am [5] as well as those of the short-lived fission products in ^{237}Np[4] are determined for the first time.

(ii) The fission yields in the mass region 134-139 in ^{238}U is unusually high (8-11%) which are confirmed from radiochemically separated samples. This has also been confirmed by measuring the yields of ^{137}Xe and ^{138}Xe in an irradiation of the sample in a sealed tube in which the noble gas fission products were not allowed to escape.

(iii) The recoil collection of fission products using 100 μm thick lexan foil in the case of ^{243}Am is a new approach to remove the interference from the gamma rays of both parent and daughter products of target actinide as well as activation products of the catcher foils[5]. This technique can infact be used for fission yield determination of any highly alpha active precious actinide.

(H. Naik, A. Ramaswami, A.G.C. Nair, A.K. Pandey, P.C. Kalsi, R.J. Singh and R.H. Iyer.)

REFERENCES

1. R.H. Iyer, R. Sampatkumar and N.K. Chaudhuri, Nucl. Instru. Methods. 115, 23 (1974).
2. R.H.Iyer, Progress Report on the Research Contract No. 6495/RB on "Measurement of absolute Fission yields in the fast neutron induced fission of actinides" for the period October 1, 1992 to June 30 1993.
3. H. Naik, A.G.C. Nair, P.C. Kalsi, A.K. Pandey, R.J. Singh, A. Ramaswami and R.H. Iyer, IX National Symposium on Solid State Nuclear Track Detectors, SSNTD-95, BARC, Bombay, March 8-10 (1995).
4. A.K. Pandey, H. Naik, P.C. Kalsi, R.J. Singh, A.G.C. Nair, A. Ramaswami and R.H. Iyer., ibid.
5. A. Ramaswami, A.G.C. Nair, A.K. Pandey, R.J.Singh, P.C.Kalsi, H. Naik and R.H. Iyer., ibid.

Table 1. Absolute Yields of Fission Products in the fast neutron induced fission of ^{238}U (99.9997 atom%)

S.No.	Nuclide	Half life	Gamma-ray Energy (keV)	Gamma abundance(%)	Fission Yield Values (%) present data	ENDF/BVI data
1.	$^{83}_{88}Br$*	2.39 h	529.5	1.3	0.187	0.393±0.024
2.	$^{89}_{36}Kr$	2.84 h	196.3	26.3	2.098±0.083	2.036±0.041
3.	$^{91}_{37}Rb$	15.2 m	1032.1	58.0	3.052±0.385	2.813±0.078
			1248.1	42.6	2.888±0.093	2.813±0.078
4.	$^{91}_{38}Sr$	9.52 h	1024.3	33.4	4.335±0.135	4.084±0.114
5.	$^{93}_{38}Sr$	2.71 h	1384.1	90.0	4.410±0.130	4.278±0.119
6.	$^{94}_{38}Sr$	7.42 m	875.9	23.9	4.560±0.091	4.933±0.296
7.	$^{95}_{39}Y$	18.7 m	918.7	56.0	4.340±0.257	4.639±0.186
8.	$^{95}_{39}Y$	10.3 m	954.1	13.4	5.032±0.061	5.150±0.103
9.	$^{97}_{40}Zr$	64.02 d	756.7	54.5	4.701±0.214	5.151±0.052
10.	$^{99}_{40}Zr$	16.9 h	743.3	92.8	6.408±0.147	5.564±0.078
11.	$^{101}_{42}Mo$	2.748 d	140.5	90.7	6.282±0.269	6.188±0.087
12.	$^{103}_{42}Mo$	14.6 m	590.9	16.4	4.799±0.276	6.197±0.372
13.	$^{104}_{44}Ru$	39.254 d	497.1	88.7	6.124±0.282	6.261±0.063
14.	$^{105}_{43}Tc$	18.3 m	358.0	89.0	5.237±0.211	5.029±0.100
15.	$^{111}_{44}Ru$	4.44 h	724.3	46.7	5.014±0.314	4.058±0.114
16.	$^{117}_{47}Ag$	7.45 d	342.1	6.7	0.083±0.014	0.071±0.001
17.	$^{117}_{48}Cd$	2.49 h	273.4	28.0	0.038±0.006	0.028±0.001
		3.36 h	1066.0	23.1		
18.	$^{127}_{51}Sb$	3.85 d	685.7	35.3	0.135±0.015	0.135±0.008
19.	$^{131}_{51}Sb$	23.03 m	943.0	44.0	3.089±0.175	3.245±0.195
20.	$^{133}_{53}I$	8.04 d	364.5	81.2	3.313±0.110	3.282±0.042
21.	$^{134}_{53}I$	20.8 h	529.9	87.0	6.755±0.216	6.769±0.332
22.	$^{135}_{52}Te$	41.8 m	566.0	18.4	8.406±0.115	6.917±0.194
23.	$^{137}_{53}I$	6.55 h	1260.4	28.6	8.422±0.118	6.965±0.139
24.	$^{138}_{54}Xe$	3.818 m	455.5	31.2	8.650±0.027	6.011±0.120
25.	$^{138}_{54}Xe$	14.08 m	434.5	20.3	8.924±0.721	5.675±0.159
26.	$^{139}_{55}Cs$	32.2 m	1435.8	76.3	11.669±0.246	5.728±0.160
27.	$^{140}_{56}Ba$	1.41 h	165.9	22.0	7.245±0.105	5.657±0.113
28.	$^{141}_{56}Ba$	12.75 d	537.3	24.4	5.646±0.154	5.846±0.058
29.	$^{141}_{56}Ba$	18.27 m	190.3	46.3	5.448±0.048	5.379±0.323
30.	$^{142}_{58}Ce$	32.5 d	145.4	48.4	5.107±0.619	5.379±0.108
31.	$^{142}_{56}Ba$	10.6 m	255.2	20.6	3.899±0.179	4.577±0.183
32.	$^{143}_{57}La$	1.542 h	641.3	47.0	6.057±0.159	4.580±0.092
33.	$^{146}_{58}Ce$	1.375 d	293.3	42.0	4.952±0.122	4.597±0.064
34.	$^{144}_{58}Ce$	13.52 m	316.7	51.0	3.572±0.225	3.426±0.096
35.	$^{147}_{58}Ce$	284.4 d	133.5	11.1	4.568±0.464	4.550±0.064
36.	$^{149}_{60}Nd$	10.98 d	531.0	13.0	2.555±0.185	2.572±0.051
37.	$^{151}_{61}Pm$*	53.08 h	286.0	2.85	1.679	1.618±0.032
38.	$^{153}_{62}Pm$	28.4 h	340.0	22.0	0.723±0.018	0.795±0.016
39.	$^{153}_{62}Sm$*	46.7 h	103.2	28.3	0.332	0.411±0.012

* based on one measurement.

Table 2. Absolute Yields of Fission Products in the fast neutron induced Fission of ^{237}Np.

a. For long lived fission products in ^{237}Np.

S.No.	Nuclide	Half life	Gamma-ray Energy (keV)	Gamma abund-ance(%)	Fission Yield Values(%) present data	ENDF/B-VI data
1.	$^{91}_{92}Sr$	9.52 h	749.9	23.6	3.655±0.190	3.933±0.236
2.	$^{95}_{92}Sr$	2.71 h	1384.1	90.0	5.155±0.345	4.455±0.267
3.	$^{97}_{95}Zr$	64.02 d	756.7	54.5	4.872±0.293	5.689±0.159
4.	$^{99}_{97}Zr$	16.9 h	743.3	92.8	6.925±0.055	6.097±0.171
5.	$^{103}_{99}Mo$	2.748 d	140.5	90.7	5.145±0.495	6.115±0.245
6.	$^{111}_{103}Ru$*	39.254 d	497.1	88.7	5.195±0.165	5.562±0.156
7.	$^{117}_{111}Ag$*	7.45 d	342.1	6.7	0.106	0.089±0.007
8.	$^{127}_{117}Cd$	2.49 h	273.4	28.0	0.016±0.003	0.018±0.0053
		3.36 h	1066.0	23.1		
9.	$^{131}_{127}Sb$	3.85 d	685.7	35.3	0.474±0.045	0.352±0.028
10.	$^{132}_{131}I$	8.04 d	364.5	81.2	3.408±0.036	3.587±0.143
11.	$^{135}_{132}Te$	3.26 d	228.3	88.2	4.928±0.020	4.804±0.192
12.	$^{138}_{135}I$	6.55 h	1260.4	28.6	6.045±0.325	6.525±0.391
13.	$^{139}_{138}Cs$	32.2 m	1435.8	76.3	5.405±0.385	5.983±0.239
14.	$^{140}_{139}Ba$	1.41 h	165.9	22.0	5.900±0.030	5.609±0.224
15.	$^{141}_{140}Ba$	12.75 d	537.3	24.4	5.640±0.698	5.472±0.077
16.	$^{142}_{141}Ce$	32.5 d	145.4	48.4	5.711±0.026	5.316±0.213
17.	$^{143}_{142}La$	1.542 h	641.3	47.0	5.525±0.285	4.830±0.193
18.	$^{144}_{143}Ce$	1.375 d	293.3	42.0	4.785±0.065	4.642±0.186
19.	$^{147}_{144}Ce$	284.4 d	133.5	11.1	4.131±0.063	4.130 0.083
20.	$^{149}_{147}Nd$	10.98 d	531.0	13.0	1.990±0.080	2.243 0.135
21.	$^{151}_{149}Pm$	53.08 h	286.0	2.85	1.138±0.217	1.300 0.052
22.	$^{153}_{151}Pm$	28.4 h	340.1	22.0	0.666±0.063	0.726 0.029
23.	^{153}Sm*	46.7 h	103.2	28.3	0.273	0.366 0.022

b. For short lived fission products.

S.No.	Nuclide	Half life	Gamma-ray Energy (keV)	Gamma abund-ance(%)	Fission Yield Values(%) present data	ENDF/B-VI data
1.	$^{89}_{93}Rb$	15.2 m	1248.3	42.6	2.212±0.137	2.523±0.202
2.	^{94}Sr	7.32 m	875.9	23.9	4.362±0.007	5.005±0.400
3.	^{95}Sr	1.235 m	1427.6	94.2	4.195±0.015	4.679±0.749
4.	^{104}Y	10.3 m	954.1	13.4	6.150±0.233	5.627±0.338
5.	^{108}Tc	18.3 m	358.0	89.0	5.375±0.135	4.133±0.231
6.	^{132g}Ru	4.55 m	164.9	28.0	1.096±0.211	1.206±0.405
7.	^{132m}Sb	4.15 m	696.9	100.0	1.044±0.243	1.343±0.309
8.	^{133}Sb	2.8 m	696.9	86.0	0.904±0.038	1.208±0.278
9.	^{137}Sb	2.36 m	1096.2	30.5	1.577±0.320	1.590±0.367
10.	^{140}Xe	3.818 m	455.5	31.2	5.391±0.040	5.895±0.472
11.	^{142}Cs	1.062 m	602.4	70.0	3.875±0.055	4.887±0.782
12.	^{145}Ba	10.6 m	255.2	20.6	3.172±0.187	4.641±0.371
13.	^{145}Ce	2.98 m	723.9	63.9	3.355±0.195	3.441±0.275

* based on one measurement.

Table 3. Absolute yields of fission products in the fast neutron induced fission of ^{243}Am

S.No.	Nuclide	Half life	γ-Energy (keV)	Gamma abundance (%)	Fission Yield Values(%) Present data	UKFY2
1.	^{89}Rb	15.2 m	1032.1	58.0	1.10 ± 0.40	1.028 ± 0.353
2.	^{91}Sr	9.52 h	1024.3	33.4	1.48 ± 0.10	1.646 ± 0.599
3.	^{92}Sr	2.71 h	1384.1	90.0	1.95 ± 0.11	2.035 ± 0.730
4.	^{92}Y	3.50 h	934.5	13.9	2.36 ± 0.11	2.047 ± 0.739
5.	^{94}Y	18.7 m	918.7	56.0	2.76 ± 1.03	2.761 ± 1.027
6.	^{95}Zr	64.02 d	756.7	54.5	4.55	3.176 ± 1.201
7.	^{97}Zr	16.9 h	743.3	92.8	3.87 ± 0.37	3.935 ± 1.476
8.	^{97}Nb	72.1 m	657.9	98.4	4.22	3.955 ± 1.484
9.	^{99}Mo	2.748 d	140.5	90.7	5.53 ± 0.03	4.488 ± 1.710
10.	^{101}Mo	14.6 m	590.9	16.4	5.91 ± 0.04	5.110 ± 1.949
11.	^{103}Ru	39.254 d	497.1	88.7	6.51	5.951 ± 2.223
12.	^{104}Tc	18.3 m	358.0	89.0	6.04 ± 0.04	6.412 ± 2.341
13.	^{105}Ru	4.44 h	724.3	46.7	6.22 ± 0.20	6.786 ± 2.391
14.	^{105}Rh	35.36 h	318.9	19.0	6.51	6.786 ± 2.392
15.	^{107}Rh	21.7 m	302.8	66.0	6.71	6.376 ± 2.165
16.	^{131}Sb	23.03 m	943.0	44.0	1.93 ± 0.06	3.092 ± 1.13
17.	^{131}I	8.04 d	364.5	81.2	3.29 ± 0.21	3.457 ± 1.261
18.	^{132}I	2.3 h	772.6	76.0	3.23	4.493 ± 1.615
19.	^{133}I	20.8 h	539.9	86.0	5.36	5.616 ± 1.982
20.	^{134}Te	41.8 m	767	29.4	5.79 ± 0.11	4.921 ± 1.66
21.	^{135}I	6.55 h	1260.4	28.6	6.69 ± 0.02	6.517 ± 2.25
22.	^{138}Cs	32.2 m	1435.8	76.3	5.58 ± 0.14	6.026 ± 2.098
23.	^{139}Ba	1.41 h	165.9	22.0	7.36 ± 0.15	5.613 ± 2.021
24.	^{140}Ba	12.75 d	537.3	24.4	6.64	5.203 ± 1.900
25	^{140}La	1.68 h	1596.6	95.4	7.10	5.205 ± 1.900
26.	^{141}Ba	18.27 m	190.3	46.3	7.40 ± 0.30	4.864 ± 1.773
27.	^{141}Ce	32.5 d	145.4	48.4	4.85	4.885 ± 1.781
28.	^{142}La	1.542 h	641.3	47.0	5.28 ± 0.28	4.600 ± 1.69
29.	^{143}Ce	1.375 d	293.3	42.0	4.74 ± 0.14	4.243 ± 1.558
30.	^{146}Pr	13.52 m	454	48.0	4.33 ± 0.05	3.019 ± 1.156

CHARGE DISTRIBUTION IN THE MASS REGION 128-134 IN LOW ENERGY FISSION OF ACTINIDES:-

Fractional cumulative yields (FCY) of ^{128}Sn, ^{131}Sb, ^{132}Te and ^{134}Te have been determined in thermal neutron induced fission of ^{233}U, ^{235}U, ^{239}Pu, ^{241}Pu and ^{245}Cm using direct gamma spectrometric and radiochemical techniques. Charge distribution systematics e.g., the width parameter (σ_Z), most probable charge (Z_p) and magnitude of charge polarization (ΔZ) have been deduced for all the four mass chains in these fissioning systems as well as in $^{249}Cf(n_{th},f)$ on the basis of the present and literature data[1,2]. It is observed that the parameter σ_Z show the effect of 50p and 82n spherical shells. Systematic increase of σ_Z values with increase in fissility parameter has been observed in all the four mass chains showing the consequence of dynamical effects. The Z_{MPE} based on liqiid drop model i.e. minimum potential hypothesis was also calculated and are shown in the figure 1 along with the ΔZ deduced from the experimental Z_p value. For a fixed heavy mass the variation of ΔZ with increase of fissility parameter is interpreted from the point of mass asymmetry effects. Detailed work is published elsewhere[3].

H. Naik, S.P. Dange, and T. Datta.

REFERENCES

1. A.C. Wahl, At Data Nucl Data Table 32, 1 (1988).
2. J.K. Dickens and J.W. Mc Connell, Phys. Rev. C23 (1981) 331; Phys. Rev. C24 (1981) 192.
3. H.Naik, S.P.Dange and T.Datta, Radiochimica Acta 62 1 (1993).

Table 1. Fractional Cumulative Yields (FCY) of ^{128}Sn, ^{131}Sb, ^{132}Te and ^{134}Te in various fissioning systems.

Fissioning Nucleus	^{128}Sn	^{131}Sb	^{132}Te	^{134}Te
$^{234}U^{*}$	0.787±0.103	0.566±0.038	0.963±0.046	0.626±0.030
$^{236}U^{*}$	0.946±0.046	0.797±0.020	0.9949±0.0011	0.898±0.023
$^{240}Pu^{*}$	0.852±0.104	0.649±0.020	0.969±0.005	0.667±0.009
$^{242}Pu^{*}$	0.931±0.039	0.784±0.025	0.9945±0.0017	0.856±0.019
$^{246}Cm^{*}$	0.748±0.055	0.647±0.033	0.945±0.019	0.562±0.026

Table 2. Charge distributions parameters for four mass chains.
a. Width of the distribution

Fissioning Nucleus	A=128	A=131	A=132	A=134
$^{234}U^{*}$	0.36	0.60	0.56	0.38
$^{236}U^{*}$	0.36	0.60	0.56	0.38
$^{240}Pu^{*}$	0.38	0.62	0.60	0.40
$^{242}Pu^{*}$	0.38	0.62	0.60	0.40
$^{246}Cm^{*}$	-	0.64	0.62	0.52
$^{250}Cf^{*}$	-	0.67	0.66	0.62

b. Most probable charge (Z_p)

Fissioning Nucleus	A=128	A=131	A=132	A=134
$^{234}U^{*}$	50.23±0.10	51.30±0.05	51.66±0.09	52.41±0.07
$^{236}U^{*}$	49.92±0.10	50.93±0.07	51.20±0.09	52.08±0.04
$^{240}Pu^{*}$	50.11±0.15	51.25±0.06	51.53±0.08	52.30±0.05
$^{242}Pu^{*}$	49.90±0.05	50.97±0.04	51.11±0.15	52.07±0.04
$^{246}Cm^{*}$	-	51.27±0.07	51.58±0.09	52.41±0.10
$^{250}Cf^{*}$	-	51.62±0.07	51.95±0.10	52.78±0.13

c. Charge polarization (Z)

Fissioning Nucleus	A=128	A=131	A=132	A=134
$^{234}U^{*}$	-0.27±0.10	-0.38±0.05	-0.49±0.09	-0.58±0.07
$^{236}U^{*}$	-0.12±0.10	-0.35±0.07	-0.49±0.09	-0.44±0.04
$^{240}Pu^{*}$	-0.26±0.15	-0.33±0.06	-0.50±0.08	-0.56±0.05
$^{242}Pu^{*}$	-0.05±0.05	-0.22±0.04	-0.49±0.15	-0.35±0.04
$^{246}Cm^{*}$	-	-0.36±0.07	-0.46±0.09	-0.46±0.10
$^{250}Cf^{*}$	-	-0.29±0.07	-0.42±0.10	-0.38±0.13

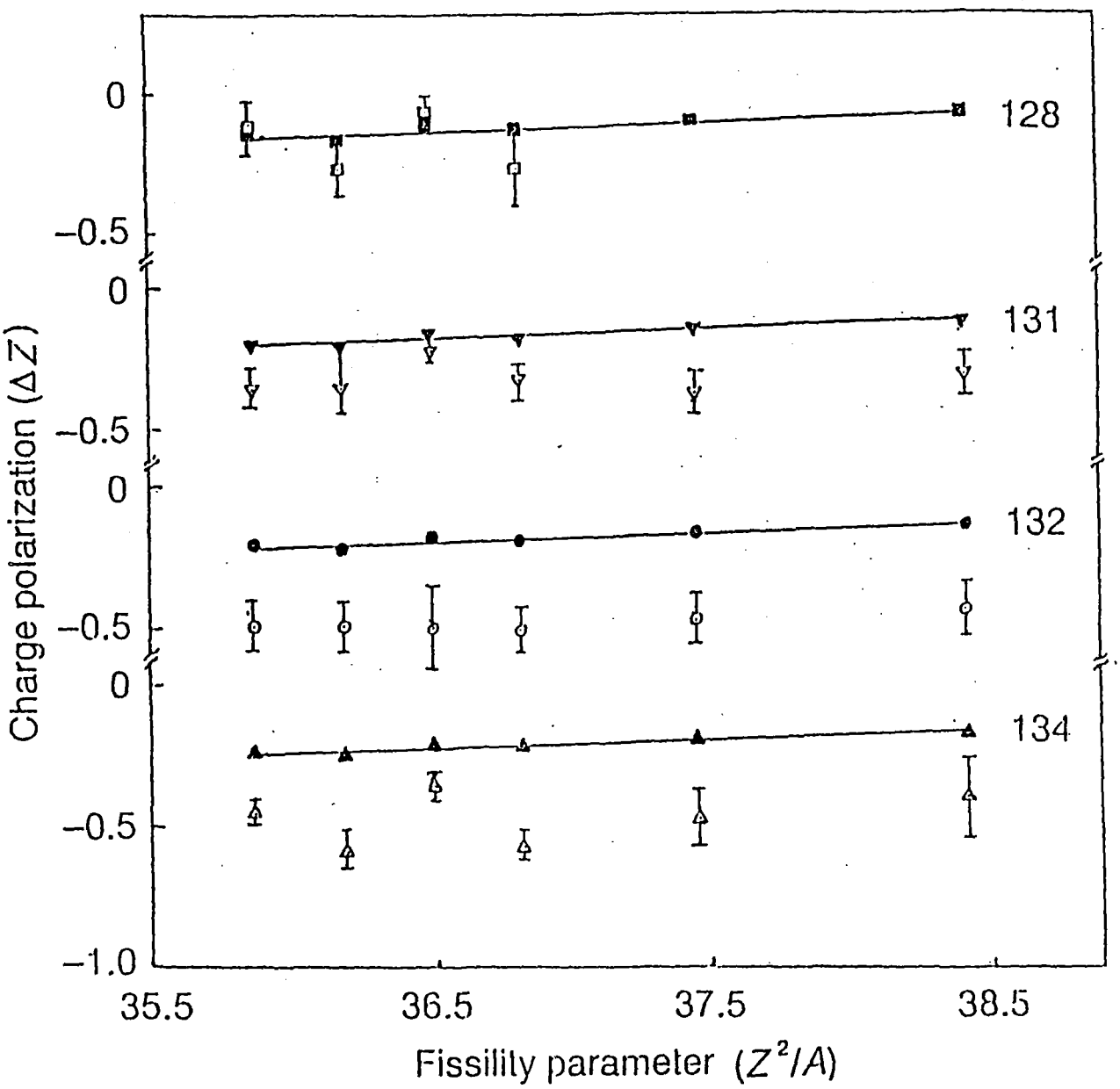

Fig. 1. Plot of charge polarization (ΔZ) for four different mass chains as a function of fissility parameters (Z^2/A) (filled points based on MPE, open points: experimental).

SYSTEMATICS OF FRAGMENT ANGULAR MOMENTUM IN LOW ENERGY FISSION OF ACTINIDES:-

Independent isomeric yield ratios of ^{128}Sb, ^{130}Sb, ^{132}Sb, ^{131}Te, ^{133}Te, ^{132}I, ^{134}I, ^{136}I, ^{135}Xe and ^{138}Cs in $^{229}Th(n_{th},f)$, for ^{136}I in $^{233}U(n_{th},f)$ and $^{239}Pu(n_{th},f)$, for ^{138}Cs in $^{235}U(n_{th},f)$, for ^{130}Sb, ^{136}I and ^{135}Xe in $^{241}Pu(n_{th},f)$, for ^{128}Sb, ^{130}Sb, ^{132}Sb, ^{131}Te, ^{133}Te, ^{134}I, ^{136}I, ^{135}Xe and ^{138}Cs in $^{245}Cm(n_{th},f)$ and for ^{128}Sb, ^{130}Sb, ^{132}Sb, ^{136}I and ^{135}Xe in ^{252}Cf(S.F.) have been determined using radiochemical and gamma ray spectrometric techniques. From the isomeric yield ratios fragment angular momenta (J_{rms}) have been deduced using spin dependent statistical model analysis and are given in the table 1a to h along with the literature data for other fission products[1] in the above fissioning systems as well as in $^{249}Cf(n_{th},f)$[3]. The yield weighted average values of fragment angular momentum of various elements in the above mentioned fissioning systems are given in table 2. The important features emerging from these data are as follows. (i) The fragment angular momentum of odd-Z products are higher than the even-Z products (fig 1 to 3) indicating the importance of single particle effect. (ii) The angular momenta for fragments with spherical 50 proton shell, 82 neutron shell are lower compared to the fragments with no shells and deformed 66 and 88 neutron shells indicating the effect of fragment deformation on scission point configuration (figs. 4-7). (iii) Fission fragment J_{rms} has a nearly inverse correlation with elemental yield in fissioning systems from $^{230}Th^{*}$ to ^{252}Cf (fig. 1-3) possibly due to coupling between the collective and intrinsic degrees of freedom. (iv) Fission product elemental yield as well as angular momentum have no definite correlation with fissionability (fig. 4-6) since both are decided near scission point. (v) From fragment J_{rms} deformation parameters (β) were deduced using statistical and pre-scission bending mode oscillation model and are given in the respective tables of fissioning systems along with calculated neck radius and kinetic energy data. The calculated β values are seen to be in good agreement with the values deduced from static scission point model Wilkins et al.[3]. Detailed work is published elsewhere[4].

H.Naik, S.P.Dange, R.J.Singh and T.Datta.

REFERENCES

1. H.Naik, Radiochemical Studies on Nuclear Fission of Actinides, Ph.D. Thesis, University of Bombay (1992).
2. J.K. Dickens and J.W. McConnell, Phys. Rev. C24 (1981) 192.
3. B.D. Wilkins, E.P. Steinberg and R.R. Chasmann, Phys. Rev C14 (1976) 1832.
4. H. Naik, S.P. Dange, R.J. Singh and T. Datta, Nucl. Phys. A (In Press).

Table 1. Independent isomeric yield ratio, fragment Jrms and different parameters related to scission point configuration.

a. $^{230}Th^{*}$

Nuclide	IY(%) (Yh+Yl)	Yh/(Yh+Yl)	Jrms (h)	β	c (F)	K.E. (MeV) Expt.	Cal.
^{128}Sb	0.026±0.003	0.530±0.053	10.4 ±0.9	0.78	1.06	171.8	172.2
^{130}Sb	0.138±0.008	0.447±0.028	9.2 ±0.3	0.50	1.04	169.8	169.0
^{132}Sb	0.794±0.022	0.338±0.025	7.1 ±0.3	0.26	1.05	171.4	170.6
^{131}Te	0.155±0.007	0.670±0.048	5.65±0.7	0.14	1.05	170.7	170.6
^{133}Te	2.331±0.221	0.568±0.058	4.7 ±0.5	0.001	1.12	171.3	182.0
^{132}I	0.034±0.005	0.433±0.062	8.3 ±0.8	0.33	1.06	171.4	171.0
^{134}I	0.570±0.049	0.394±0.082	7.8 ±1.0	0.19	1.06	170.0	171.0
^{136}I	3.667±0.573	0.667±0.072	8.2 ±1.4	0.24	1.03	166.7	166.2
^{135}Xe	0.408±0.023	0.573±0.063	4.7 ±0.6	0.001	1.12	168.0	180.0
^{138}Cs	0.467±0.044	0.642±0.080	8.7 ±0.8	0.34	1.03	164.3	164.6

b. $^{234}U^{*}$

Nuclide	IY(%) (Yh+Yl)	Yh/(Yh+Yl)	Jrms (h)	β	c (F)	K.E. (MeV) Expt.	Cal.
^{128}Sb	0.132±0.009	0.530±0.047	10.4 ±0.8	0.80	1.07	178.2	178.6
^{130}Sb	0.79 ±0.064	0.456±0.063	9.3 ±0.9	0.57	1.07	178.0	178.6
^{132}Sb	1.14 ±0.162	0.263±0.065	6.35±0.65	0.12	1.08	179.5	180.3
^{131}Te	1.44 ±0.078	0.653±0.055	5.5 ±0.55	0.17	1.08	179.5	179.8
^{133}Te	3.57 ±0.212	0.569±0.054	4.7 ±0.6	0.01	1.12	178.8	186.5
^{132}I	0.169±0.006	0.425±0.037	8.2 ±0.4	0.33	1.08	179.5	179.3
	0.192±0.014	0.427±0.061	8.2 ±0.8	0.33	1.08	179.5	179.3
^{134}I	2.15 ±0.13	0.391±0.038	7.7 ±0.5	0.19	1.07	178.0	177.6
	1.79 ±0.072	0.430±0.028	8.2 ±0.4	0.32	1.08	178.0	177.6
^{136}I	1.33 ±0.13	0.666±0.085	8.2 ±1.8	0.28	1.06	175.2	175.9
^{133}Xe	0.056+0.004	0.704±0.094	6.1 ±1.9	0.31	1.08	178.8	178.6
^{135}Xe	1.433±0.091	0.552±0.080	4.5 ±0.7	0.001	1.16	176.3	191.8
	1.64 ±0.078	0.616±0.042	5.1 ±0.4	0.04	1.07	176.3	177.0
	1.52 ±0.086	0.559±0.047	4.9 ±0.7	0.001	1.08	176.3	178.6
^{138}Cs	1.01 ±0.07	0.720±0.040	10.2 ±0.8	0.69	1.05	173.0	172.9
	1.17 ±0.067	0.709±0.065	10.0 ±1.3	0.65	1.05	173.0	172.9
^{148}Pm	1.17±0.14	0.750±0.125	11.8 ±2.8	0.87	1.02	161.0	161.9
	E-06	0.800±0.060	13.6 ±2.2	0.99	0.94	161.0	149.2

Yh and Yl- Yield of high and low spin isomer.

c. $^{236}U^{*}$

Nuclide	IY(%) (Yh+Yl)	Yh/(Yh+Yl)	Jrms (h)	ß	c (F)	K.E. (MeV) Expt.	K.E. (MeV) Cal.
^{131}Sn	0.0112±.0043	0.670±0.02	5.7 ±0.2	0.50	1.09	181.8	181.7
^{128}Sb	0.024±0.003	0.456±0.087	9.3 ±1.3	0.56	1.06	175.5	176.3
^{130}Sb	0.49 ±0.064	0.449±0.101	9.2 ±1.5	0.58	1.09	180.8	181.3
	0.622±0.084	0.405±0.063	8.6 ±0.9	0.45	1.09	180.8	181.3
^{132}Sb	2.0 ±0.31	0.190±0.050	5.55±0.6	0.001	1.14	180.8	189.6
	1.946±0.137	0.310±0.031	6.8 ±0.3	0.25	1.09	180.8	181.3
^{131}Te	0.32 ±0.028	0.656±0.085	5.5 ±1.2	0.18	1.09	181.0	180.8
	0.359±0.041	0.643±0.08	5.4 ±1.0	0.16	1.09	181.0	180.8
^{132}Te	1.603±0.151	0.280±0.04	5.3 ±0.4	0.12	1.09	180.8	180.8
^{133}Te	3.46 ±0.224	0.566±0.047	4.6 ±0.4	0.01	1.14	180.5	189.1
	3.31 ±0.242	0.585±0.074	4.7 ±0.8	0.01	1.12	180.5	185.8
		0.608±0.064	4.9 ±0.8	0.02	1.09	180.5	180.8
^{132}I	0.022±0.0035	0.446±0.037	8.4 ±0.4	0.40	1.09	180.8	180.2
	0.022±0.002	0.454±0.061	8.6 ±0.8	0.44	1.09	180.8	180.2
^{134}I	1.16 ±0.11	0.352±0.019	7.3 ±0.25	0.12	1.09	180.3	180.2
	0.92 ±0.08	0.412±0.046	8.0 ±0.6	0.29	1.09	180.3	180.2
	0.78 ±0.06	0.462±0.031	8.6 ±0.5	0.43	1.09	180.3	180.2
^{136}I	2.643±0.503	0.677±0.176	8.4 ±2.4	0.34	1.07	177.0	176.9
^{133}Xe	0.0024±.0002	0.751±0.063	6.9 ±1.5	0.55	1.10	180.5	181.2
^{135}Xe	0.258±0.027	0.648±0.104	5.4 ±1.0	0.14	1.09	179.6	179.6
	0.233±0.022	0.644±0.104	5.4 ±1.5	0.14	1.09	179.0	179.6
	0.284±0.017	0.669±0.053	5.65±0.7	0.21	1.09	179.6	179.6
^{138}Cs	0.42 ±0.042	0.711±0.045	10.0±1.1	0.67	1.06	174.0	173.9
^{148}Pm	-	0.720±0.139	11.0±2.7	0.73	1.02	161.8	161.3

d. $^{240}Pu^{*}$

Nuclide	IY(%) (Yh+Yl)	Yh/(Yh+Yl)	Jrms (h)	ß	c (F)	K.E. (MeV) Expt.	K.E. (MeV) Cal.
^{128}Sb	0.127±0.009	0.520±0.048	10.2 ±0.7	0.75	1.06	181.5	180.9
^{130}Sb	1.08 ±0.086	0.537±0.078	10.5 ±1.15	0.83	1.08	185.0	184.3
^{132}Sb	1.75 ±0.228	0.303±0.074	8.75±0.75	0.24	1.09	185.8	186.0
^{131}Te	1.34 ±0.064	0.679±0.049	5.8 ±0.6	0.26	1.09	186.0	185.7
^{133}Te	4.31 ±0.22	0.617±0.045	5.1 ±0.4	0.07	1.09	186.0	185.7
^{132}I	0.165±0.008	0.426±0.036	8.2 ±0.7	0.35	1.09	185.8	185.2
	0.23 ±0.014	0.478±0.052	8.9 ±0.7	0.51	1.09	185.8	185.2
^{134}I	2.42 ±0.19	0.394±0.047	7.8 ±0.5	0.25	1.09	185.8	185.2
	2.34 ±0.08	0.470±0.030	8.7 ±0.4	0.46	1.09	185.8	185.2
^{136}I	2.67 ±0.07	0.701±0.049	8.8 ±1.1	0.45	1.08	183.0	183.5
^{133}Xe	0.042±0.002	0.782±0.057	7.7 ±1.5	0.69	1.10	186.0	186.3
^{135}Xe	1.114±0.061	0.591±0.045	4.9 ±0.5	0.01	1.09	184.3	184.6
	1.29 ±0.07	0.659±0.053	5.55±0.55	0.18	1.09	184.3	184.6
	1.17 ±0.07	0.581±0.043	4.8 ±0.4	0.001	1.10	184.3	186.3
^{138}Cs	0.87 ±0.22	0.670±0.060	9.2 ±1.0	0.51	1.07	180.0	180.6
	0.84 ±0.07	0.690±0.092	9.5 ±1.5	0.58	1.07	180.0	180.6

e. $^{242}Pu^{*}$

Nuclide	IY(%) (Yh+Yl)	Yh/(Yh+Yl)	Jrms (h)	β	c (F)	K.E. (MeV) Expt.	K.E. (MeV) Cal.
^{128}Sb	0.026±0.015	0.530±0.080	10.4 ±1.4	0.82	1.08	184.0	183.7
^{130}Sb	0.85 +0.094	0.410±0.053	8.0 ±0.6	0.33	1.10	187.5	187.1
^{132}Sb	2.529±0.132	0.226±0.043	6.0 ±0.4	0.08	1.11	188.2	188.8
^{131}Te	0.295±0.034	0.643±0.061	5.3 ±0.5	0.16	1.11	188.0	188.4
^{133}Te	3.635±0.134	0.536±0.075	4.3 ±0.7	0.001	1.20	188.0	203.6
^{132}I	0.025±0.003	0.450±0.030	8.5 ±0.4	0.45	1.11	188.2	187.9
^{134}I	1.531±0.077	0.405±0.043	7.9 ±0.6	0.30	1.11	187.4	187.9
^{136}I	4.365±0.383	0.669±0.085	8.2 ±1.8	0.34	1.09	185.0	184.5
^{135}Xe	0.231±0.015	0.650±0.060	5.45±0.6	0.17	1.10	186.5	185.6
^{138}Cs	0.553±0.197	0.650±0.110	8.9 ±1.6	0.46	1.08	181.5	181.6

f. $^{246}Cm^{*}$

Nuclide	IY(%) (Yh+Yl)	Yh/(Yh+Yl)	Jrms (h)	β	c (F)	K.E. (MeV) Expt.	K.E. (MeV) Cal.
^{128}Sb	0.214±0.007	0.570±0.032	11.1 ±1.6	0.99	1.11	193.5	193.5
	0.161±0.032	0.558±0.072	10.9 ±1.4	0.96	1.11	193.5	193.5
^{130}Sb	1.155±0.032	0.510±0.030	10.0 ±0.5	0.79	1.12	194.5	195.2
	1.349±0.108	0.509±0.055	10.0 ±0.9	0.79	1.12	194.5	195.2
^{132}Sb	1.678±0.031	0.335±0.034	7.1 ±0.4	0.36	1.11	194.0	193.5
^{131}Te	1.001±0.014	0.704±0.060	6.1 ±1.2	0.37	1.12	194.5	194.9
	1.067±0.07	0.729±0.081	6.5 ±1.8	0.47	1.12	194.5	194.9
^{133}Te	3.226±0.138	0.563±0.049	4.6 ±0.4	0.001	1.14	193.0	198.4
	2.928±0.199	0.593±0.068	4.9 ±0.5	0.04	1.11	193.0	193.2
^{132}I	0.232±0.044	0.482±0.044	8.9 ±0.6	0.55	1.12	194.0	194.6
^{134}I	2.49 ±0.17	0.446±0.037	8.4 ±0.5	0.42	1.11	192.0	192.8
		0.450±0.051	8.5 ±0.7	0.44	1.11	192.0	192.8
^{136}I	2.329±0.275	0.697±0.143	8.7 ±2.2	0.45	1.09	190.0	189.3
	2.255±0.142	0.679±0.075	8.4 ±1.6	0.38	1.09	190.0	189.3
^{135}Xe	1.003±0.032	0.685±0.062	5.85±0.65	0.27	1.10	190.5	190.6
^{138}Cs	1.039±0.019	0.649±0.051	8.9 ±0.9	0.48	1.09	187.5	188.3

g. $^{250}Cf^{*}$

Nuclide	IY(%) (Yh+Yl)	Yh/(Yh+Yl)	Jrms (h)	β	c (F)	K.E. (MeV) Expt.	K.E. (MeV) Cal.
^{128}Sb	0.332±0.044	0.669±0.104	13.2 ±2.3	0.99	0.92	198.0	164.2
^{130}Sb	1.128±0.071	0.620±0.059	12.1 ±1.4	0.99	1.01	199.5	180.3
^{131}Te	1.613±0.179	0.737±0.093	6.6 ±1.2	0.50	1.12	199.8	199.7
^{133}Te	2.136±0.304	0.611±0.134	5.0 ±1.4	0.09	1.12	198.8	199.7
^{132}I	0.763±0.132	0.511±0.126	9.3 ±1.2	0.64	1.12	199.5	199.4
^{134}I	2.483±0.093	0.463±0.081	8.65±1.15	0.47	1.11	197.0	197.6
^{136}I	1.482±0.369	0.621±0.164	7.5 ±1.9	0.17	1.10	195.0	195.9
^{138}Cs	3.002+0.209	0.676±0.250	9.3 ±3.0	0.57	1.09	193.0	193.3
^{154}Pm	0.403±0.03	0.776±0.261	9.7 ±3.6	0.47	1.02	176.5	176.7

h. ^{252}Cf

Nuclide	IY(%) (Yh+Yl)	Yh/(Yh+Yl)	Jrms (h)	β	c (F)	K.E. (MeV) Expt.	K.E. (MeV) Cal.
^{128}Sb	0.027±0.003	0.534±0.076	10.5 ±1.4	0.81	1.06	189.0	188.6
^{130}Sb	0.515±0.058	0.456±0.066	8.9 ±1.3	0.51	1.08	191.7	192.1
^{132}Sb	0.882±0.043	0.374±0.037	7.5 ±0.5	0.42	1.09	193.8	193.9
^{131}Te	0.401±0.041	0.641±0.078	5.3 ±1.0	0.14	1.10	195.0	195.5
^{133}Te	1.996±0.31	0.546±0.071	4.4 ±0.6	0.01	1.18	195.5	209.7
^{132}I	0.134±0.047	0.565±0.072	10.2 ±1.1	0.80	1.10	196.0	195.2
^{134}I	1.10 ±0.137	0.549±0.066	9.9 ±1.0	0.73	1.10	195.5	195.2
^{136}I	1.776±0.115	0.755±0.055	10.0 ±1.5	0.72	1.09	193.8	193.4
^{135}Xe	0.315±0.032	0.651±0.059	5.5 ±0.65	0.18	1.10	195.5	194.8
^{138}Xe	2.3 ±0.345		6.7	0.43	1.08	191.0	191.3
^{140}Xe	1.5 ±0.225		10.05	0.99	1.04	189.5	184.2
^{138}Cs	0.701±0.119	0.582±0.068	7.9 ±0.9	0.23	1.08	191.0	190.8
^{142}Ba	2.9 ±0.435		8.2	0.69	1.06	187.5	186.8
^{144}Ba	3.6 ±0.540		7.2	0.47	1.06	186.5	186.8
^{146}Ba	1.01 ±0.152		5.9	0.16	1.05	185.5	185.0
^{146}Ce	1.04 ±0.156		8.8	0.78	1.06	185.5	185.5
^{148}Ce	2.31 ±0.323		8.9	0.77	1.05	183.0	183.7
^{150}Ce	>0.98±0.147		8.9	0.74	1.04	181.0	182.0
^{152}Nd	>0.6 ±0.090		8.85	0.71	1.03	178.5	178.7
^{154}Nd	>0.4 ±0.060		9.75	0.84	1.02	176.5	177.0
^{158}Sm	>0.15±0.023		11.1	0.99	0.99	171.5	169.9

Table 2. Yield weighted average angular momentum of different elements in various fissioning systems.

	$^{230}Th^*$	$^{234}U^*$	$^{236}U^*$	$^{240}Pu^*$	$^{242}Pu^*$	$^{246}Cm^*$	$^{250}Cf^*$	^{252}Cf
Sn	-	-	5.7	-	-	-	-	-
Sb	7.49	7.74	6.77	8.27	6.53	9.03	12.35	8.06
Te	4.76	4.93	4.98	5.27	4.38	4.96	5.69	4.55
I	8.11	8.01	8.15	8.45	8.12	8.53	8.40	9.97
Xe	4.7	4.86	5.5	5.13	5.45	5.85	-	7.83
Cs	8.7	10.1	10.0	9.35	8.9	8.9	9.3	7.9
Ba	-	-	-	-	-	-	-	7.24
Ce	-	-	-	-	-	-	-	8.87
Nd	-	-	-	-	-	-	-	9.39
Pm	-	11.8	11.0	-	-	-	9.7	-
Sm	-	-	-	-	-	-	-	11.1

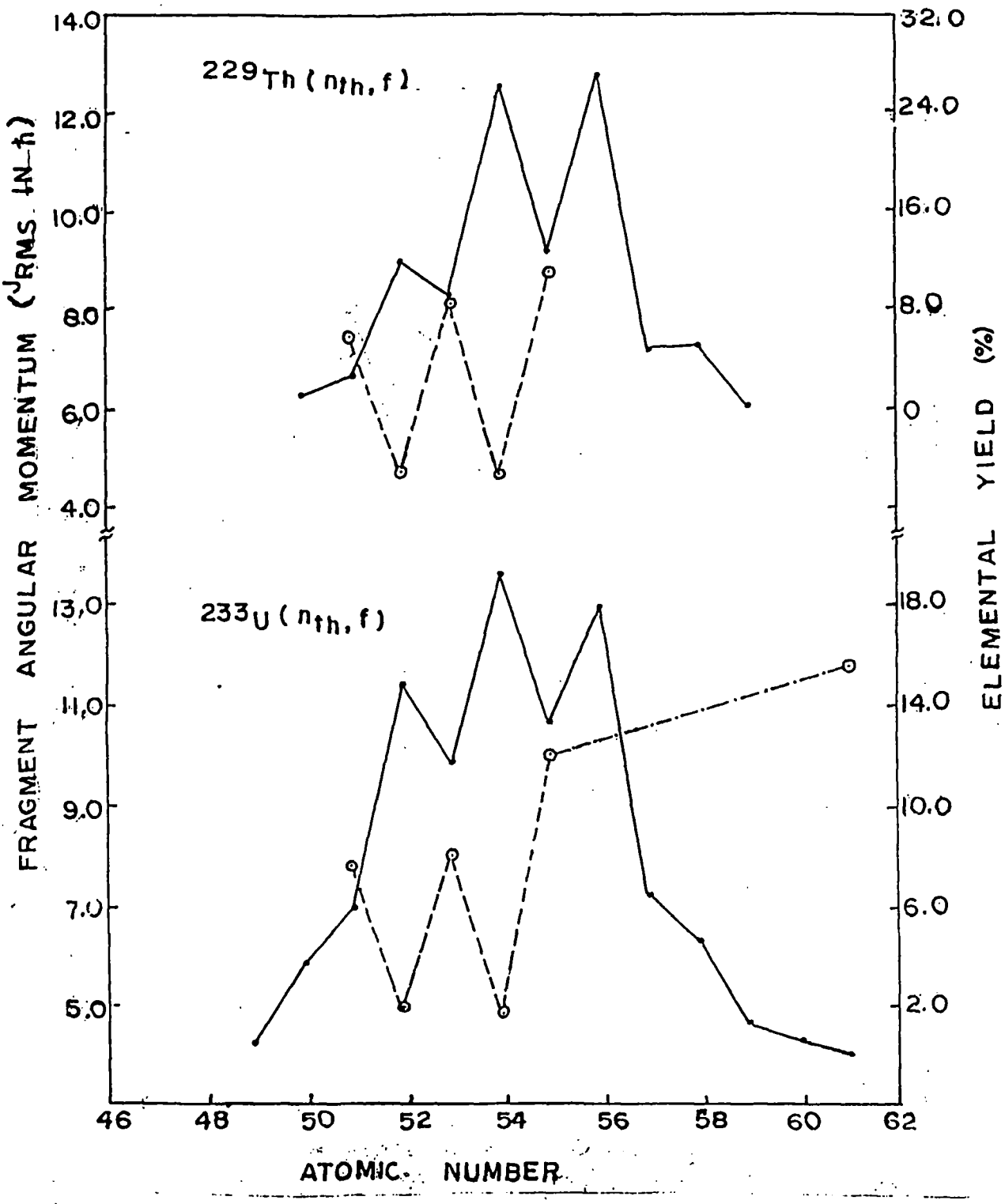

FIG.1. CORRELATION OF FRAGMENT ANGULAR MOMENTUM AND ELEMENTAL YIELDS IN $^{229}Th(n_{th},f)$ AND $^{233}U(n_{th},f)$.

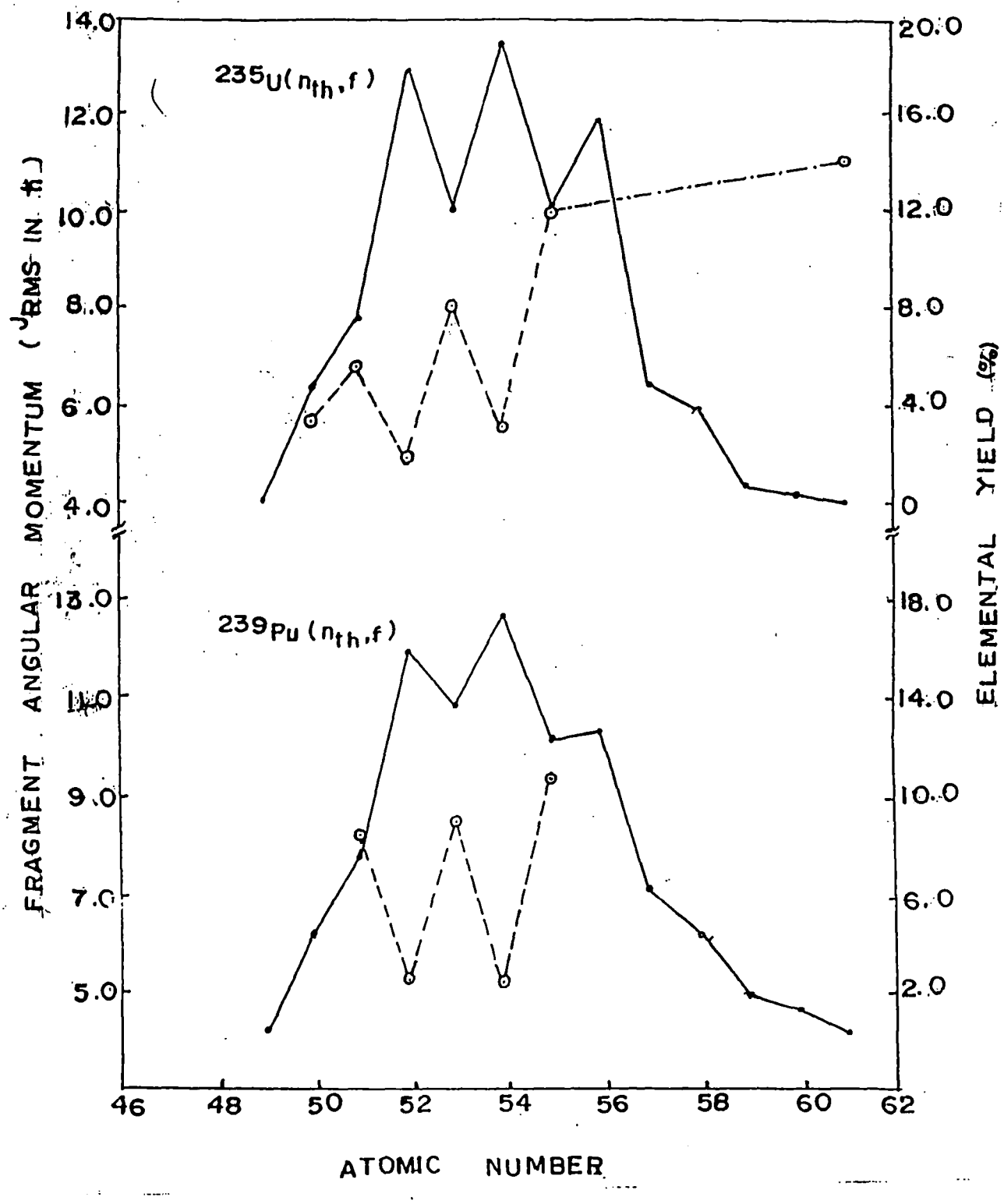

FIG.2. CORRELATION OF FRAGMENT ANGULAR MOMENTUM AND ELEMENTAL YIELDS IN $^{235}U(n_{th},f)$ AND $^{239}Pu(_{th},f)$.

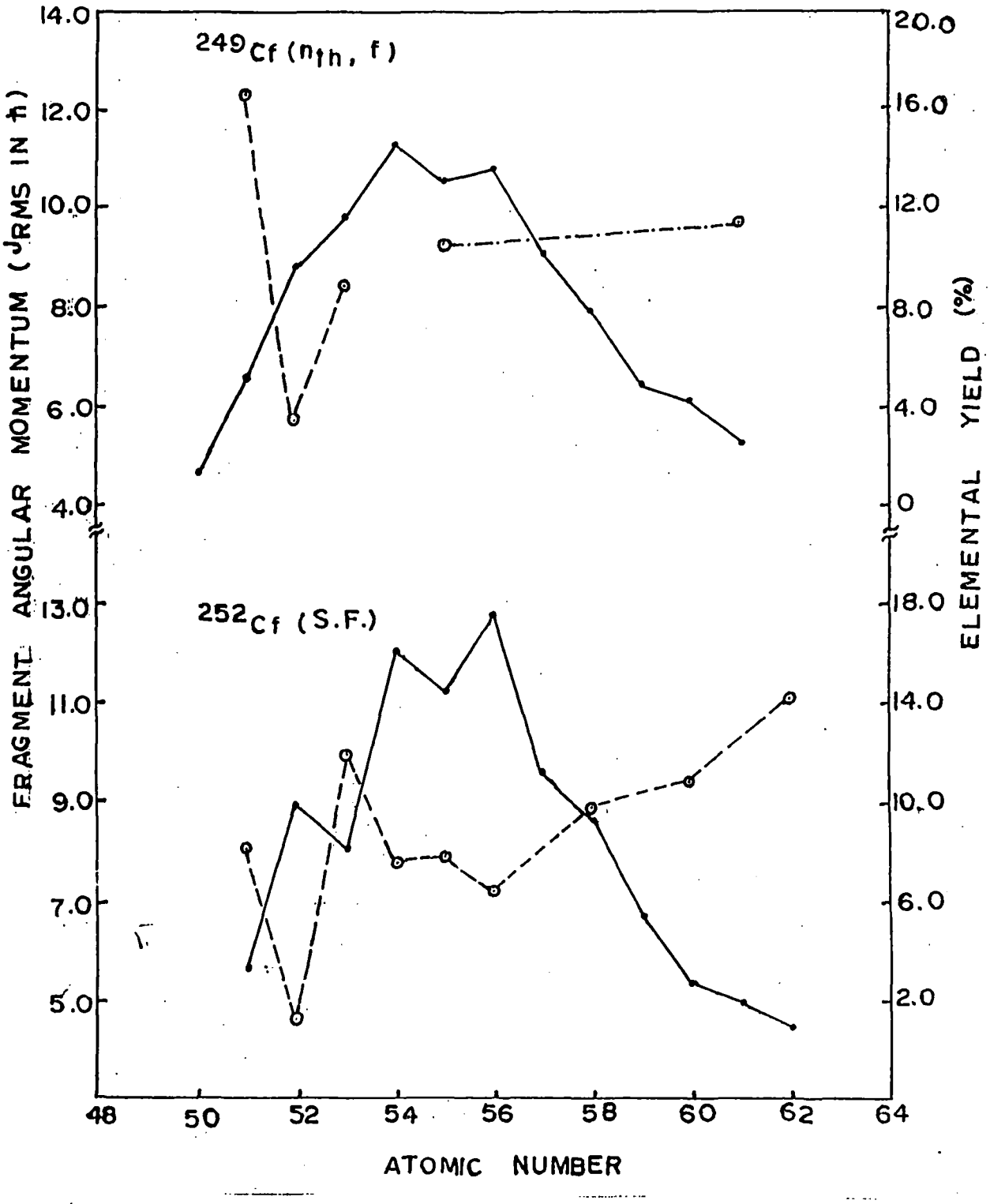

FIG.3. CORRELATION OF FRAGMENT ANGULAR MOMENTUM AND ELEMENTAL YIELDS IN $^{249}Cf(n_{th},f)$ AND $^{252}Cf(S.F.)$.

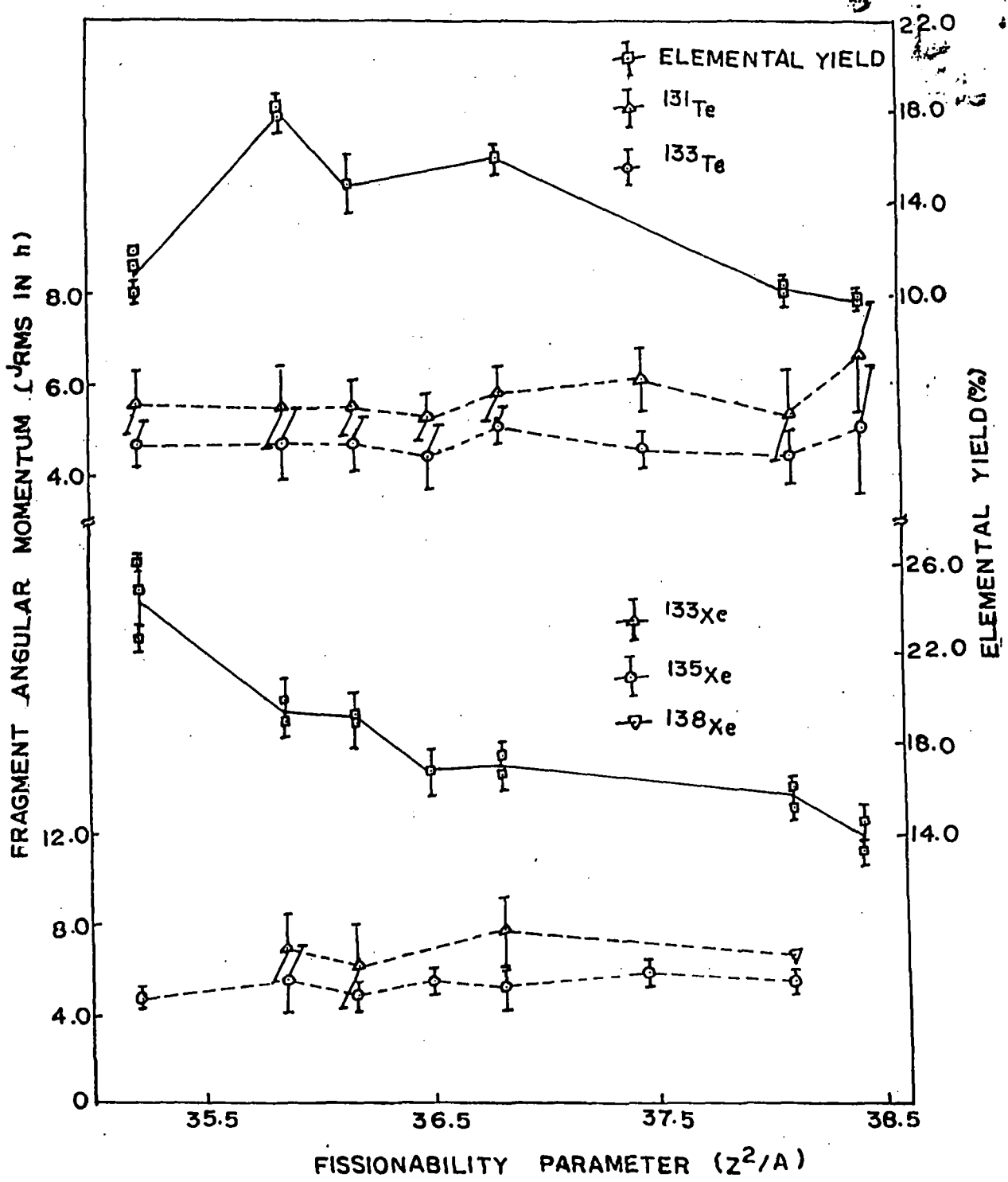

FIG.4. COMPARISON OF FRAGMENT ANGULAR MOMENTUM OF ^{131}Te, ^{133}Te, ^{133}Xe, ^{135}Xe AND ^{138}Xe WITH THEIR ELEMENTAL YIELD IN DIFFERENT FISSIONING SYSTEMS.

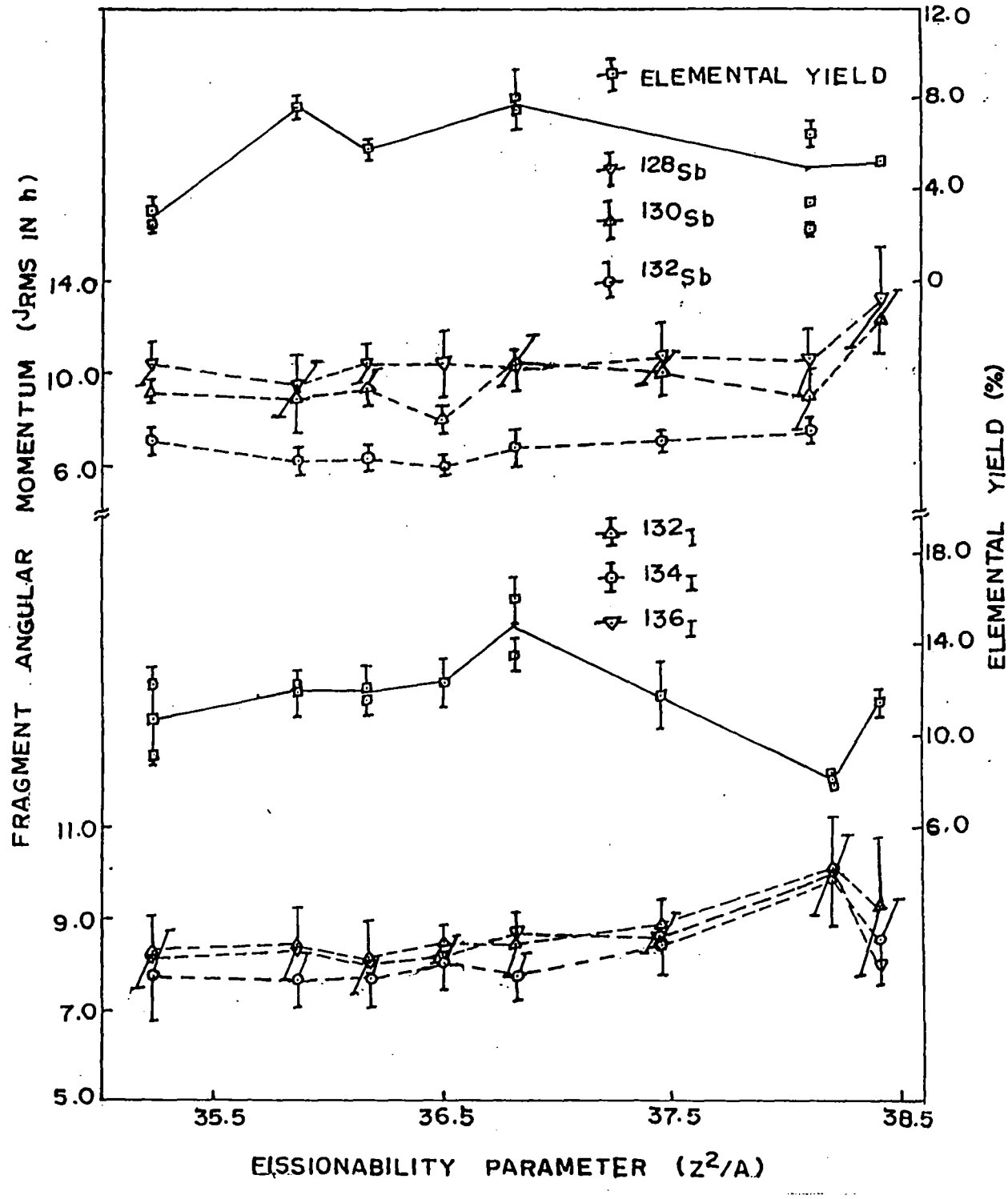

FIG.5. COMPARISON OF FRAGMENT ANGULAR MOMENTUM OF ^{128}Sb, ^{130}Sb, ^{132}Sb, ^{132}I, ^{134}I AND ^{136}I WITH THEIR ELEMENTAL YIELD IN DIFFERENT FISSIONING SYSTEMS.

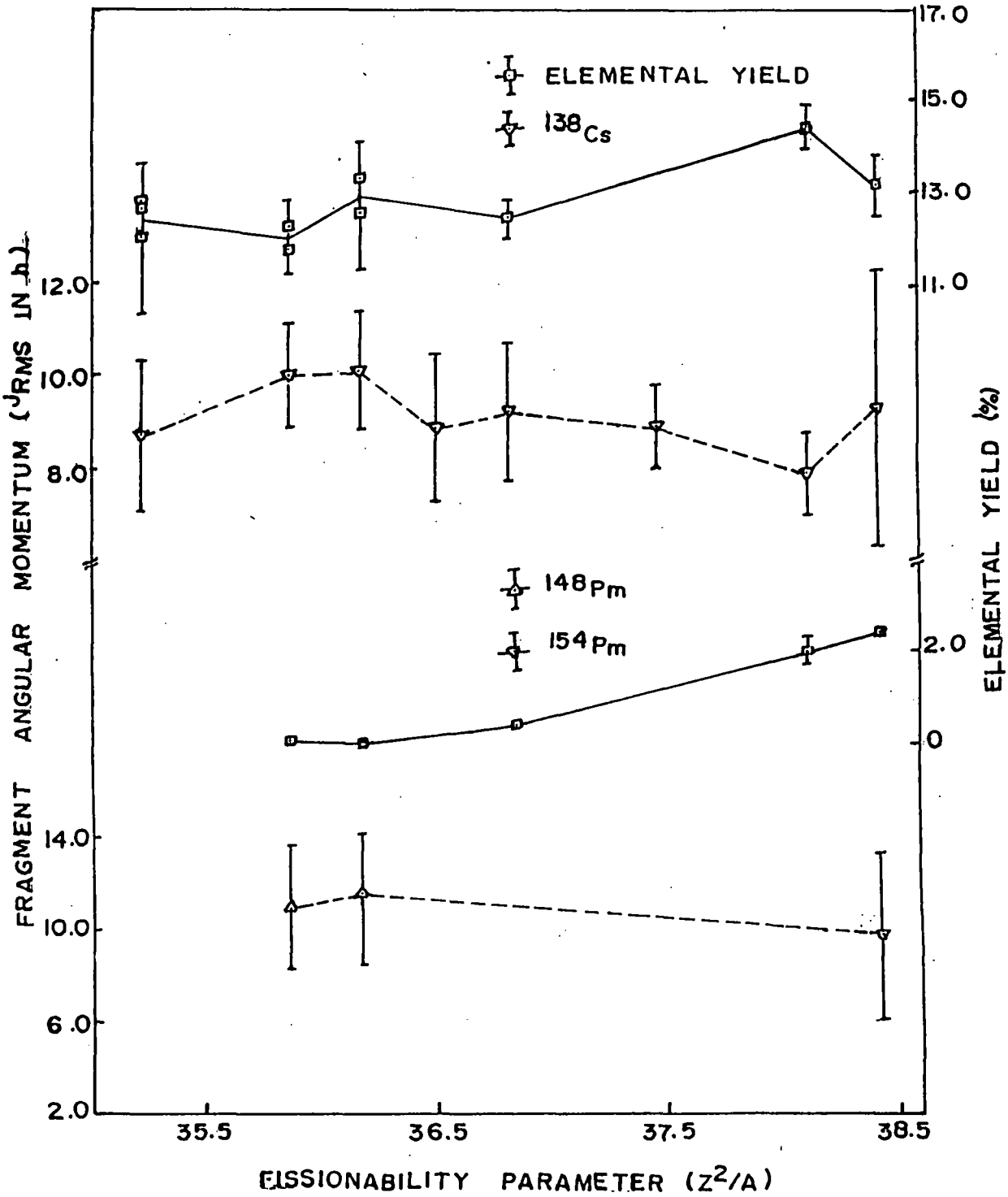

FIG.6. COMPARISON OF FRAGMENT ANGULAR MOMENTUM OF ^{138}Cs, ^{148}Pm, AND ^{154}Pm WITH THEIR ELEMENTAL YIELD IN DIFFERENT FISSIONING SYSTEMS.

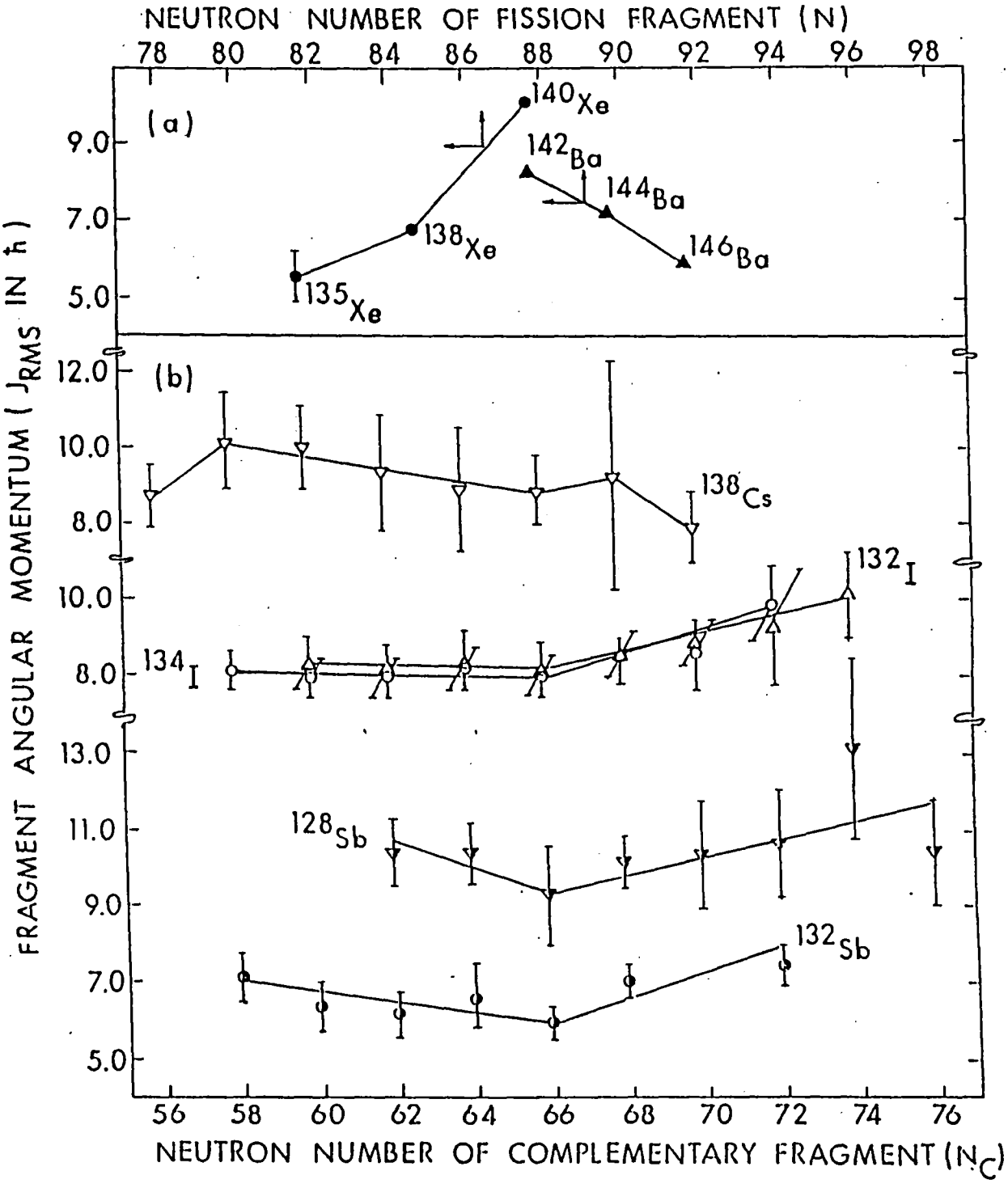

FIG.7. EFFECT OF DEFORMED 88 AND 66 NEUTRON SHELL ON ITS ANGULAR MOMENTUM.

A. Single-neutron transfer process has been studied at near-barrier energies in $^{197}Au+^{12}C$ and $^{197}Au+^{16}O$ reactions at the BARC-TIFR Pelletron facility. In these reactions high spin fractions(HSF) for ^{196}Au were measured at different bombarding energies using stack-foil irradiation, radiochemical separation and high resolution gamma-spectrometric techniques. The data are shown in table-1 at different energies(E_{cm}) along with the corresponding values for input angular momenta and Q_{eff} values that provide the interpretations.

- T.Datta, S.P.Dange, H.Naik, P.K.Pujari and S.B.Manohar.

B. Fission fragment (^{134}I) spin has been measured as a function of fragment emission angles in an odd-Z system $^{237}Np(\alpha_{29MeV},f)$ and even-Z system $^{238}U(\alpha_{39MeV},f)$. Effects of the collective rotational degrees (esp. tilting) and single particle spin ($j \geq k \approx 4h$) in odd-Z ^{241}Am fission and only of the collective degrees in even-Z ^{242}Pu fission were seen, as shown in fig-1. Fragment spin were deduced from independent isomeric yields at six emission angles($90° \geq \theta \geq 10°$) and statistical model based code GROGI2. Indèpendent isomeric yield ratios at different θ were obtained employing recoil-catcher collection and off-line high resolution gamma-spectrometric techniques.

- T.Datta, H.Naik and S.P.Dange

: Phys. Rev. C-46,1445(1992) & Phys.Rev. C (communicated)(1995).

C. Fission fragment angular distributions as a function of mass-asymmetry were determined in the even-Z fissioning systems $^{232}Th(\alpha,f)$ and $^{238}U(\alpha,f)$ and in the odd-Z system $^{237}Np(\alpha,f)$ at different energies($E\alpha$). Recoil-catcher collection and off-line gamma spectrometric techniques were used and average angular anisotropy, W(0)/W(90), for the asymmetric and symmetric modes in each fissioning system were deduced. Fig-2 shows W(0)/W(90) in the even-Z systems along with literature data at various energies. Theoretical plots deduced employing the transition-state model and considering multichance fission and individual mode's tilting mode variances(K_0^2) seem to be adequate. For the odd-Z ^{241}Am fission, similar theoretical evaluation is inadequate (table-2) due to contribution, $\langle k^2 \rangle$, from single particle spin to K_0^2. The deduced $\langle k^2 \rangle$ values are shown in table-2.

- T.Datta, S.P.Dange, H.Naik and S.B.Manohar

: Phys.Rev. C-48,221,(1993) & Z.Phys. A-(1995)(In Press).

Table-1. HSF for ^{196}Au from ^{12}C and ^{16}O reactions on ^{197}Au.

Reaction	E_{cm} MeV	$\langle l \rangle$ $\hbar$	HSF	Q_{eff} MeV
$^{197}Au+^{12}C$	55	8.1	0.04	0.0
V_C=62MeV	66	12.4	0.15	-2.9
	76	20.6	0.20	-5.5
	82	24.7	0.21	-6.8
$^{197}Au+^{16}O$	74	9.2	0.03	0.0
V_C=81MeV	81	9.6	0.07	-1.1
	84	11.8	0.11	-1.5
	93	21.3	0.13	-3,2

Error on HSF values ≈10-12%.

Table-2 : Experimental Average Angular Anisotropy values for the Symmetric and Asymmetric modes in the system $^{237}Np(\alpha,f)$ at Eα= 29 and 44 MeV and Theoretical Analysis for K_0^2 and odd-proton spin contribuion $\langle k^2 \rangle$.

(Target spin=5/2).

MODE:	Asymmetric	Symmetric
$I_{\perp Rigid}(\hbar^2/MeV)$	306.1	214.9
$I_{\parallel Rigid}(\hbar^2/MeV)$	75.6	84.3
- AT Eα= 29 MeV.	E^*= 22.9 MeV.	$\langle J \rangle$= 9.0 $\hbar$
$W(0)/W(90)_{CM}$	1.22±0.09	1.13±0.06
K_0^2 ($\hbar^2$) :calc.	80	112
K_0^2 ($\hbar^2$) :expt.	90±10	128±14
$\langle k^2 \rangle_p$	≈10	≤ 18
- AT Eα= 44 MeV.	E^*= 37.8 MeV.	$\langle J \rangle$=15.4 $\hbar$
$W(0)/W(90)_{CM}$	1.51±0.05	1.35±0.05
K_0^2 ($\hbar^2$) :calc.	110	154
K_0^2 ($\hbar^2$) :expt.	120±13	170±20
$\langle k^2 \rangle_p$	≈10	≤ 16

* Error on $\langle k^2 \rangle$ ≈15-30 %

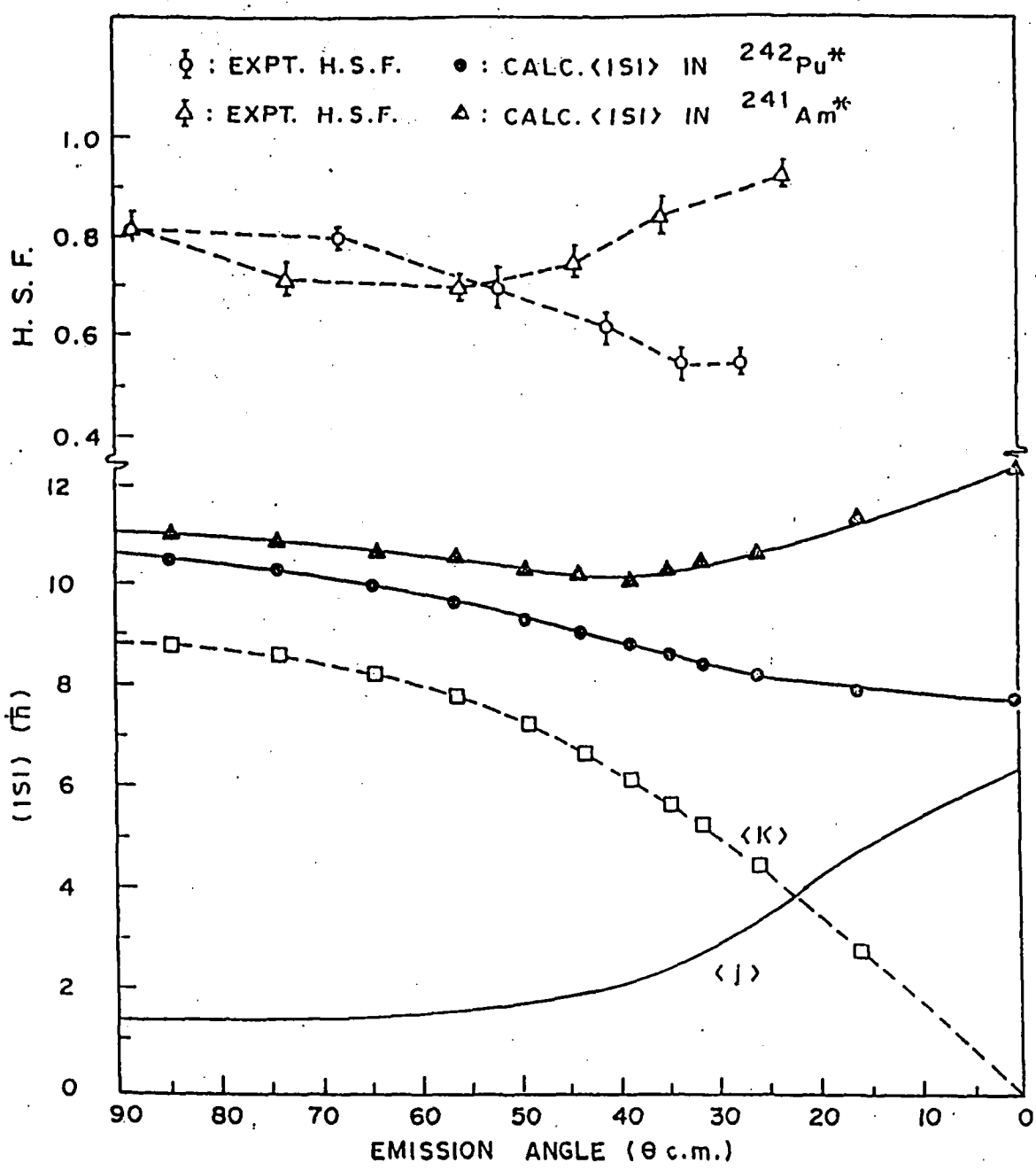

FIG.-1. VARIATIONS OF ODD-Z FRAGMENT SPIN [⟨ISI⟩] AND HIGH SPIN FRACTION [Ym/(Ym+Yg)] WITH EMISSION ANGLES IN EVEN-Z AND ODD-Z FISSIONING NUCLEI.

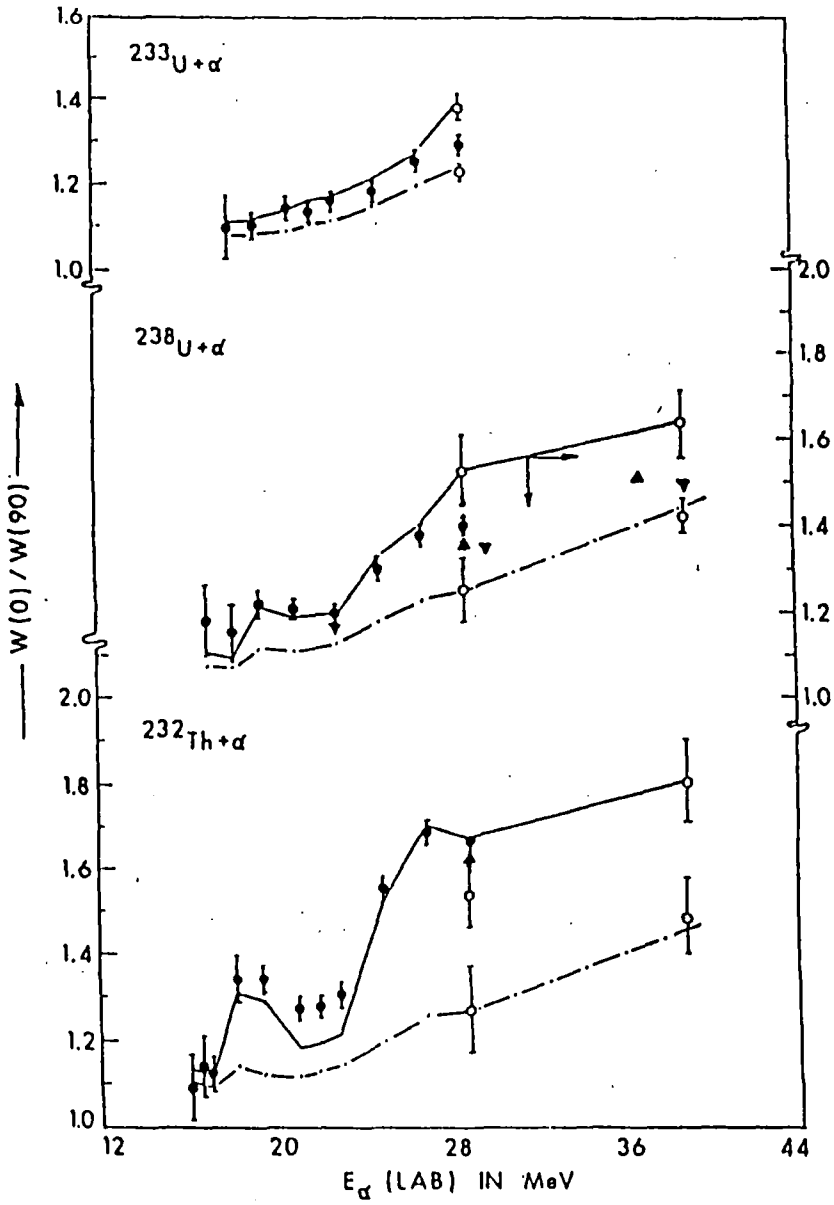

FIG.- 2. COMPARISON OF THEORETICAL & EXPERIMENTAL ANGULAR ANISOTROPY IN $^{232}Th(\alpha, f)$, $^{238}U(\alpha, f)$ & $^{233}U(\alpha, f)$.
EXPT. DATA : o THIS LAB., • Ref.(5), ▲ Ref.(6), ▼ Ref.(7)
THEORETICAL PLOTS: —— ASYMM. MODE,
·-·-·- SYMM. MODE.

1. Recoil range distribution (RRD) of radioactive evaporation residues in ^{12}C + ^{93}Nb and ^{16}O + ^{89}Y.

B.S.Tomar, A.Goswami, S.K.Das, A.V.R.Reddy, P.P.Burte, S.B.Manohar and B.John

Recoil range distribution (RRD) of radioactive evaporation residues in 63 and 77.5 MeV ^{12}C + ^{93}Nb and 68 MeV ^{16}O + ^{89}Y have been measured using recoil catcher technique followed by gamma ray spectrometry(1). The RRDs of ^{101}Pd and ^{100}Pd showed a Gaussian curve with the mean range equal to that expected for complete fusion (CF) products. On the other hand the RRDs of ^{99}Rh showed two components representative of CF and incomplete fusion (ICF). In the case of ^{12}C + ^{93}Nb the technetium products showed a predominantly low range (ICF) component while in the case of ^{16}O + ^{89}Y the RRDs of technetium products was a broad Gaussian with mean range equal to that expected for CF. Figures 1-3 show the RRDs for the evaporation residues in the three systems.

The experimental RRDs were compared with those predicted for CF. In the case of products showing ICF components the CF curves were subtracted from the experimental curves to obtain the ICF cross sections. Table 1. gives the CF and ICF cross sections obtained by summing the ICF contributions in the individual evaporation residues.

References:

1. B.S.Tomar, A.Goswami, S.K.Das, A.V.R.Reddy, P.P.Burte, S.B.Manohar and B.John Phys. Rev. C49, 941 (1994).

Table 1.

Complete fusion and incomplete fusion cross sections

System	Cross section (mb)	
	CF	ICF
63 MeV ^{12}C + ^{93}Nb	950±27	138±14
77.5 MeV ^{12}C + ^{93}Nb	1400±37	180±12
68 MeV ^{16}O + ^{89}Y	770±20	86±9

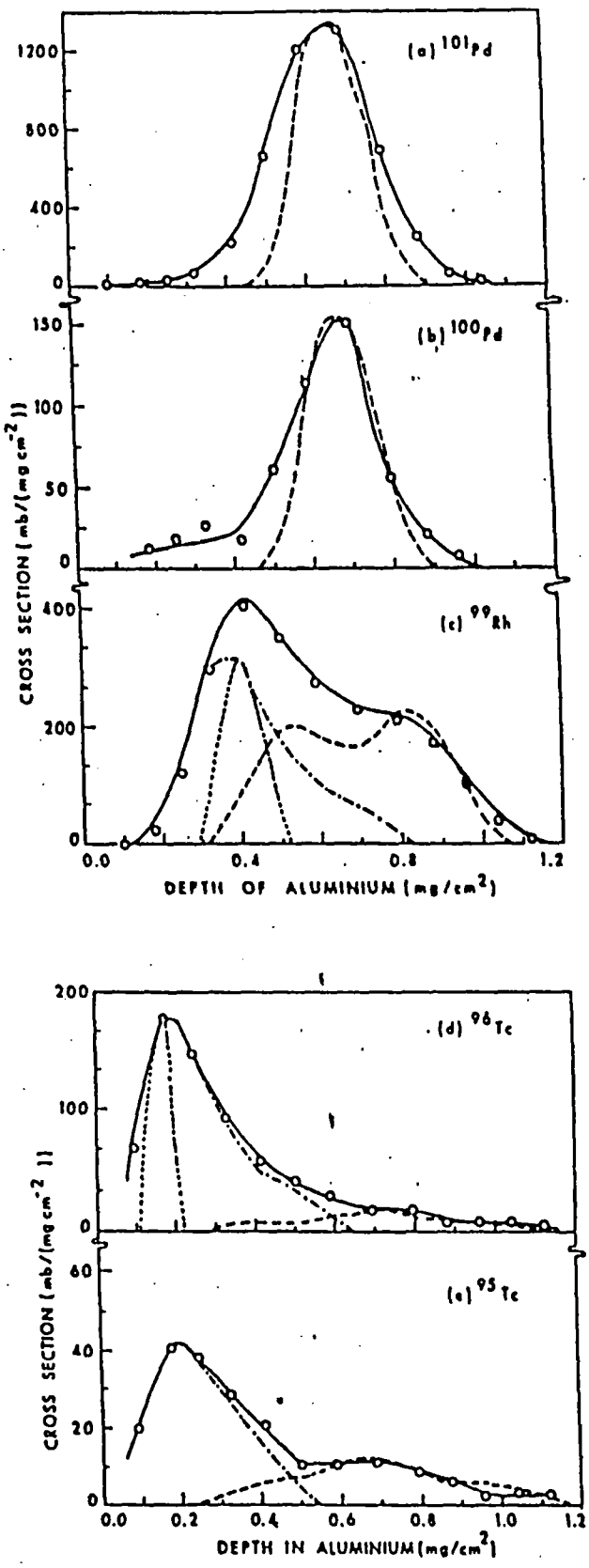

FIG. 1. Recoil range distributions in 63 MeV $^{12}C+^{93}Nb$. The solid lines are guides to the experimental data. Dashed lines are the PACE2 curves for the CF process. The dotted lines are obtained by simulation of the ICF process based on the breakup fusion model. The dash-dotted curves are the ICF components obtained by subtracting the CF part from the experimental curves.

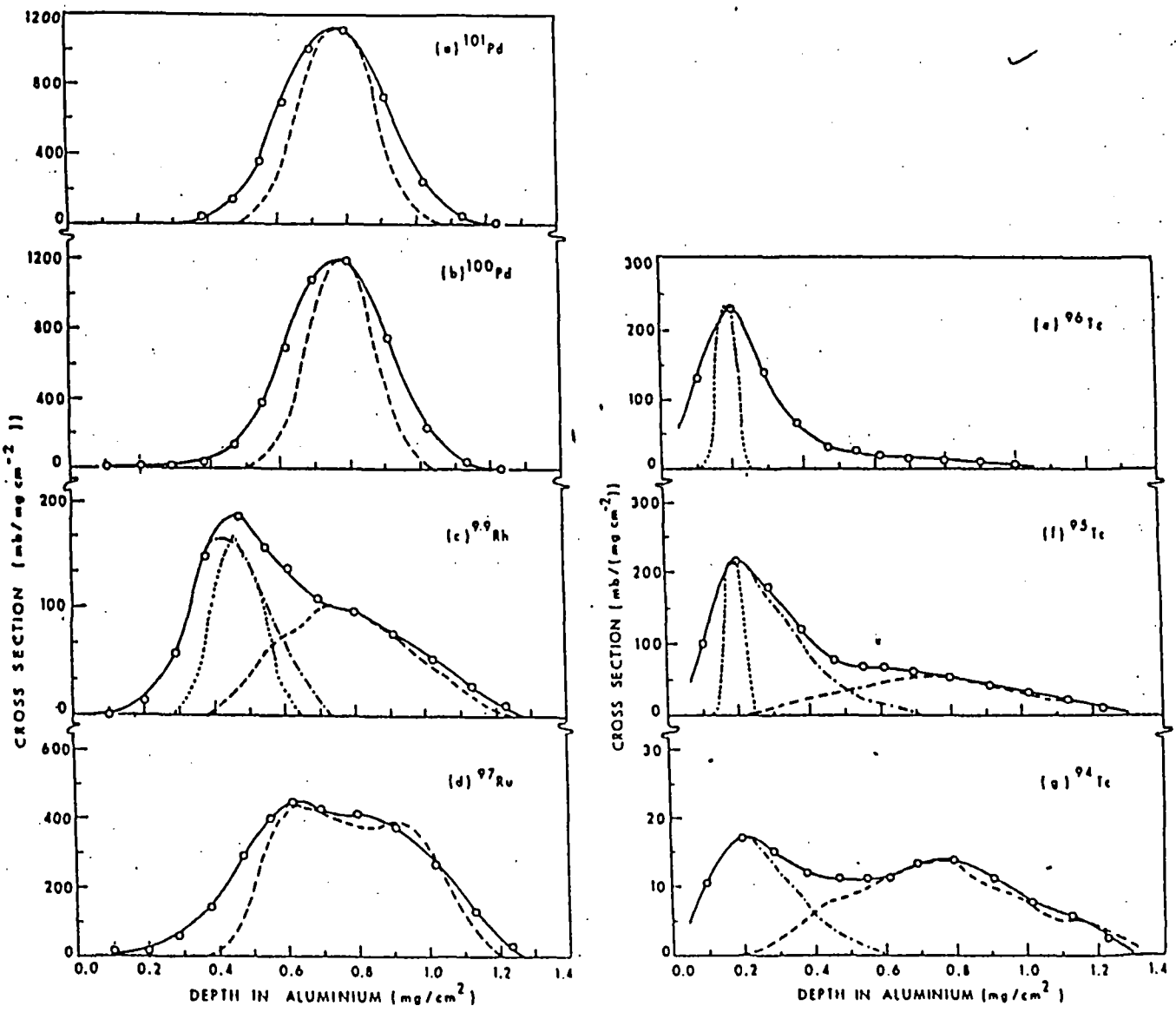

FIG. 2. Recoil range distributions in 77.5 MeV ^{12}C+^{93}Nb. The notation is the same as in Fig. 1.

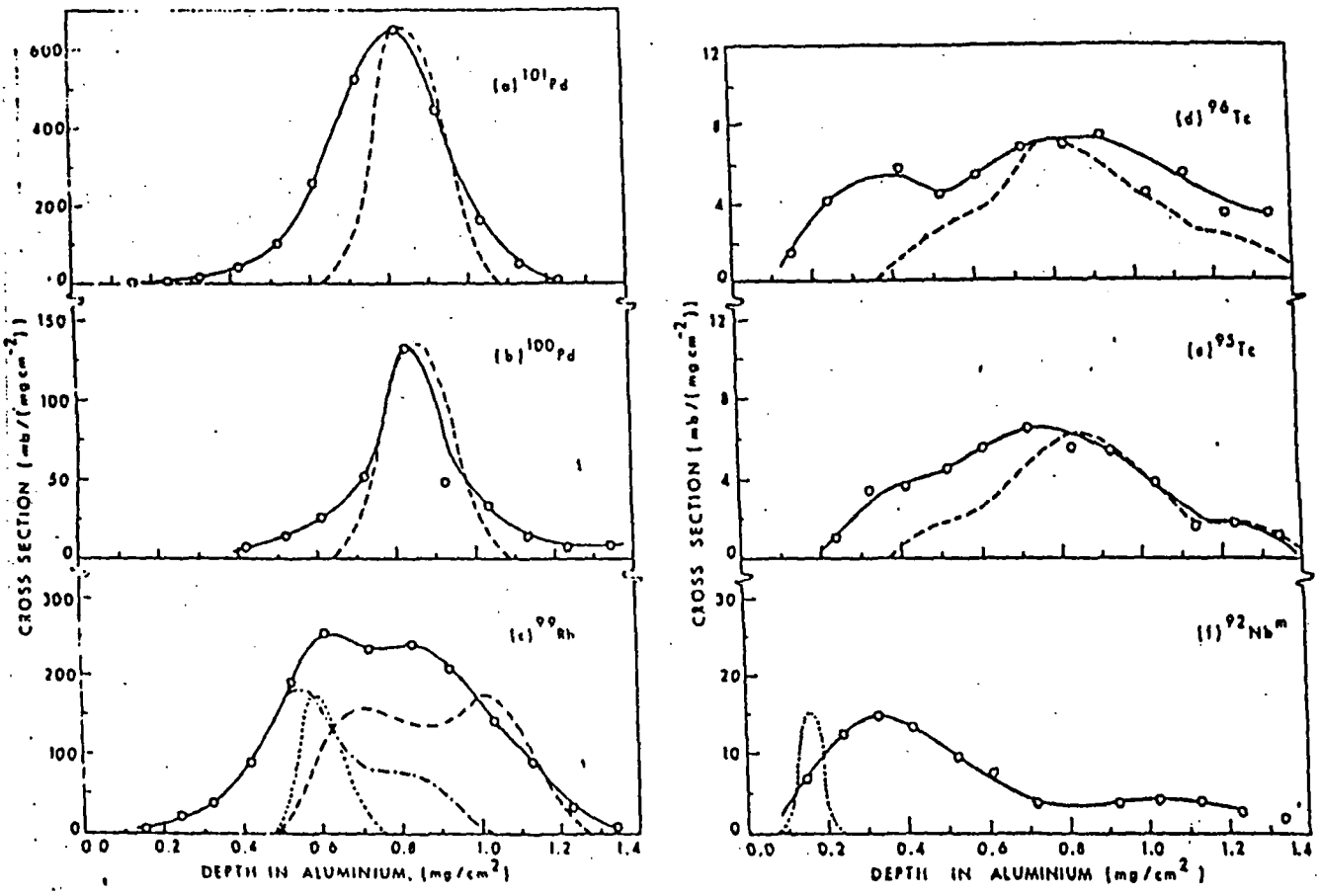

FIG. 3. Recoil range distributions in 68 MeV ^{16}O+^{89}Y. The notation is the same as in Fig. 1.

2. Mass distribution in ^{16}O induced fission of ^{232}Th.

A.Goswami, A.V.R.Reddy, B.S.Tomar, P.P.Burte, S.B.Manohar and B.John

Recoil catcher and gamma spectrometry of fission products were used to determine the cumulative/ independent cross sections of 18 fission products in 92 and 105 MeV ^{16}O induced fission of ^{232}Th(1). The charge distribution parameters were obtained from the best fit of the mass distribution. Figure 4. shows the mass distribution curves. The fission cross sections at 91 and 105 MeV beam energy are 386±35 and 595±48 mb and the total number of neutrons emitted per fission are 8.4±1.4 and 10.2±1.2 respectively.

References:

1. A.Goswami, A.V.R.Reddy, B.S.Tomar, P.P.Burte, S.B.Manohar and B.John Radiochim. Acta 62, 173 (1993)

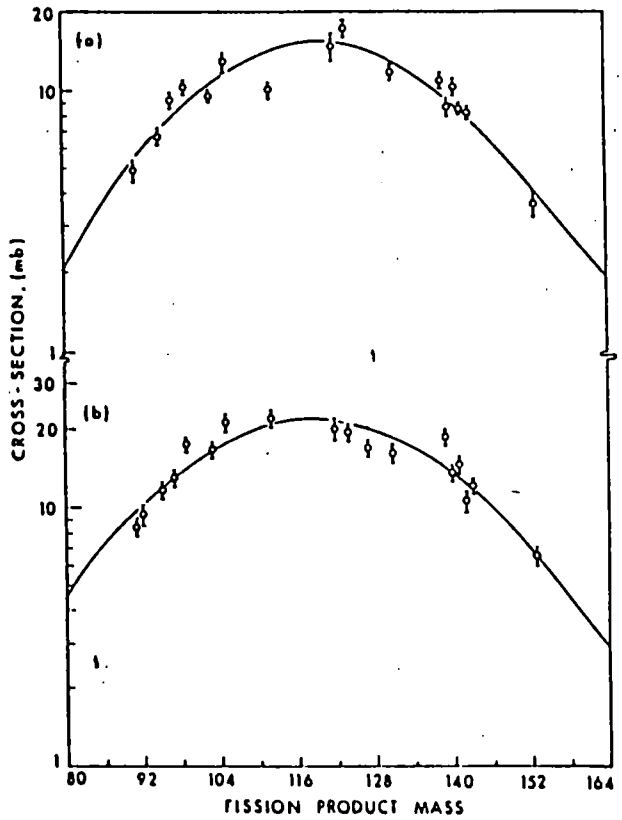

Fig. 1. Mass yield distribution in (a) 92 MeV and (b) 105 MeV ^{16}O-induced fission of ^{232}Th.

3. Charge distribution in 96 MeV ^{16}O induced fission of ^{238}U

A.V.R.Reddy, A.Goswami, B.S.Tomar, S.B.Manohar, S.K.Das, P.P.Burte and Satya Prakash

Independent yields of iodine isotopes in 96 MeV ^{16}O induced fission of ^{238}U have been determined radiochemically(1). These yields were used to calculate the width and the most probable mass of the isotopic yield distribution. The values obtained are 2.07±0.09 and 129.7±0.1 mass units respectively. Figure 5 shows the measured isotopic yield distribution. Using the unchanged charged distribution (UCD) hypothesis the total number of neutrons in this reaction was calculated as 9.3±0.3.

References:

1.A.V.R.Reddy, A.Goswami, B.S.Tomar, S.B.Manohar, S.K.Das, P.P.Burte and Satya Prakash Radiochim. Acta 64,149(1994).

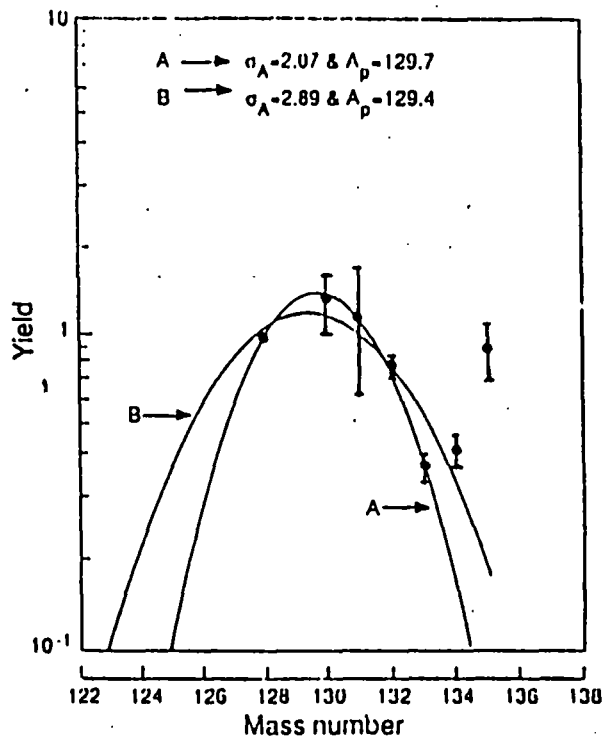

Fig. 2. Isotopic yield distribution of iodine in $^{16}O + ^{238}U$ (one page).

Excitation function of ^{4}He-ion-induced fission of Dy (Natural)

As part of a long-range programme of work on the measurement of fission excitation functions of low Z (Z < 80) elements[1,2], the fission cross sections of Nat. Dysprosium (Z=66) induced by ^{4}He-ions in the energy range 35-50 MeV were measured using the sensitive "fission track" technique using lexan polycarbonate plastic as detectors. Targets of (spec. pure grade) high purity Dy_2O_3 ,further purified by a series of anion exchange technique, deposited on high purity (99.9999%) silver foils were irradiated with ^{4}He-ions of different energies from the Variable Energy Cyclotron at Calcutta. The heavy elements contents of both the dysprosium oxide and the silver foils were estimated to be not more than 1-3 ppb. The experimental ^{4}He-ion-induced fission cross sections of natural Dysprosium ($^{162.5}$Dy) is shown in Table-1.

Table-1 Experimental Fission Cross Sections of $^{4}He+^{162.5}Dy$ system :

E_L MeV	E^* MeV	σ_R (Reaction cross section) cm^2	σ_f (Fission)* cm^2
35	33.4	1.569×10^{-24}	$(9.5\pm6.5)\times10^{-35}$
40	38.3	1.740×10^{-24}	$(2.29\pm0.15)\times10^{-33}$
45	43.2	1.866×10^{-24}	$(2.58\pm0.21)\times10^{-32}$
50	48.05	1.961×10^{-24}	$(8.39\pm0.52)\times10^{-32}$

* Error quoted in cross sections are statistical error only. Accuracy from 40-50 MeV = 30-40% and at 35 MeV = 70%.

From the experimental cross section, the ratio, Γ_f/Γ_n , which measures the competition between fission and neutron emission was calculated. For low Z elements this ratio is very nearly equal to σ_f/σ_R where σ_R is the total reaction cross section which can be computed by standard optical model codes. These ratios i.e. $\Gamma_f/\Gamma_n \approx \sigma_f/\sigma_R$,were analysed using the statistical model expression given by Vandenbosch and Huizega[3] to get the fission barrier E_f and the level density parameters a_n and a_f. A least square fitting procedure was used to fix the experimental Γ_f/Γ_n

ratios by varying the values of a_f and a_n. The best fit values are E_f = 27.5±3.5 MeV, a_f= 15.136 MeV^{-1}, a_n =15.136 MeV^{-1} and a_f/a_n = 1.00. This experimental fission barrier ($^{162.5}Dy+^{4}He$ --> $^{166.5}Er$) obtained by analysis of the excitation function was compared with fission barriers calculated by theoretical models such as the simple liquid drop model (LDM)[4], rotating liquid drop model (RLDM)[5], shell-corrected liquid drop model[6] and rotating finite range models (RFRM) of Sierk[7]. These are summarized in the table-2. For comparison, data on a few other lighter elements based on our earlier work[1,2] are also included in the Table. These results provide some excellent systematics on fission barriers and level density parameters over a wide range of Z.

Target	C.N.	a_f MeV^{-1}	a_f/a_n	Exp. E_f (MeV)	E_f(LDM) (MeV)	E_f(RLDM) (MeV)	E_f(Shell-cor.) (MeV)	E_f(RFRM) (MeV)
Nat.Dy	$^{166.5}Er$	A/11	1.00	27.5±3.5	33.93	32.55	32.9	27.8
^{159}Tb	^{163}Ho	A/12	1.01	31.5±3.5	36.98	33.6	34.3	28.4
^{165}Ho	^{169}Tm	A/12	1.04	29.8±3.0	34.6	31.2	32.6	26.6
Nat.Er	$^{171.3}Yb$	A/12	1.03	27.8±3.0	33.1	29.7	31.1	25.3

REFERENCES:

[1] R.H. Iyer, A.K. Pandey, P.C. Kalsi and R.C. Sharma. Physical Review C, Vol. 44, No. 6, 2644-2652 (1991).

[2] R.H.Iyer, A.K.Pandey, P.C.Kalsi and R.C.Sharma, Phys. Rev. C , 48, 87-94 (1993).

[3] R. Vandenbosch and J.R. Huizenga, Nuclear Fission (Academic, New York, 1973).

[4] S.Cohen and W.J. Swiatecki, Ann.Phys. (N.Y.) 22, 406 (1963).

[5] S.Cohen, F.Plasil, W.J.Swiatecki, Ann. Phys. 82, 557 (1974).

[6] W.D. Myers and W.J. Swiatecki, Lawerence Radiation Laboratory Report No. UCRL/11980 (1965).

[7] A.J. Sierk, Phys. Rev. C 33, 2039 (1986).

[P.C.KALSI, A.K.PANDEY, R. SAMPATH KUMAR and R.H.IYER]

FISSION PROPERTIES OF ^{183}Os COMPOUND NUCLEUS FORMED BY $^{171}Yb+^{12}C$ THE REACTION

The study of heavy-ion-induced fission of low Z elements at moderate excitation energies, provides unique opportunities to understand the fission properties of high spin fissioning systems and to test theoretical models. In our earlier studies[1-3], the fission cross sections and fragment angular distributions of the ^{181}Re compound nucleus produced by two target + projectile combinations ($^{12}C+^{169}Tm$ and $^{16}O+^{165}Ho$) and the compound nucleus ^{213}Fr ($^{16}O+^{197}Au$) were studied at several bombarding energies above the fusion barriers. It is seen from these studies that the best fits to the experimental fission cross sections data are provided by using the angular momentum dependent fission barrier, $E_f(J)$ from the Rotating Finite Range Model, RFRM of Sierk[4].

In order to test the valadity of the theoretical models predicting angular momentum dependent fision barriers particularly in the lighter elements region, the fission properties of ^{183}Os compound nucleus produced by the ^{12}C induced reaction on isotopically enriched ^{171}Yb were investigated. The experiments were carried out at the 14 UD BARC-TIFR Pelletron facility in TIFR Bombay at bombarding energies 80, 84, 87 MeV using identical techniques as described in our earlier papers[1&5]. The experimental results and data analysis are given in Table-1. This study also indicates that the 'best fit' to the experimental fission cross sections are provided by statistical model using angular-momentun-dependent fission barriers from RFRM of Sierk[4].

TABLE-1 $^{171}Yb+^{12}C$ System (X=0.65)

E_{lab} (MeV)	E^* (MeV)	σ_f(Exp.) mb	σ_f(Cal.)[a] mb	$\langle l \rangle_{av}$[b] h	W_{168}/W_{90} (Expt.)
80	58.8	3.66	3.46	24.18	3.30
84	62.6	8.53	7.66	25.51	4.44
87	65.4	15.81	11.45	26.84	4.59

a-Calculated by statistical model using $a_f=A/8$, $a_f/a_n=1.03$(best fit) and $E_f(J)$ values 15.7, 15.4 and 15.2 respectively from RFRM.
b- Calculated from Bass model.

REFERENCE:

[1] A.K.Pandey, R.C.Sharma, P.C.Kalsi and R.H.Iyer, DAE Symp. on Nuclear Physics, Proceedings vol. 34 B, page no. 13., Bombay (1991).

[2] A.K.Pandey, P. C. Kalsi, R.C.Sharma and R.H. Iyer, DAE symposium on Nuclear and Radiochemistry, Andhra University, Visakhapatnam , Dec 21-24 (1992)

[3] A. K. Pandey, P. C. Kalsi and R.H.Iyer, DAE symp. on Nuclear Physics Symposium, Calicut Univ., Calicut ,27-30 Dec. 1993, Proceedings Vol 36B, p. no. 146.

[4] A.J. Sierk , Phys. Rev. C33, 2039 (1986)

[5] R.H.Iyer, A.K.Pandey, P.C.Kalsi and R.C.Sharma, Phys. Rev. C, 48, 87-94 (1993).

[A.K.PANDEY , P.C.KALSI and R.H.IYER]

REACTION MECHANISM STUDIES IN ALPHA INDUCED REACTIONS

M.K. Bharadwaj, I.A. Rizvi and A.K. Chaubey

Department of Physics, Aligarh Muslim University
Aligarh 202002 (India)

Our research programme is on going programme on "Reaction Mechanism Studies in Alpha Induced Reactions (pre-equilibrium) at IUC-DAEF using VEC at Calcutta. So far all the experiments done are off-beam experiments. Stack foil technique was used and alpha particle beams of energies upto 50MeV (available at VECC) was utilized. The induced activities due to different (α,xnyp) reactions were measured using HP-Ge detector with associated electronics and multi channel analyser. This type of study is very helpful in studying reaction mechanism, contribution of pre-equilibrium decay at different energies and compound nuclei formation. The analysis and theoretical calculations were done using computer code ALICE-82 and 91. Still data is scanty and needs further measurement.

In the above mentioned period one student got the Ph.D. Degree.

Name of Student : M.K. Bhardwaj, Year : 1992

Topic of Thesis : Study of Excitation Functions for α-induced reactions in some nuclei at cyclotron energies.

Papers published

1. Excitation function studies for the alpha induced reactions in indium
M.K. Bhardwaj, I.A. Rizvi and A.K. Chaubey
Int. J. Mod. Phys. E 01, 389, 1992.

2. Alpha induced reactions in Iridium
M.K. Bhardwaj, I.A. Rizvi and A.K. Chaubey
Phys. Rec. C45, 2338, 1992.

3. Pre-equilibrium fractions in some nuclei for alpha induced reactions,
I.A. Rizvi, M.K. Bhardwaj, R.P.Gautam & A.K. Chaubey
Proc. Nucl. Phys. Symposium 36B, 248, 1993.

4. Non-equilibrium emission of multi-particles in alpha induced reactions in cesium and iodine,
A.K. Chaubey, M.K. Bhardwaj, I.A. Rizvi & Nishi Agarwal
Proc. Nucl. Phys. Symposium 37B, 293, 1994.

5. Alpha induced reactions in antimony
M.K. Bhardwaj, I.A. Rizvi and A.K. Chaubey
Int. J. Mod. Phys. E03, 239, 1994.

TOWARDS ESTABLISHING NUCLEAR DATA ONLINE SERVICES

S. Ganesan and V.K. Sundaram*
Neutron Physics Division
Bhabha Atomic Research Centre (BARC)
Bombay 400 085
(email: ganesan@magnum.barct1.ernet.in)

Efforts were successfully made to access online the internationally available nuclear data bases through INTERNET. Using Kermit, the work site at the BARC was connected to the Sunsparc workstation at the Pellatron laboratory. From the Sunsparc Workstation, invoking internet access, the online retrieval of the entire ENDF/B-VI library (ENDF/B-VI tapes 100 to 129 including all updates as on the date of retrieval) from the IAEA Nuclear Data Section, Vienna was successfully completed.

Using Internet acces, the latest version of the Pre-processing programs and the utility programs of ENDF/B have also been successfully downloaded. The latest version of the pre-processing programs, LINEAR, RECENT, SIGMA1, GROUPIE, SIXPAC, COMPLOT, EVALPLOT etc have been commissioned successfully at the BARC.

Efforts have been initiated to create a parallelized version of the RECENT, the program to reconstruct resonance cross sections, on the BARC Parallel computer as the RECENT code takes too much CPU time in the case of isotopes with large number of resonances (e.g. Fe-56, U-238 etc).

---

*Radiation Safety and Systems Division, BARC

USE OF NEW CROSS SECTION DATA FOR URANIUM AND BORON ISOTOPES OBTAINED FROM RECENT ENDF/B-VI FILES

V.Jagannathan, R.P.Jain and S.Ganesan*
Theoretical Physics Division, *Neutron Physics Division
Bhabha Atomic Research Centre, Bombay - 400 085, India

The Indian thermal power reactor calculations are done with WIMS cross section library obtained in sixties from U.K. It has been observed from the feedbacks from TAPS BWRs as well as from the Indian PHWRs that there is a systematic overprediction of calculated eigenvalue or K-effective in cold reactor states while in hot power operating conditions the eigenvalues are somewhat underpredicted. Similar trends were observed in the IAEA benchmark analyses of other reactor types such as Spanish PWR, Russian VVER and Mexican BWRs. Such discrepancies had in fact been observed world over and the reason was traced to the U-235 eta values in thermal energy range (below 0.3 eV), improved resonance integrals for U-238 etc [1].

Recently nuclear data for a few selected isotopes, as part of preliminary results of the IAEA WIMS Library Update Project derived from ENDF/B-VI, were made informally available (Dr.Jung Do Kim, KAERI, Korea & Dr.A.Trikov, Ljubljana, Slovania). The data in WIMS library format was generated by them using the latest version of the NJOY code system by processing the ENDF/B-VI library. These data were incorporated in our WIMS69 data library. The eta values for U-235 are compared in Fig.1 in the energy range from 0.005 eV to 0.3 eV. The U-238 resonance integrals are now available up to 1100 °K compared to earlier tabulations of up to 900°K. The new (WIMSKAL-88) B-10 cross sections in thermal energy range are seen to be higher by about 2 % as compared to old WIMS data.

Some preliminary analysis of the cold and hot critical data of KAPS-I & II reactor cores has been carried out with both old and new nuclear data. In general the results do indicate a definite decrease in calculated Keff values when new cross sections for both uranium and boron isotopes are used while there is no appreciable change in hot operating conditions, thus reducing the discrepancy between calculation and measurements.

References

1. M.J.Halsall, 'Recent Adjustments To The WIMS Nuclear Data Library',EPRI NP-2855, Project 975-1, Proceedings, Feb 1983.

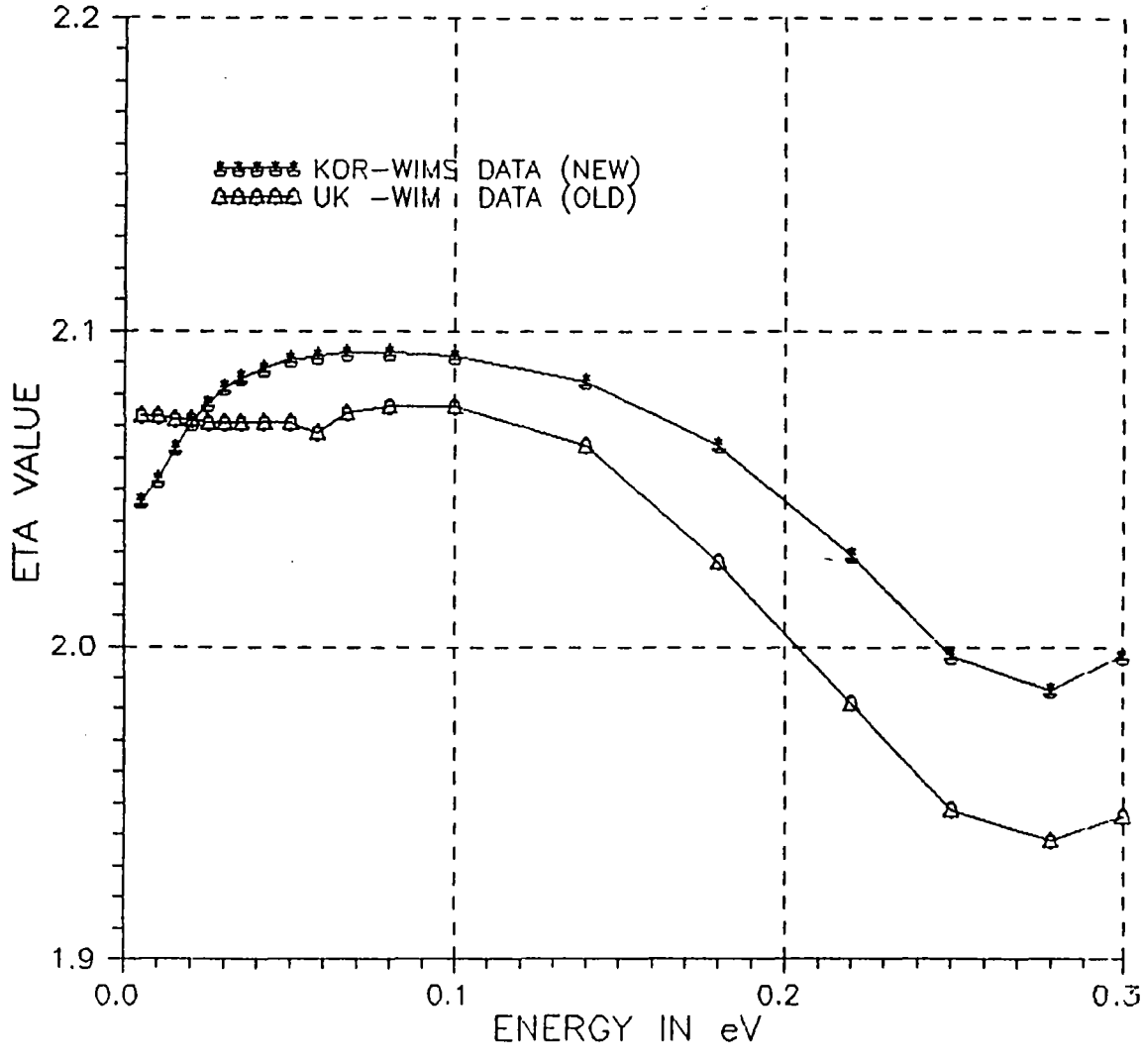

FIG.1 U-235 ETA - vs ENERGY

ENTRANCE CHANNEL DEPENDENCE OF FISSION FRAGMENT ANISOTROPIES FOR $^{6,7}Li$, ^{11}B, ^{12}C, ^{16}O AND ^{19}F + ^{238}U SYSTEMS

A.Samant, S.Kailas, A.Chatterjee, A.Navin, A.Shrivastava, P.Singh,
M.S.Samant* and S.S.Kapoor
Nuclear Physics Division, Bhabha Atomic Research Centre,
Bombay 400 085 * T.I.F.R., Bombay 400 005

Fission fragment angular distributions have been measured for the systems ^{11}B + ^{238}U at E = 57.5, 61.5, 65.5 and 69.5 MeV and ^{19}F + ^{238}U at E = 104, 108 and 112 MeV using the BARC-TIFR pelletron [1]. Combining these with the ones available in the literature for other projectiles like $^{6,7}Li$, ^{12}C and ^{16}O, it has been possible to bring out the entrance channel dependence of measured fission fragment anisotropies. This observation is consistent with the prediction of pre-equilibrium fission model proposed earlier by the Trombay group [2]. A detailed paper on this work is being prepared for publication.

[1] A. Karnik et al. Proc.Int.workshop on heavy-ion fusion, Padova, Italy 1994 to be published.
[2] V.S.Ramamurthy and S.S.Kapoor Phys.Rev.Lett. 54,178(1985); V.S.Ramamurthy et al. Phys.Rev.Lett. 65,25(1990)

INVESTIGATION OF PRESCISSION NEUTRON EMISSION IN ^{235}U (n_{th}, f) THROUGH FRAGMENT-NEUTRON ANGULAR CORRELATION STUDIES

M.S. Samant*, R.P. Anand. R.K. Choudhury, S.S. Kapoor and D.M. Nadkarni
Nuclear Physics Division, Bhabha Atomic Research Centre, Bombay 400 085

*TIFR, Bombay

Abstract

Measurements of prompt neutron energy spectra and angular distributions from mass and kinetic energy selected fission fragments were carried out in the thermal neutron fission of ^{235}U. Neutron energy was determined by the time of flight technique and fission fragment energy and angle were measured using a back-to-back gridded ionization chamber. The measured angular distributions of neutrons emitted from fragment pairs of various mass and kinetic energy were compared with results of Monte Carlo calculations asuming neutron emission from fullv accelerated fragments to determine the component of neutrons which may be emitted in the prescission stage. The calculations were carried out using as inputs the measured center of mass neutron energy spectra and multiplicities and assuming isotropic emission of neutrons in the centre of mass frame of both the fission fragments, and a three source fitting of the angular distributions was done to deduce the component of prescission neutrons. The value of the prescission neutron multiplicity ν_{pre} averaged over all fragment masses is found to be 0.25 ± 0.05 (about 10% of the total neutron multiplicity). The value of ν_{pre} is found to be nearly same for all fragment masses except in the region of doubly closed heavy fragment shell region, where it is somewhat larger. It is also seen that ν_{pre} shows an increase with fragment total kinetic energy Calculations carried out under the assumptions of the statistical model give an estimate of the time scale from saddle-to-scission transition which is compatible with the values obtained from heavy ion fusion-fission experiments. The present results have been discussed on the basis of the energy damping and timescale of the saddle to scission transition in the thermal neutron induced fission process.

PROMPT NEUTRON EMISSION SPECTRA AND MULTIPLICITIES IN THE THERMAL NEUTRON INDUCED FISSION OF ^{235}U

M.S. Samant, R.P. Anand, R.K. Choudhury, S.S Kapoor, K. Kumar,
D.M. Nadkarni and A. Saxena
Nuclear Physics Division, Bhabha Atomic Research Centre,
Bombay 400 085, India

Abstract. The emission spectra of prompt fission neutrons from mass and kinetic energy selected fission fragments have been measured in $^{235}U(n_{th}, f)$. Neutron energies were determined from the measurement of the neutron time of flight using a NE213 scintillation detector. The fragment energies were measured by a pair of surface barrier detectors in one set of measurements and by a back-to-back gridded ionization chamber in the second set of measurements. The data were analysed event by event to deduce neutron energy in the rest frame of the emitting fragment for the determination of neutron emission spectra and multiplicities as a function of the fragment mass and total kinetic energy. The results are compared with statistical model calculations using shell and excitation energy dependent level density formulations to deduce the level density parameters of the neutron rich fragment nuclei over a large range of fragment masses.

Nuclear Data Section
International Atomic Energy Agency
P.O. Box 100
A-1400 Vienna
Austria

e-mail, INTERNET: SERVICES@IAEAND.IAEA.OR.AT
e-mail, BITNET: RNDS@IAEA1
fax: (43-1) 20607
cable: INATOM VIENNA
telex: 1-12645 atom a
telephone: (43-1) 2060-21710

online: TELNET or FTP: IAEAND.IAEA.OR.AT
username: IAEANDS for interactive Nuclear Data Information System
username: NDSOPEN for FTP file transfer